Final

Engineering Development of Coal-Fired High Performance Power Systems Phase II and III

DE-AC22-95PC95144

Quarterly Progress Report

October 1 - December 31, 1996

Prepared for

Pittsburgh Energy Technology Center
Pittsburgh, Pennsylvania

United Technologies Research Center
411 Silver Lane, East Hartford, Connecticut 06108

Abstract

This report presents work carried out under contract DE-AC22-95PC95144 "Engineering Development of Coal-Fired High Performance Systems Phase II and III." The goals of the program are to develop a coal-fired high performance power generation system (HIPPS) by the year 2000 that is capable of:

- >47% thermal efficiency (HHV)
- NOx, SOx, and particulates > 10% NSPS
- coal providing ≥ 65% of heat input
- all solid wastes benign
- cost of electricity 90% of present plant

Work reported herein is from:

1. Task 1.3 HIPPS Commercial Plant Design,
2. Task 2.2 HITAF Air Heater; and
3. Task 2.4 Duct Heater Design.

Table of Contents

List of Exhibits

List of Exhibits (Continued)

Executive Summary

This report presents work carried out under contract DE-AC22-95PC95144 "Engineering Development of Coal-Fired High Performance Systems Phase II and III." The goals of the program are to develop a coal-fired high performance power generation system (HIPPS) by the year 2000 that is capable of:

- >47% thermal efficiency (HHV)
- NOx, SOx, and particulates > 10% NSPS
- coal providing ≥ 65% of heat input
- all solid wastes benign
- cost of electricity 90% of present plant

Work reported herein is from Task 1.3 HIPPS Commercial Plant Design, Task 2.2 HITAF Air Heater; and Task 2.4 Duct Heater Design.

The impact on cycle efficiency from the integration of various technology advances is presented. The criteria associated with a commercial HIPPS plant design as well as possible environmental control options are presented.

The design of the HITAF air heaters, both radiative and convective, is the most critical task in the program. In this report, a summary of the effort associated with the radiative air heater designs that have been considered is provided. The primary testing of the air heater design will be carried out in the UND/EERC pilot-scale furnace; progress to date on the design and construction of the furnace is a major part of this report. The results of laboratory and bench scale activities associated with defining slag properties are presented. Correct material selection is critical for the success of the concept; the materials, both ceramic and metallic, being considered for radiant air heater are presented. The activities associated with the duct heater are also presented.

Introduction

The High Performance Power Systems (HIPPS) electric power generation plant integrates a combustion gas turbine and heat recovery steam generator (HRSG) combined cycle arrangement with an advanced coal-fired boiler. The unique feature of the HIPPS plant is the partial heating of gas turbine (GT) compressor outlet air using energy released by firing coal in the high temperature advanced furnace (HITAF). The compressed air is additionally heated prior to entering the GT expander section by burning natural gas. Thermal energy in the gas turbine exhaust and in the HITAF flue gas are used in a steam cycle to maximize electric power production. The HIPPS plant arrangement is thus a combination of existing technologies (gas turbine, heat recovery boilers, conventional steam cycle) and new technologies (the HITAF design including the air heaters, and especially the heater located in the radiant section).

The HITAF provides heat to the compressor outlet air using two air heaters, a convective air heater (CAH), and a radiant air heater (RAH). The HITAF is a slagging furnace which contains the radiant air heater, as well as waterwalls and steam drum for the high pressure (HP) steam system. Hot flue gas leaving the HITAF furnace passes over the CAH prior to entering heat recovery steam generator (HRSG) #2. Hot exhaust gas from the gas turbine is ducted to HRSG #1 in a typical combined cycle arrangement. The HITAF, gas turbine and HRSGs are configured to achieve the required high efficiency of the HIPPS plant.

The key to the success of the program is the development of integrated combustor/air heater that will fire a wide range of US coals with minimal natural gas and with the reliability of current coal-fired plants. The compatibility of the slagging combustor with the high temperature radiant air heater is the critical challenge.

Results and Discussions

The body of this report provides a status of the ongoing effort by task and presents both results during the last quarter and a discussion of those results by task.

Conclusions

The body of this report provides a status of the ongoing effort by task and presents within that discussion any conclusions reached during the reporting quarter

Task 1.3 Powerplant Description

The confusion surrounding the deregulation of the electric utility industry and the formation of the new organizations that will provide electric power in the 21st century will have a profound effect on the type of generation equipment purchased in the next several decades. The industry is changing from today's operations in which regulation was based on cost of service. This method of operation was not flexible enough to ensure that capacity was added to the systems at the right time and the right price. Capitalization was straightforward and of low risk. The industry will now be market driven meaning that the groups that can supply the grid with the right type capacity, timed to demand, and at the lowest cost will be rewarded.

While the exact configuration of the future utility industry is undefined, one version in current favor is shown in Exhibit 1.3-1. Although the flow of energy is clear, most of the mechanisms for deciding who furnishes the power and at what cost are not. The configuration shown in Exhibit 1.3-1 is called "POOLCO".

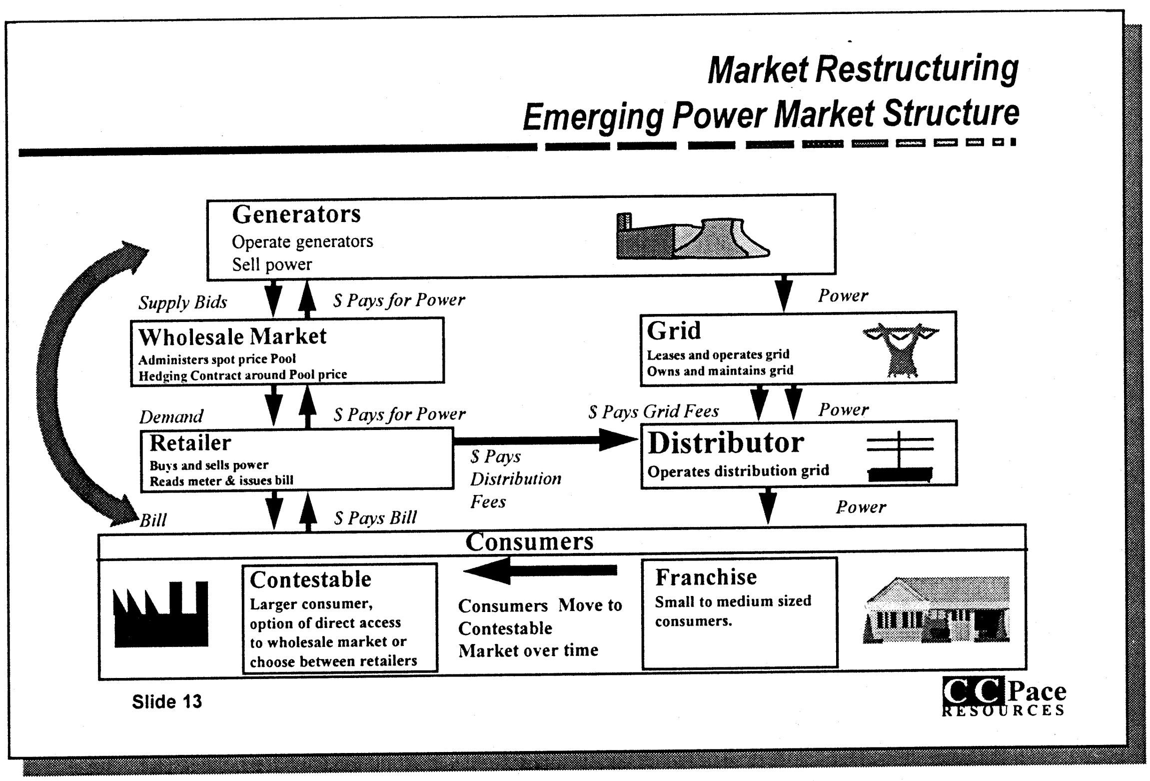

Exhibit 1.3-1
POOLCO Configuration of the Electric Power Industry

Introduction of a competitive POOLCO presents both energy suppliers and users with new issues:

- All existing generation assets will have to be revalued
- Potential risk is created in placing new capital investment in the system
- Incremental changes in generation to create value added will be important in divestiture decisions (i.e., emissions control, life extension, repowering)
- Fuel arrangements will become either a competitive advantage or a liability
- Balancing of spot, short-term, and long-term purchase/sales will be a key to market survival.

While all the ramifications of deregulation have not been identified, it does appear that the market opportunities will accrue to new power technologies that offer high efficiencies, rapid dispatch and response, fuel flexibility, and low capital costs. The HIPPS approach to repowering could be one of the more attractive coal-based new technologies.

In addition to continued review of deregulation, with the emphasis on how it will affect repowering, the Commercial Plant design of Phase I has been revisited. The purpose of the new investigation has been to evaluate possible alternative configurations which would bring the HIPPS closer to typical power plant operating characteristics.

Operating Changes in Commercial Plant Design

The Commercial Plant Design models have been revised to reflect several changes in operation. Three alternative plants were analyzed:

1. original design but with HITAF stack at 300 F to account for sulfur (Stream 15 in Exhibit 1.3-2)
2. air preheater replacing GT exhaust for combustion air; 300 F stack (Exhibit 1.3-3)
3. same as above with no recirculation for quench (Exhibit 1.3-4)

The effect of increasing the HITAF stack temperature from 240F to 300F (Case 1) was a reduction in plant efficiency from 48.4% to 47.9%. The use of a more or less standard air preheater to heat the HITAF combustion air in lieu of using the GT exhaust resulted in an overall efficiency of 47.8%. When the recirculation stream was eliminated, the performance declined by another 0.1 point to 47.7%. The foregoing results are as would be expected. As long as the heat from the GT cycle is used in the steam cycle without significant change in duty, the only effect on overall performance would be due to changes in recovery of heat in the HITAF exhaust, i.e., less heat is recoverable since the stack temperature is higher. The results also indicate that the cycle is relatively insensitive to configuration changes

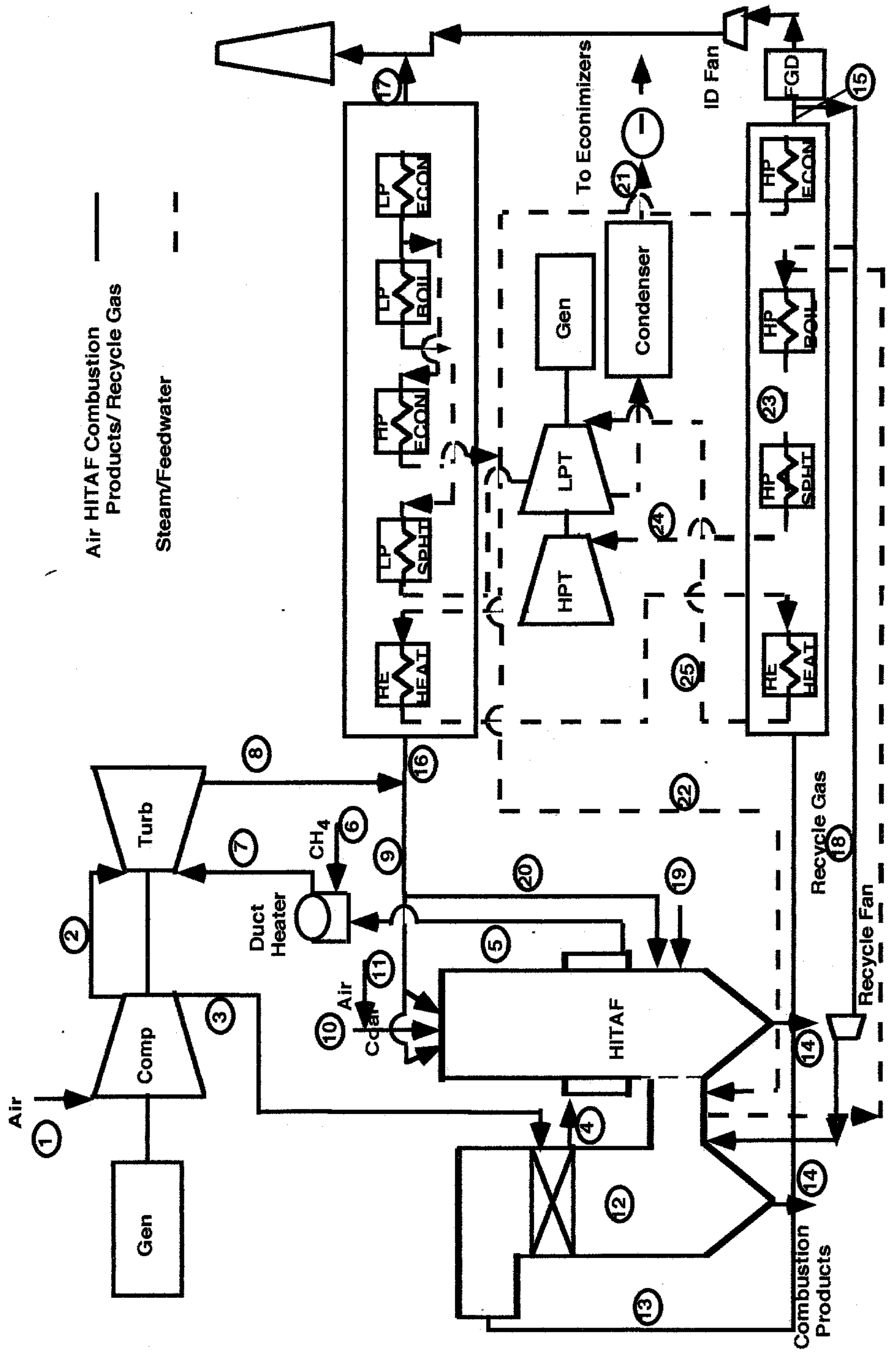

Exhibit 1.3-2
Baseline Commercial Plant Design

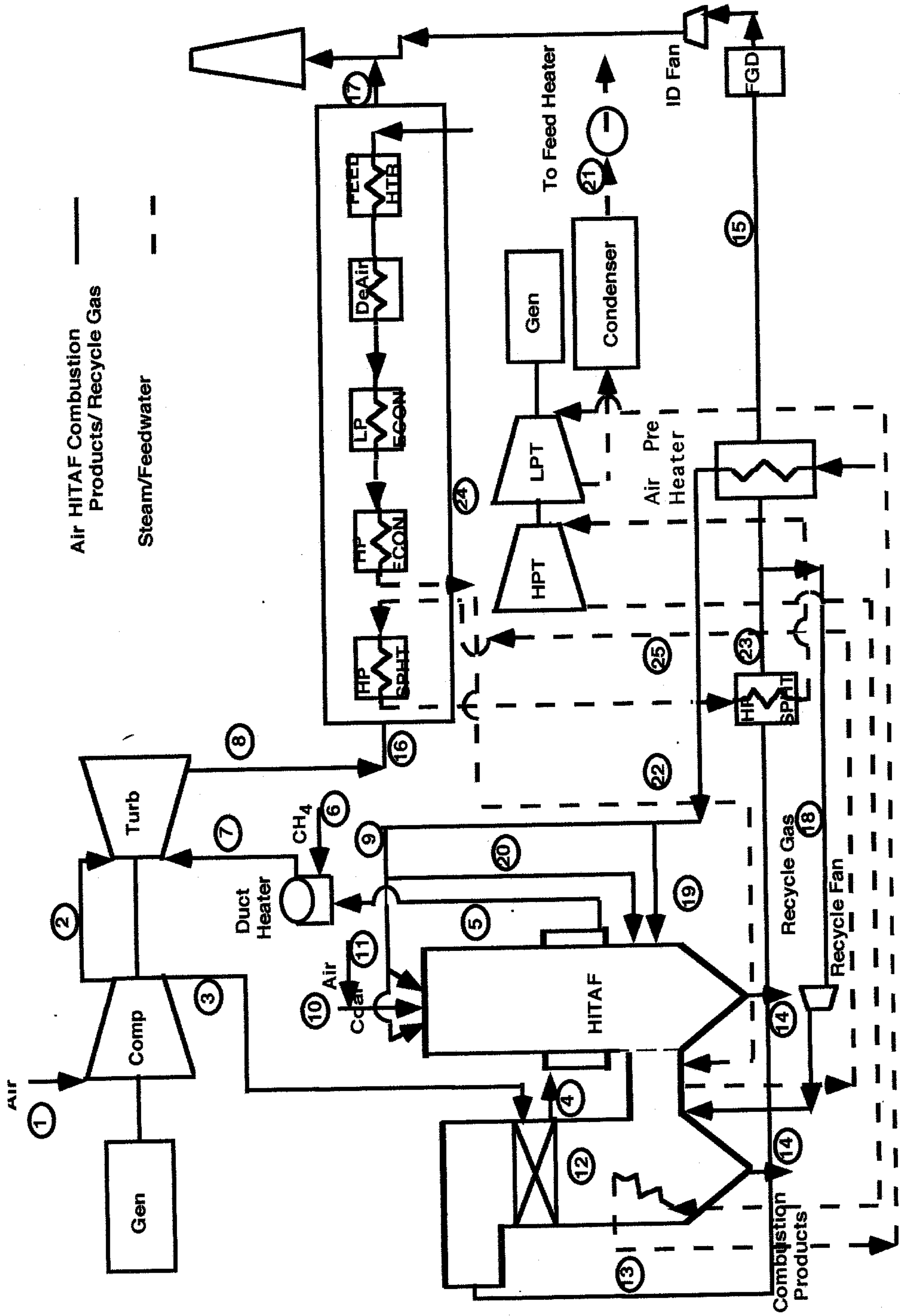

Exhibit 1.3-3
Commercial Plant Design with Air Preheater

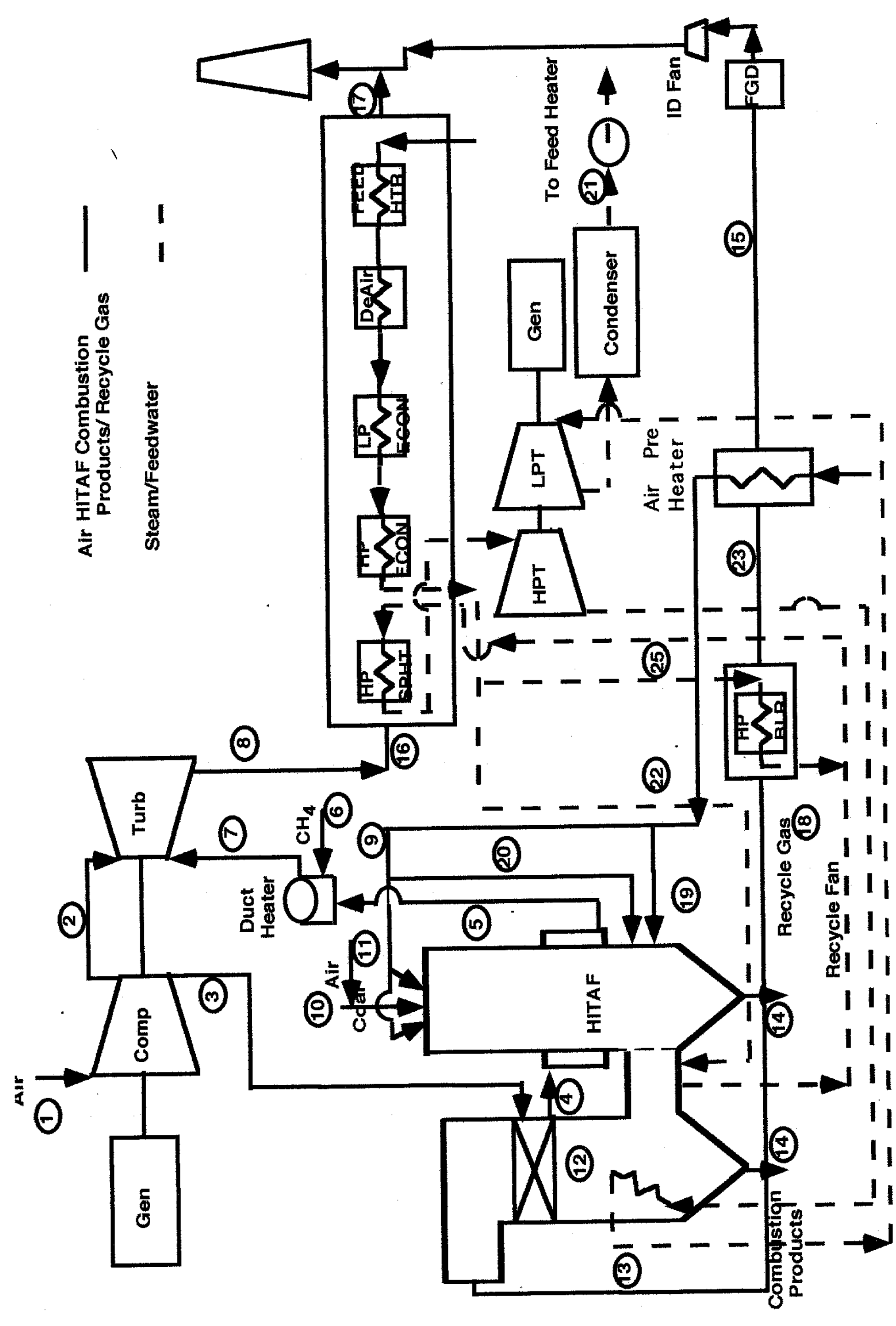

Exhibit 1.3-4
Commercial Plant Design /Air Preheater w/o Recycle

FT4000 HAT

A revised model of the FT4000 HAT has been under construction. Early versions have been used to estimate HIPPS/HAT performance (in the 53-55% range HHV). The model continues to be updated as information on cooling and flow characteristics is received from Pratt & Whitney. A gas-fueled version, which will define the baseline HAT performance characteristics, is shown schematically in Exhibit 1.3-5. Note that the combustor exit temperature is several hundred degrees C above that of the ATS technology engines. Airfoil cooling is based on an industrial adaptation of techniques that have been demonstrated in programs for the very high performance military aircraft engines. These techniques are significantly enhanced with an intercooled engine such as the FT4000 I/C. Further advantage accrues when a HAT cycle version is considered.

HIPPS Commercial Plant Design and Operations Review

The commercial plant conceptual design and properties of the major process flow streams were reviewed. Enthalpies of the streams were calculated with different sets of heat capacity data: Kobe, Hougen et al and JANAF tables. After discussions with UTRC, it was agreed to use the JANAF tables, which are consistent with UTRC's calculations.

Review of the flow sheet raised a question about the proper flue gas exit temperature, in view of the coal's sulfur content and acid gas dew point considerations. Review of literature, discussion with other Bechtel specialists and communications with equipment suppliers indicated that the flow sheet temperature of 258 °F was low. A new exit gas temperature of 300 °F was established as the practical limit. This change and others that are expected from UTRC will require revision of the flow sheet and the stream properties.

Much of the process work this quarter has been to better understand and define the technologies available to meet the project's emission control limits. In order to evaluate and propose a system for the team to use in the commercial design, recent literature was reviewed and informal contacts made with emission control process developers. Flue gas properties were estimated to define the stream being cleaned to meet the DOE requirements.

Data is being collected for sulfur dioxide, nitrogen oxides and particulate controls. Cost and technical information has been requested, and partially received from the following organizations.

- AirPol Inc., Parsippany, NJ
- ABB Environmental Systems, Knoxville, TN
- Babcock & Wilcox, Baberton, OH
- Dravo Lime Company, Pittsburgh, PA
- Environmental Elements Corporation, Baltimore, MD
- Environmental Systems, Lebanon, PA
- Krupp Koppers, Essen, Germany
- Haldor Topsoe, Inc., Houston, TX
- NOXSO Corporation, Bethel Park, PA
- Pure Air, Allentown, PA

Other developers and equipment suppliers will be contacted as the requirements for more information expands.

A potential revision to the process is the addition of coal drying ahead of the pulverization and combustion step. Currently the coal is “warmed” and a small amount of moisture removed. The coal solids are effectively “dried” in the pulverizer, but this is only to enhance the solids handling and transportability operation; the moisture from the coal remains entrained with the transport gases, and has a detrimental effect on efficiency in the furnace. A technical investigation was requested by UTRC, and has started, to determine if drying ahead of the pulverizer, in a separate step, is worth adding. Questions such as the supply of drying heat/energy; the cost of new equipment and its auxiliary power consumption; equipment savings from the present scheme; and the efficiency improvements with dried coal (for calculations -- zero percent moisture) used in the HITAF are part of the investigation.

Bechtel continues to contact potential suppliers of BOP equipment and systems. Data from the suppliers will enhance the process calculations, adding practical information to the conceptual design. Also, the suppliers are being asked to provide cost data, lead-times for procurement, and for selected specifics about materials of construction, footprint and energy consumption.

As the process and its energy and material balance become more defined, the equipment list will be revised. One of the primary goals of this preliminary equipment list data will be to highlight items and/or systems where tradeoffs may exist between efficiency and cost. Process efficiency, especially in Phase I, has been given the highest attention during process design. As the BOP, the HITAF and the gas turbine system are more defined and costs detailed, alternatives to the base process will become targets for tradeoff calculations to determine if costs can be reduced without significantly reducing efficiency. The possible use of coal drying ahead of the HITAF (as discussed above) is one example of such work to be performed in the second (Federal fiscal year) quarter.

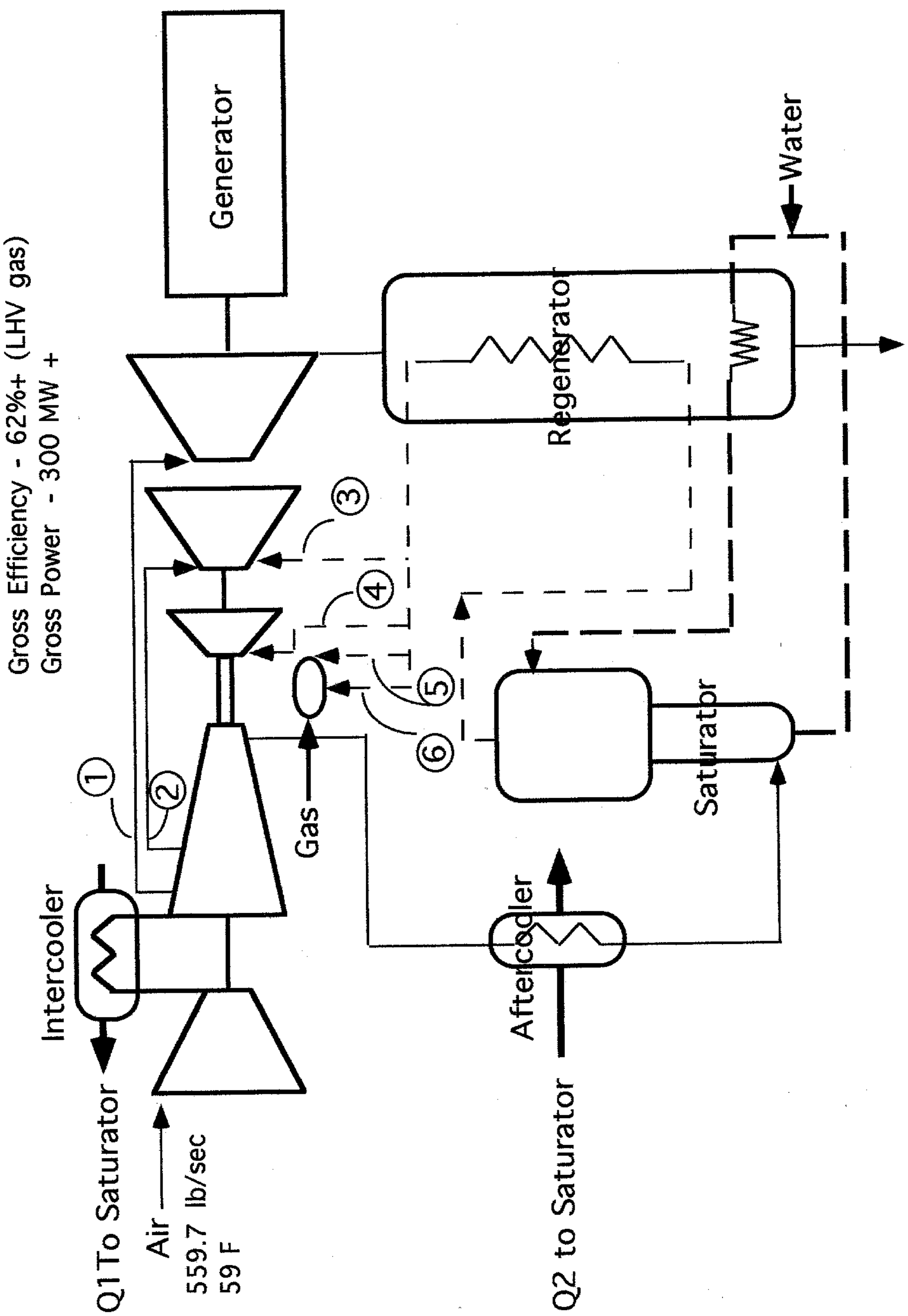

Exhibit 1.3-5
FT4000 HAT cycle Schematic Task 2.2 HITAF Air Heaters

Task 2.2 HITAF Air Heaters

The last quarter of 1996 was spent primarily in designing the three test heater panels to be employed in the U.N.D. Pilot scale test:

1. Large RAH panel
2. Small RAH panel
3. CAH insert.

The following sections define the testing priorities of each heat exchanger, and then describe the heat transfer analysis.

Description and Testing Priorities

Large RAH Panel

The testing priorities for the large RAH panel were listed in the last Quarterly report. The main goals of the heat transfer testing are to

1. prove that the air can be heated from 1300 F to 1700 F [704 C to 927 C], with
2. materials which can withstand the environment, and
3. that we can correlate our design models to the test data

For these reasons it is important that the compressed air be supplied at the design temperature of 1300 F, and that the flow rate be such that 1700 F is maintained at the output.

Exhibit 2.2-40 in the Structural Analysis section shows the large RAH panel design It has the following features:

2.5 in [.064 m] OD tubes with 0.25 inch [.0064 m] walls made from MA754.

These are the same tubes that have been identified for use in the full scale RAH, but will require an insert tube to enhance the air-side heat exchange (see below).

Three tubes in a box:

The full scale RAH will have 6 tubes per box, however, this many tubes cannot fit into the pilot scale test port. To test the radiative transfer within the box it is necessary to have both center tubes and end tubes. It is felt that three tubes will be sufficient to allow validation of the heat transfer models.

The ceramic bricks

These bricks face the flame and will be made from the current best candidate material, and will be identical in shape to the proposed commercial scale design with the exception that they will be 18 inches [0.46 m] rather than 30 inches [0.76 m] wide (to accommodate the narrow RAH port opening).

In the commercial plant it is intended that a 400F rise will be obtained over 60 feet [18.3 m] of tube length. In the pilot-scale test this same rise will be accomplished in less than 6 [1.83 m] feet. If the heat flux per unit brick face area is the same, then the air flow per tube will need to be

~1/10th of the commercial plant design. For this reason an insert tube will be used to both enhance the air-side convective coefficient, and provide enough pressure drop so that the flow can be uniformly distributed among the three tubes.

Small RAH Panel

A schematic of the small RAH panel is shown in Exhibit 2.2-1. A detailed design has not yet been finalized. The primary purpose of the small RAH panel is to provide a means of testing alternative ceramic brick designs and attachment schemes. For this reason it is not important for the cooling air to be supplied at 1300 F; hotter air will enable a more uniform temperature to be achieved on the back side of the bricks. In this panel a center support rail will be employed so that the slag seal between adjacent bricks can also be tested. The active height of the small RAH panel will be 36 inches [.91 m].

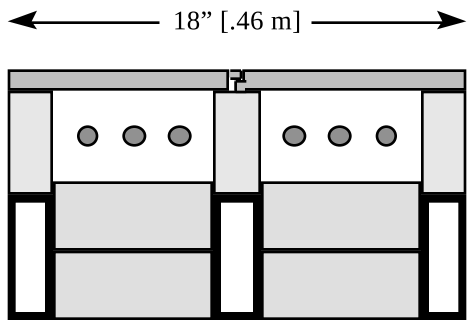

Exhibit 2.2-1
Preliminary Schematic of Small RAH Panel

CAH Insert

A drawing of the CAH insert is shown in Exhibit 2.2-37. The primary goals of the CAH test are to:

1. determine the outside (flue-gas to tubes) convective coefficient,
2. determine the rate of coal deposition on the tubes, and
3. test the metal alloy tube which is exposed to the slag for resistance to corrosion at key temperatures. (The hottest tube wall temperature in the commercial design is expected to be ~1600 F [871 C]. Materials will also be tested at lower temperatures where corrosive alkalies form.

It is believed that the internal convective heat transfer is easily calculated and need not be explicitly checked in the pilot scale tests.

The commercial plant CAH design requires (according to the Phase II proposal) that the compressed air be heated from 730 to 1300 F [388 to 704 C], while the flue gas is cooled from 1800 down to 1200 F [980 to 650 C]. Depending upon the convection coefficient achieved on the flue-gas side, the tube temperature will likely vary from ~1000 to ~1600 F [540 to 870 C]. In this reduced scale test it will not be possible to test the full range of tube temperatures during a single test at EERC. Each test condition will simulate a single section of the full CAH.

Each exposed section of tube will be 13 inches [.33 m] long. The CAH will have 7 active tubes, and 5 dummy tubes. The reason for fewer active tubes is to increase the air-flow per tube and therefore have less axial temperature gradient over each tube length. The dummy tubes help set up the proper turbulent flow regime over the tubes which will be monitored for heat transfer.

An earlier specification to EERC stipulated that the CAH compressed air be supplied at 1000 F [538 C]. A tube design was found (see below) which will heat air from 1000 to just under 1200 F [538 to 648 C] in a single pass (using bayonet style tube-within-a-tube) with the maximum tube wall temperature at ~1600 F [871 C]. Multiple path arrangements were not attempted in this small scale due to the headering complexities which would arise. The cooler tube temperatures can easily be achieved by lowering the inlet air temperature to the CAH.

Heat Transfer Analysis

Large RAH Panel

The large RAH panel heat transfer was analyzed using the same code that was developed for the commercial plant design with a few minor modifications.

RAH Code: Modification to air convection and pressure drop.

The pilot scale design uses concentric tubes with the middle tube plugged. The flow area, perimeter, and equivalent diameter for pressure drop and convection calculations become:

$$A_c = \frac{\pi}{4}\left(D_1^2 - D_2^2\right) \qquad P = \pi\left(D_1 + D_2\right)$$

$$D_e \equiv \frac{4\,A_c}{P} = \frac{D_1^2 - D_2^2}{D_1 + D_2} = D_1 - D_2 \quad \text{which is 2 times the gap.}$$

Spiral spacers will be necessary to mix the flow from the tubes hot side (facing the hot brick) to its cold side (facing the re-radiating insulation). This mixing occurs naturally in an open tube, but in the concentric tube design it is possible for the air to be at different temperatures circumferentially around the tubes. With spiral spacers at angle θ (θ = 0 is no spiral, θ = 90 is blocked) the flow area and length are modified as:

$$A_c = \frac{\pi}{4}\left(D_1^2 - D_2^2\right) * \cos(\theta)$$

Length = L0 / cos(θ)

The mixing length is the axial distance per _ turn: $L_{mix} = \frac{\pi\, D}{2\tan(\theta)}$.

For 2 inch [0.051 m] tubes:

θ	L_{mix}
30°	5.44 in [0.138 m]
45°	3.14 in [0.078 m]

RAH code Inputs

The inputs indicated in Exhibit 2.2-2 to the RAH code:

Exhibit 2.2-2
RAM Code Input

Outer Tube OD	2.5 in	0.064 m
Outer Tube ID	2.0 in	0.051 m
Inner Tube OD	1.625 in	0.041 m
Spiral Angle	45 degrees	
Length of Active Heat Exchanger	54 in	1.37 m
Flow rate air (was varied in order to obtain the desired output temperature)	890 #/hr (195 scfm)	.112 kg/s
Refractory Thickness	1.5 in	.038 m
Refractory Conductivity	3.2 (Btu/hr-ft-F)	5.5 W/m-K
Air-side convection, based on spiraled thin annular gap (derivation not shown here).	70 (btu/hr-ft^2-F)	400 W/m^2-K
Radiation box transfer coefficient is determined from another code (not shown here) and is a function of temperature.		

RAH code Output:

Exhibit 2.2-2 is a graph of the output temperature profiles from the Modified RAH code. The metal temperature is not shown but lies in the range between the refractory temperature and the air temperature. It is hotter on the side which faces the refractory. The Profiles shown here mimic those expected in commercial design, except that they occur over 5 feet [1.52 m] rather than 60 [18.3 m].

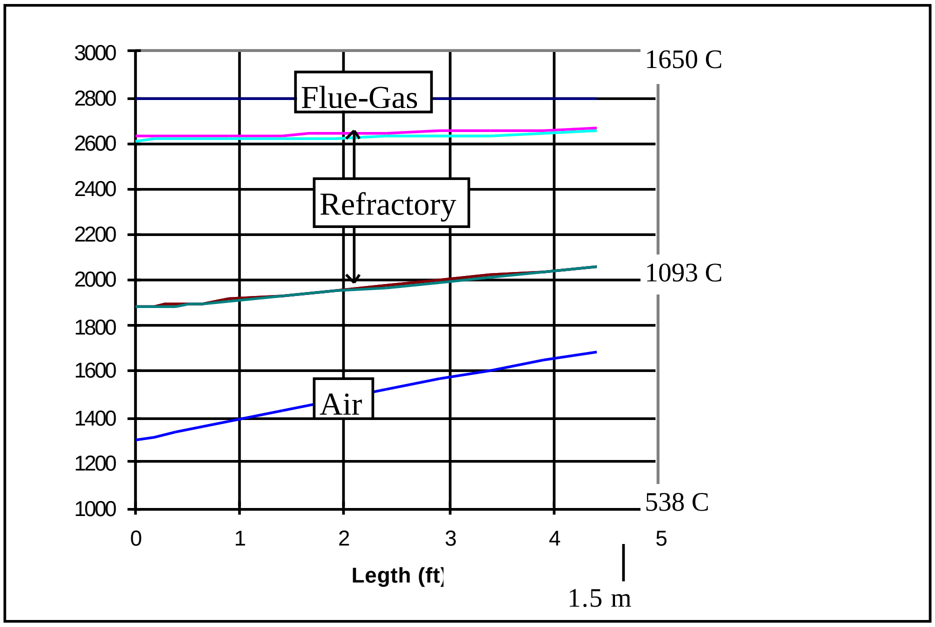

Exhibit 2.2-3
Large RAH Panel Temperature Profiles (flow = 890 #/hr) [.112 kg/s]

Small RAH Panel

The small RAH panel design has only been roughed out at this time. The goal is to use the same thickness refractory brick panels facing the flame as in the large RAH (as in the commercial plant design). In order to properly test the bricks, it is necessary to achieve roughly the same temperature gradient across them. If that can be done, then the heat flux will be prescribed, and will be proportional to the thermal conductivity of the brick. Since it is not expect that 1300 F air will be available for cooling these bricks, the tube design will not be identical to that in the large RAH. It is currently intended that use air at 1000 F or less be used, and that the tubes be bayonet style (tube-within-a-tube). With the colder tubes it will be possible to use cheaper tube material. In addition, the colder tubes will need to be smaller to provide less of a radiation sink for the bricks.

CAH Insert Heat Transfer

The CAH insert was design using two codes. The Kays code, which automates calculations found in his book, Compact Heat Exchanger Design, was used to find the convective coefficient between the flue-gas and the outside of the tubes. A second program was then written to determine the temperature profiles as a function of axial position along the tubes. This program simply solves for the net heat flux to each wall element by following the air flow (down the inside tube, and then back up the annulus between the two tubes) and then relaxes the tube wall temperatures with time until a steady-state solution is found. Exhibits 2.6-4 and -5 display the input to the code and the output from the temperature profile code, respectively. Exhibits 2.2-6 and -7 display the input and the output to the Kays' code.

Exhibit 2.2-4
Inputs to the Temperature Profile Code

Outside Tube OD	2 (in)	.051 m
Outside Tube Wall Thickness	3/16 (in)	.0048 m
Active Heat Exchange length	13 (in)	.33 m
Length for Pres. Drop. Calc.	20 (in)	.51 m
Spiral Angle	45 (deg)	
Total air flow	100 (scfm)	.057 kg/s
Temp Air Entering	1000 (F)	538 (C)
Temp Flue Gas	1800 (F)	982 (C)
h convection outside (from Kays' code, see below)	23 (btu/hr-ft^2-F)	130 W/m^2-K
k tube is high.		

Exhibit 2.2-5
Outputs From Code Temperature Profile

#	Number of Active Tubes	OD of inner tube (in)	Temp Air out (F)	Temp Tube bottom (F)	Temp Tube Top (F)
1	5	1.25	1185	1405	1490
2	7	1.25	1218	1459	1545
3	7	1.125	1192	1505	1571
4	**7**	**1.0**	**1173**	**1538**	**1591**
5	5	1.0	1149	1488	1543
metric:					
4	7	.0254 m	634 C	837 C	866 C

Case #4 was chosen for the CAH design.

Exhibit 2.2-6
The Inputs For Kays' Code

type of cross flow	Single Pass
Cross-sectional area	13 X 14 (in)
Length	16 (in) (4 deep)
Flue Gas flow rate	4720 (#/hr)
Flue Gas Properties • density • viscosity • specific heat • Pr • Pressure	 0.018 (#/ft^3) 0.28 (#/ft-hr) 0.29 (Btu/#-F) 0.74 15 (psia)
Tube designation used	T31 and T24 (nominally 1 inch tubes with 2 inch spacings)
Scaling factor	X 2

Exhibit 2.2-7
Outputs from Kays' code for outside of tubes

	T31	T24
Reynold's Number	27,000	27,000
Convection Coefficient	22.3	23.3

(Actual desired tube arrangement lies between case T24 and T31.)

Tube stress analysis

The analysis done above implied that there is no circumferential variation in tube temperature or flux. In fact, the convective coefficient provided by Kays' code is an integrated average. Although sufficient for determining the net heat flux, in order better represent the tube wall temperature distribution for determining thermal stress, the outside convective coefficient was re-generated as a function of circumference around the tube. A function was derived which matched the profile found in *Kreith*, Principle of Heat Transfer, and which was scaled to give the same integrated average value as calculated by Kays' code.

The finite element code MARC was used to solve for the thermal stresses of the outside tube as indicated in the Structural Analysis section The following were provided as boundary conditions:

Outside convective coefficient =	function of circumferential position around the tube
Inside convective coefficient =	constant
Outside Temperature =	1800 F [982 C].
Inside temperature =	function of axial position.

Pilot-Scale Testing

EERC activities this past quarter include the design, procurement, and construction of the pilot-scale high-temperature slagging furnace. Final design activities have been completed for all major system components with the exception of a few details concerning the RAH panels and CAH tube bank. Final design packages were completed, reviewed, and approved for the system refractory selection/installation, slag screen, dilution/quench zone, CAH section, and the cooling air preheaters in the past quarter. To date, UTRC has approved the final designs and specifications for the baghouse, tube-and-shell heat exchangers, primary and auxiliary burners, slagging furnace and slag pot shells, slag screen, dilution/quench zone, CAH section, cooling air preheaters, refractory selection/installation, coal feeder, and system fans. Completion of final design details concerning the RAH panels and CAH tube bank is expected early next quarter. The remainder of this section will discuss the status of design, procurement, fabrication, and installation activities concerning the pilot-scale slagging furnace system.

Structural Steel Design, Procurement, Fabrication, and Erection

Structural steel design, drafting, and procurement activities were essentially completed in April 1996; fabrication and erection were completed in May; and priming and painting continued through June of 1996. Ongoing structural steel activities have addressed support requirements for the installation of specific system components. Further priming and painting will be completed as individual system components are installed and area touch-up is required.

In the past quarter, structural supports have been added for the slagging furnace and the coal feed systems. In addition, short beam sections have been installed to support two of the four system fans. Partial guardrails were installed around the egress ladder openings in the fifth and sixth floors. Structural steel support activities for the refractory-lined duct sections and system piping and fans will be completed in the next quarter. Also in the next quarter, process component supports will be installed for the refractory-lined duct sections and two remaining system fans. Structural steel design data and fabrication and erection drawings will be updated to document recent and future changes. This information is on file at the EERC and available upon request. A photograph documenting the status of the structural steel as of December 31, 1996 is presented in Exhibit 2.2-8 (showing slagging furnace, slag pot, slag screen, dilution/quench zone, CAH section, cooling air preheater section, coal feeder, two system fans, flue gas stack penetrating the roof, baghouse/ash line, insulated tube-and-shell heat exchangers, and egress ladder location).

Preliminary Design of the Pilot-Scale Slagging Furnace

The final preliminary design package for the pilot-scale slagging furnace system was completed and approved by July 1996. The package contained a process description, process flow diagram, plan and elevation views of major components, P&IDs, and an instrumentation list. Exhibit 2.2-8 is a simplified illustration of the overall slagging furnace system. The EERC initiated procurement of system instrumentation and components for the data acquisition system in August with procurement activities continuing on a limited basis through December. Equipment procurement activities will continue through at least February 1997 and possibly through system shakedown.

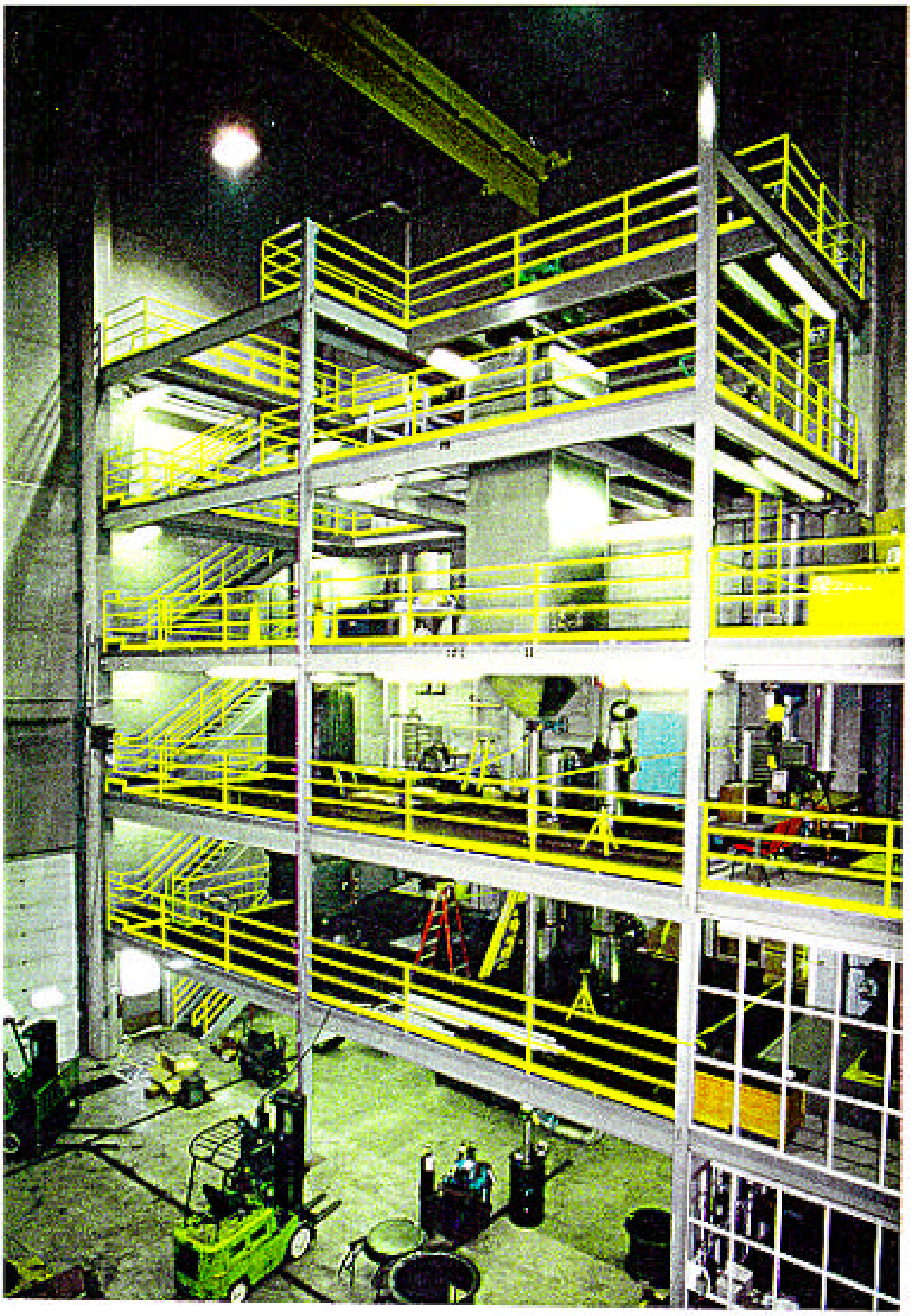

Exhibit 2.2-8
Photograph Illustrating The Status Of The Structural Steel And Component Installation

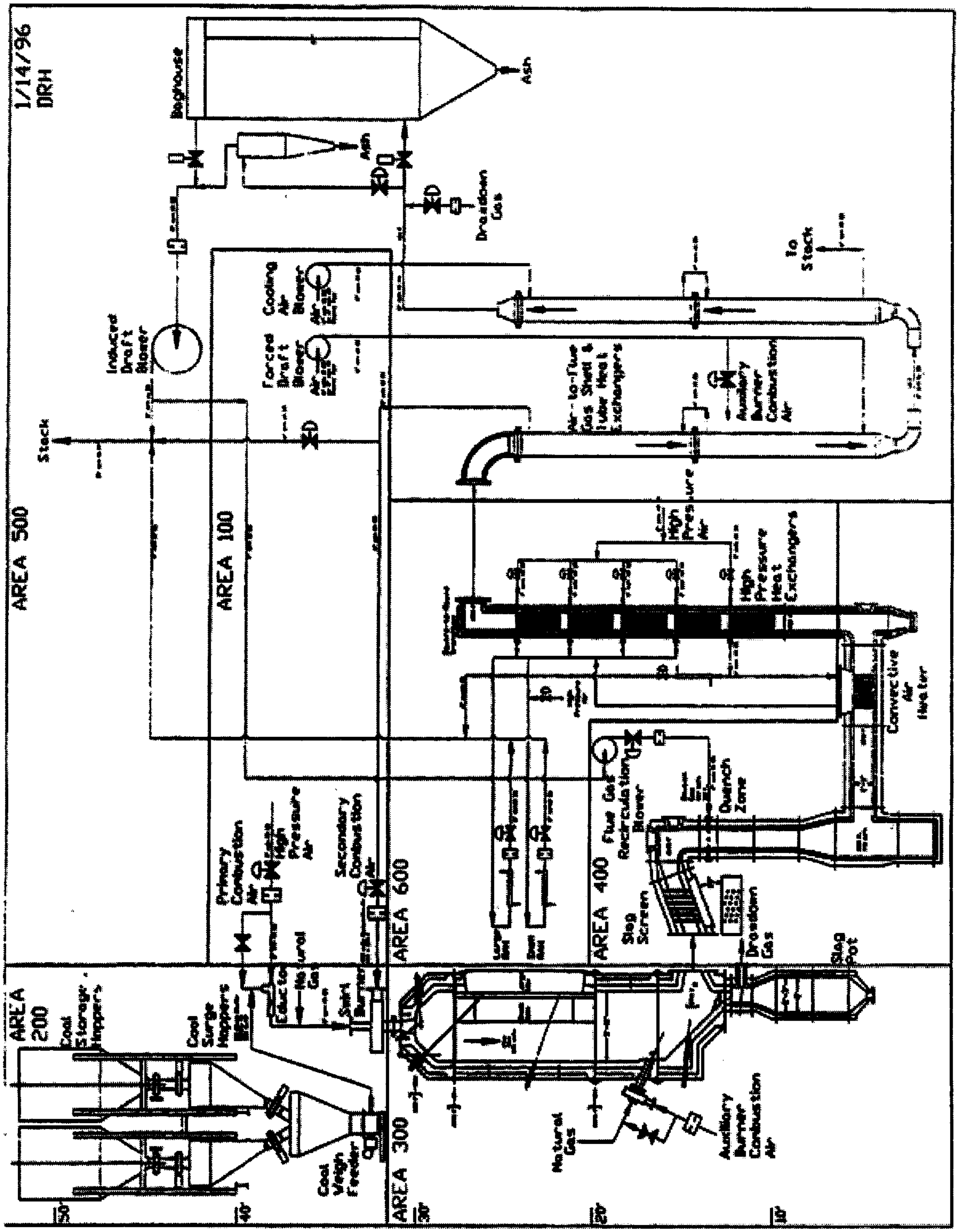

Exhibit 2.2-9
Combustion 2000 Slagging Furnace And Support Systems

Installation of electrical lighting and 110-, 208-, and 440-volt circuits was initiated in July and continued through September 1996. All of the light fixtures have been installed, and fixture wiring has been completed on all six floors. Weatherproof instrument and electrical wire trays have been run on all six floors and into the control room. Electrical circuits (110-volt) to support installation of the various system components have been installed on all six floors. Installation of circuit breaker panels (110-, 208-, and 440-volt) was completed in December, with wiring activities to continue through February 1997. The focus of electrical work will be final electrical hookups as system components are installed. Electrical procurement and work will continue through February as equipment installation continues. The remainder of this section presents the current design assumptions and the status of the final system and component designs.

Fuel Feed System

Work on the fuel feed system during the past quarter focused on the installation of the coal feeder, designing and fabricating two coal hoppers, and fabricating and installing the natural gas supply header required to support the primary and auxiliary burners. Coal feeder specifications were prepared by July 1996. Coal feeder specifications included pulverized coal density (40 lb/ft^3 or 641 kg/m^3) and particle size (70% <0.0030 in. or 75 :m; 300-μm top size). Other specifications included feed rate range (200-500 lb/hr or 91-227 kg/hr), minimum hopper capacity (10 ft^3 or 0.3 m^3), nonpulsing feed (twin-screw preferred), gravimetric (loss-in-weight) feed mode, minimum 20-bit resolution load cell (high-resolution digital preferred), and a user-programmable microprocessor control.

A bid package was distributed to several vendors requesting formal bids on the coal feeder. Coal feeder bids were received from four prospective vendors in August, and a purchase order was subsequently issued to Winger Associates for a K-Tron coal feeder. The coal feeder arrived in late October and was installed on the fourth floor of the high-bay structure in November. Fabrication drawings for two intermediate coal hoppers were completed in early December followed by material procurement. Fabrication of the coal hoppers began in December 1996 and will be completed in January 1997, followed by coal hopper installation. Level controllers for the coal hoppers arrived in November and will be installed after installation of the coal hoppers has been completed. The programming of the controller for the coal feeder and its integration with the data acquisition system began in December and should be completed in January.

Natural gas requirements were finalized with the local supplier in August 1996 concerning line and header size and delivery pressure. The local supplier installed a 2-in. (5-cm) meter and regulator to deliver natural gas at 10 psig (0.7 bar). Based on the components installed by the gas supplier, the EERC elected to design and fabricate a 2-in. (5-cm) natural gas header to be operated at 10 psig (0.7 bar). This header will supply natural gas to the primary and auxiliary burners. Header design, fabrication, and installation have been completed. Installation of the natural gas control system and lines to the individual burners is anticipated in January 1997. Procurement of valves, regulators, and flow control devices for the natural gas system has been completed. Procurement of some small quantities of pipe (1- and 0.5-in. [2.5- and 1.3-cm]) and fittings to support gas connections to the primary and auxiliary burners will be completed in early January.

Pilot-Scale Slagging Furnace

The pilot-scale slagging furnace design is intended to be as fuel-flexible as possible, with maximum furnace exit temperatures of 2700 to 2900 F (1483 to 1593C) in order to maintain desired slag flow. It will have a nominal firing rate of 2.5 million Btu/hr (2.6 x 10^6 kJ/hr) and a range of 2.0 to 3.0 million Btu/hr (2.1 to 3.2 x 10^6 kJ/hr) using a single burner. The design is based on a bituminous coal (Illinois No. 6 - 11,100 Btu/lb or 25,800 kJ/kg) and a nominal furnace residence time of 3.4 sec. Resulting flue gas flow rates will range from roughly 425 to 640 scfm (12 to 18 m^3/min), with a nominal value of 530 scfm (15 m^3/min) based on 20% excess air. Firing a subbituminous coal or lignite will increase the flue gas volume, decreasing residence time to roughly 2.7 sec. However, the high volatility of the low-rank fuels will result in high combustion efficiency (>99%). The EERC will orient the furnace vertically (downfired) and has based the burner design on a swirl burner currently used on two EERC pilot-scale pulverized coal (pc)-fired units that are fired at 600,000 Btu/hr (633,000 kJ/hr). Slagging furnace dimensions will be 47-in. (119-cm) inside diameter (ID) by roughly 18 ft (5.5 m) in length. Exhibit 2.2-9 illustrates the furnace, slag tap/pot, slag screen, dilution/quench zone, CAH section, and cooling air preheaters.

The vertically oriented furnace shell has been designed to include four distinct furnace sections that, when bolted together, make up the pilot-scale slagging furnace. The top section of the furnace will support the primary burner connection and is shown in the photographs in Exhibit 2.2-18. The top section of the furnace was installed in November and then removed in December in preparation of refractory-pouring activities. The RAH panels will be located in the upper-middle furnace section (on the opposite wall) shown in the Exhibit 2.2-12 photograph. The lower middle furnace section will support the auxiliary gas burner; the bottom section of the furnace includes the furnace exit to the slag screen as well as the slag tap opening. Exhibit 2.2-13 is a photograph of the two lower sections of the furnace showing the auxiliary burner flange connection, several sight ports, slag screen, slag tap, and the top of the slag pot.

Construction materials for the furnace shell were mostly carbon steel. The only exceptions were the flanged pipe connections for the primary and auxiliary burners and the sight ports, since their refractory protection will be limited. The primary burner piping connection to the furnace is 8-in. (20-cm) Schedule 40 stainless steel material (shown in Exhibit 2.2-11). The auxiliary burner piping connection to the furnace is 3.5-in. (8.9-cm) Schedule 40 stainless steel material, which can be seen in Exhibit 2.2-13.

Temperature measurement in the furnace is extremely important. Furnace exit temperature will be measured using a minimum of two methods. Methods to characterize the furnace during shakedown will include Type S thermocouples, an optical method, and a high-velocity thermocouple (HVT). A minimum of four additional thermocouple locations has been designated for the furnace interior in the final design. Temperature measurements at the interface between the high-density and intermediate refractory layers are planned, as well as between the intermediate and insulating refractory layers. Thermocouple data will be automatically logged into the data acquisition system. A pressure transmitter and gauges will be used to monitor static pressures in order to monitor furnace performance. These data will be automatically logged into the data acquisition system and recorded manually on data sheets on a periodic basis, as backup.

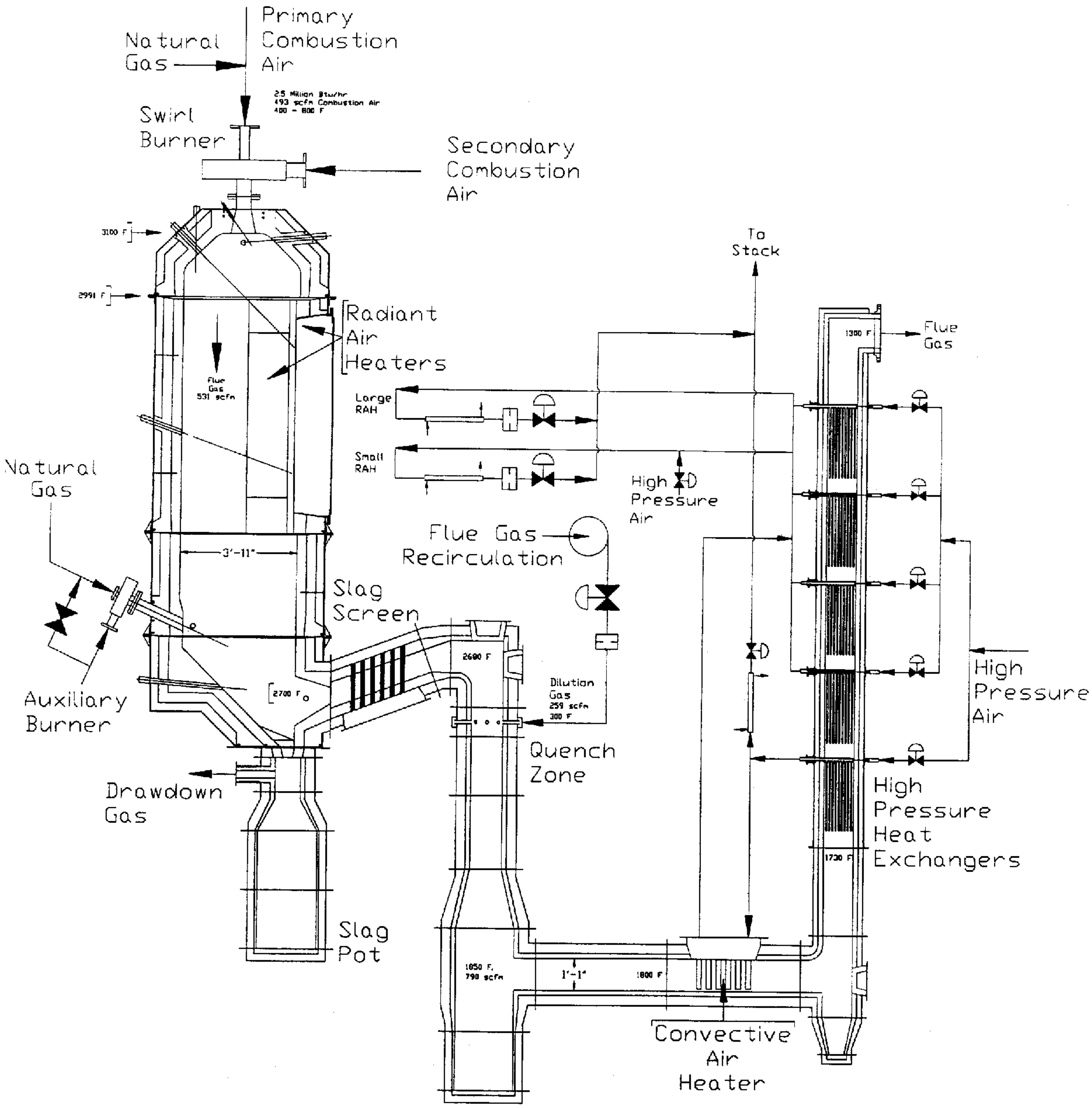

Exhibit 2.2-10
Combustion 2000 Slagging Furnace And Refractory Components

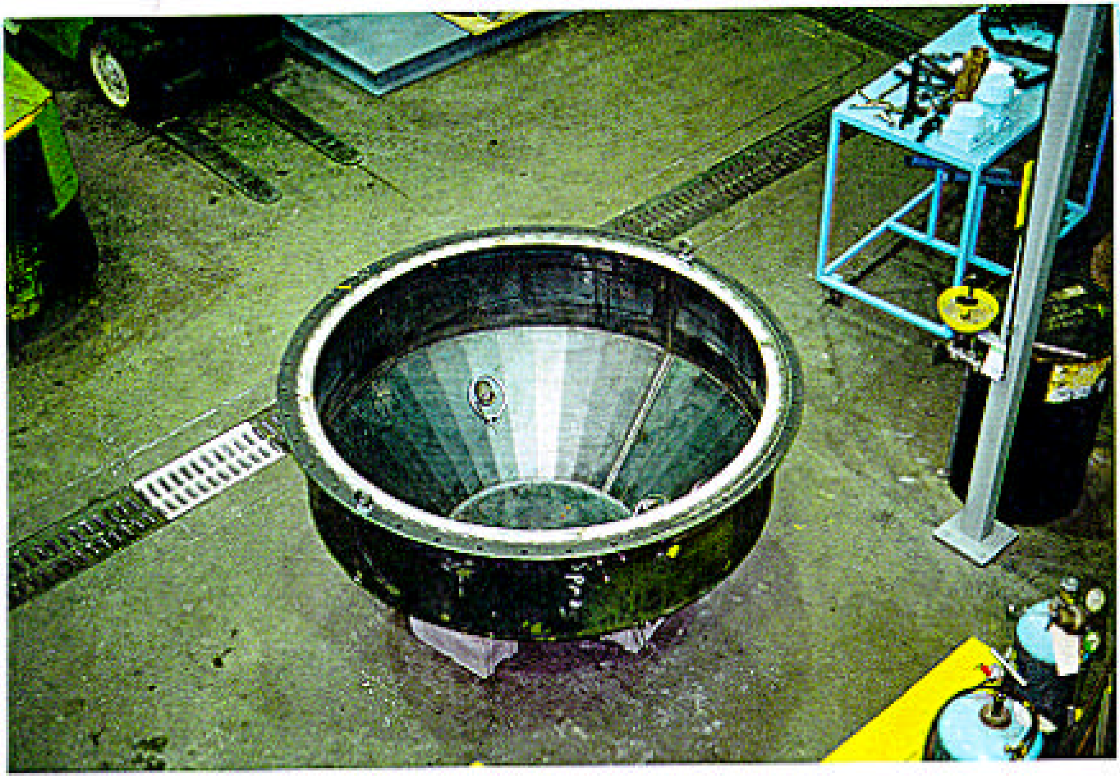

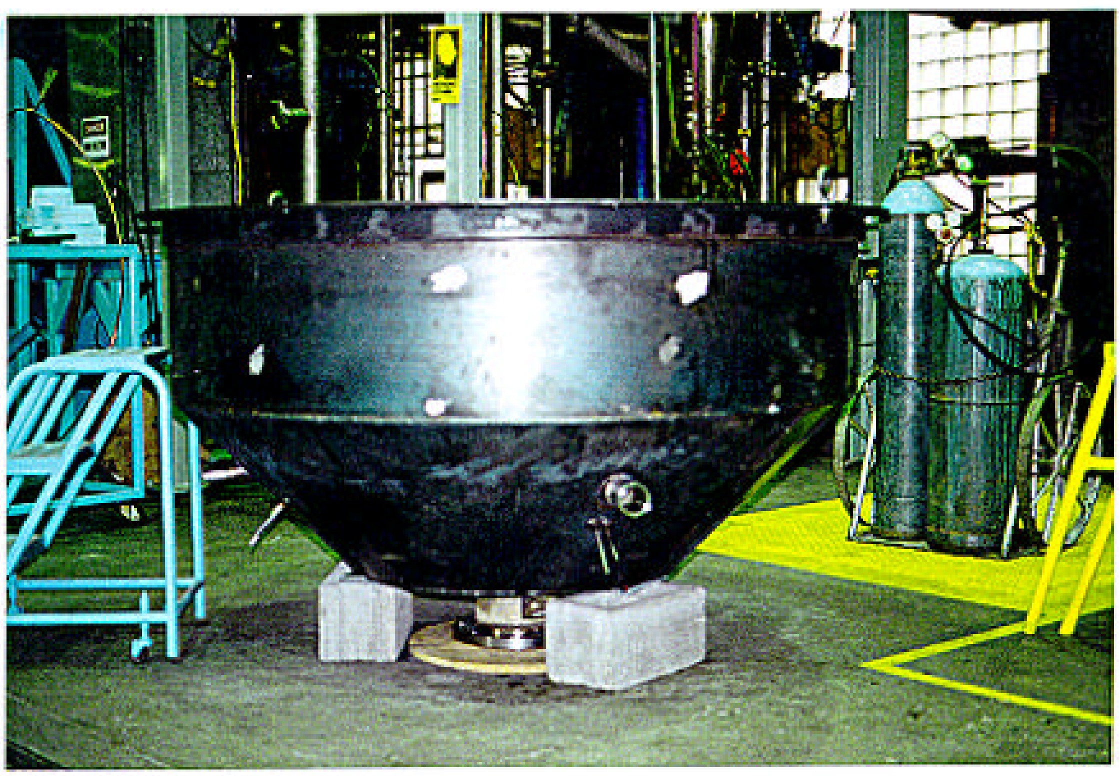

Exhibit 2.2-11
Photographs Of Furnace Top Inverted In Preparation For Refractory Pouring

Exhibit 2.2-12
Photograph Of Upper-Middle Furnace Section Located On The Third Floor Of The High Bay

Exhibit 2.2-13
Photographs Of The Two Lower Furnace Sections, Slag Screen,
Slag Tap, And Top Of Slag Pot Located On The Second Floor Of The High Bay

Observation ports were located in the furnace to permit visual observation of the primary burner flame, auxiliary burner flame, RAH panels, slag screen, and slag tap. With the exception of the furnace exit (inlet to the slag screen), there are no plans at this time to include additional sampling ports in the furnace walls. However, in order to adequately characterize the furnace during shakedown, and since RAH test panels will not necessarily be available for all furnace operating periods, the first set of doors built for the RAH panel locations will have ports to permit the insertion of temperature and heat flux measurement probes.

The slag tap is intended to be as simple and functional as possible. To that end, the current slag tap design is a simple refractory-lined hole in the bottom of the furnace. The diameter of the slag tap will be 4 in. (10 cm) initially, with the potential to reduce the diameter to 2 in. (5 cm) by simply repouring refractory. To minimize heat losses associated with the slag tap, slag will be collected in an uncooled, dry container with refractory walls. A design feature of the slag tap will involve drawing a small amount of flue gas through the slag tap to maintain temperature and promote slag flow. The exact flow rate of the drawdown gas required will be determined during system shakedown, but will be <10% of the total flue gas flow rate. The drawdown gas temperature will be reduced using indirect cooling, and the gas will reenter the system upstream of the baghouse. Alternative slag tap design options were also considered. The most complicated option would involve the use of water-cooled hearth plates with a slag tap burner originally designed for use on a 1-ton/hr slagging gasifier. However, the EERC believes that the combination of the auxiliary gas burner near the furnace exit and the drawdown gas option will result in effective slag tap operation.

The slag pot will consist of several refractory-lined modular components. Two of these modular components are shown hanging from the bottom of the furnace in the background of the photograph in Exhibit 2.2-14. The refractory in the slag pot will consist of two layers: 1.5 in. (3.8 cm) of high-density material and 2.5 in. (6.4 cm) of insulating refractory. The high-density refractory is intended to be sacrificial when slag samples are collected for analysis and maintenance performed after a test. The actual size of the slag pot will be 2-ft (0.6-m) ID and allow for a variable length (3 to 9 ft/0.9 to 2.7 m) with the installation of as many as four spool piece sections. Depending on the frequency and duration of system operation, it may be necessary to have two complete slag pots. The use of a single slag pot for a week of operation is desirable.

Construction materials for the slag pot shell are carbon steel. The only exception is the flanged pipe connection for the drawdown gas, because its refractory protection will be limited. The drawdown gas piping connection to the slag pot is 6-in. (15-cm) Schedule 10 stainless steel material. An observation port was installed in the slag pot to permit visual evaluation of slag tap performance. The key to its value will be proper location and the ability to keep it clean.

Temperature measurement in the slag pot near the slag tap may be useful as an indicator of slag tap performance. Therefore, a thermocouple will be located in the top section of the slag pot opposite the drawdown gas exit. Thermocouple data will be automatically logged into the data acquisition system. A pressure indicator will be used to monitor static pressure in the same location in order to monitor slag tap performance. These data will be recorded manually on data sheets on a periodic basis.

Exhibit 2.2-14
Photograph Showing Furnace Slag Pot Shell Sections In The Background And The CAH Shell Sections In The Foreground

Combustion air preheat capabilities will range from 300 to 800F (149 to 427C). The EERC intends to make use of two tube-and-shell heat exchangers operated in series to recover heat from the flue gas to preheat combustion air. However, it may also be necessary to include an electric air preheater to achieve desired flexibility with respect to combustion air temperature control. The need for an electric air preheater will be based on performance data developed during system shakedown.

The refractory walls in the slagging furnace will consist of three castable refractory layers: 4 in. (10.2 cm) of high-density (14 Btu-in./ft^2-F-hr or 2.0 W/m-K) slag-resistant material; 4 in. (10.2 cm) of an intermediate refractory (4.0 Btu-in./ ft^2-F -hr or 0.6 W/m-K); and 3.25 in. (8.3 cm) of a low-density insulating refractory (1.3 Btu-in./ ft^2-F -hr or 0.2 W/m-K). Three refractory layers will be necessary to avoid overheating the low-density insulating refractory. Selection of the high-density, intermediate, and insulating refractories has been made. Refractory selection and approach to installation were summarized in October. Exhibit 2.2-15 summarizes refractory properties, and Exhibit 2.2-16 illustrates refractory layout for the slagging furnace. Refractory procurement began in December and will be completed in January. Refractory forms were fabricated and installed in the top furnace section in December, and the insulating refractory layer will be poured in early January.

Exhibit 2.2-17 summarizes the volumetric flow rate and temperature data upon which the furnace design was based. This table has been recently updated from previous submissions to reflect minor changes resulting from design modifications and revised calculations. Detailed fabrication drawings for the furnace and slag pot shells were completed in June 1996. Fabrication drawings were completed in July followed by the release of a materials list and drawings for some limited vendor fabrication and material estimates. Vendor estimates were reviewed in August, and a purchase order was issued for the materials and limited fabrication activities. Final delivery of the furnace and slag pot materials and fabricated components was anticipated in late September. Although some materials were delivered and the EERC initiated furnace fabrication, most of the furnace and slag pot materials were not delivered until the first week of October. Furnace and slag pot shell fabrication was completed in October, except for structural support components and various wall penetrations. The furnace was installed in the high bay in November and most furnace penetrations were completed in December. Fabrication drawings will be updated, with penetrations added for thermocouples, pressure taps, and sight ports. These updated drawings will be submitted to UTRC for information purposes when completed.

Exhibit 2.2-15
Refractory Properties

Refractory	Plicast Cement Free 96	Narco Cast 60	Plicast LWI-28	Plicast LWI-20	Harbison-Walker 26
Function	High-density	High-density	Insulating	Insulating	Insulating
Density, lb/ft^3	186	145	80	55	66
K, Btu-in./hr-(ft^2)-EF @ 2000EF	14.0	6.5	4.0	NA[1]	2.2
K, Btu-in./hr-(ft^2)-EF @ 1500EF	14.2	6.0	3.0	1.7	1.9
K, Btu-in./hr-(ft^2)-EF @ 1000EF	15.0	5.6	2.7	1.3	1.7
Hot MOR[2] @ 2500EF, psi	1400	NA	NA	NA	NA
Hot MOR[2] @ 1500EF, psi	2000	1000	250	100	110
Cold Crush Strength @ 1500EF, psi	10,000	NA	750	400	350
Typical Chemical Analysis, wt% (calcined)					
Al_2O_3	95.3	62.2	54.2	39.6	53.8
SiO_2	3.8	28.0	36.3	31.5	36.3
Fe_2O_3	0.1	1.0	0.8	5.4	0.5
TiO_2	0.0	1.7	0.5	1.5	0.6
CaO	0.1	2.8	5.7	19.5	7.2
MgO	0.0	0.1	0.2	0.8	0.2
Alkalies	0.2	0.2	1.5	1.4	1.4

[1] Not applicable.

[2] Modulus of rupture.

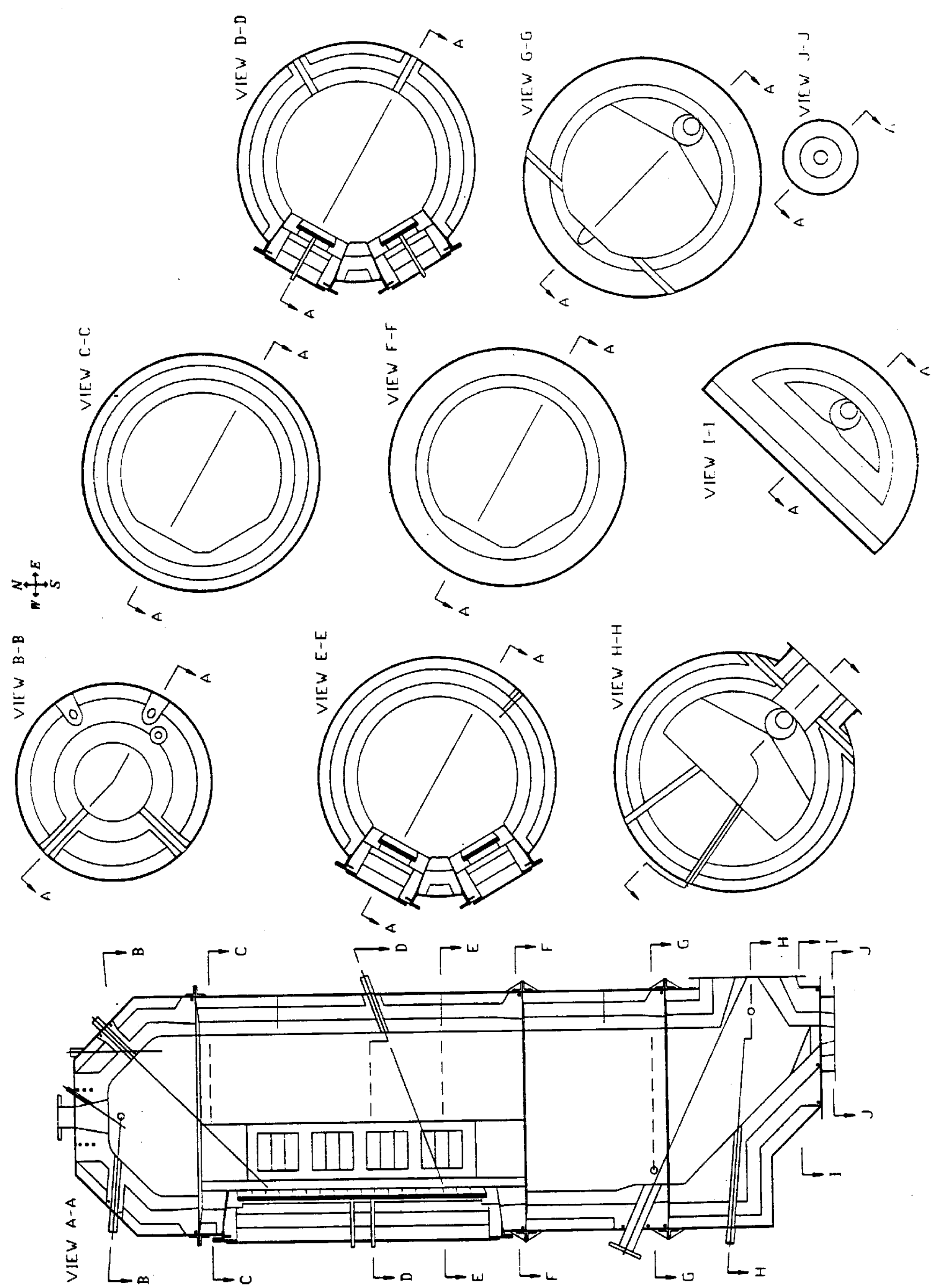

Exhibit 2.2-16
Cross-Sectional Views Of The Furnace Refractory Layout

Exhibit 2.2-17
Flow and Heat-Transfer Calculations for Combustion 2000 Slagging Furnace and Refractory Ducts

Illinois No. 6 Bituminous

Furnace			Furnace		
Furnace ID, in.	47	47	Furnace ID, in.	47	47
Firing Rate, MMBtu/hr	2.5	3.0	Firing Rate, MMBtu/hr	2.50	3.0
Coal Feed Rate, lb/hr	225	270			
Air Flow Rate, scfm	493	592	Slag Screen Inlet		
Flue Gas Flow Rate, scfm	531	638	Gas Temp., °F	2700	2900
Flue Gas Flow Rate, acfm	3431	4245	Flue Gas Flow Rate, acfm	3227	4122
Furnace Gas Velocity, ft/s	4.7	5.9	Gas Velocity, ft/s	59.6	76.1
Exit Gas Velocity, ft/s	29.8	38.1			
Flue Gas Residence Time, s	3.4	2.7	Dilution Gas Requirements		
			Gas Velocity in, ft/s	57.5	73.4
Auxiliary Burner, MMBtu/hr	0.095	0.217	Exit Gas Temp., °F	1860	1860
Wall Losses, MMBtu/hr	0.195	0.199	Dilution Gas Temp., ∞F	300	300
Other Losses, MMBtu/hr	0.200	0.200	Calc. Dilution Gas, scfm	286	425
			Total Flue Gas Flow, scfm	817	1063
Furnace Sect. Length, ft	16	16	Flue Gas Flow Rate out, acfm	3645	4743
Refract. 1 Thickness, in.	4	4	Gas Velocity out, ft/s	33.6	43.8
Refract. 2 Thickness, in.	4	4			
Refract. 3 Thickness, in.	3.25	3.25	Dilution Gas Nozzles		
Furnace Weight, tons	14.4	14.4	Nozzle Diameter, in.	1.25	1.25
			No. of Nozzles	8	8
Inlet Gas Temp., ∞F	3100	3100	Dilution Gas Flow, acfm	418	621
Avg. Gas Temp., ∞F	2900	3000	Dilution Gas Velocity, ft/s	102	152
Exit Gas Temp., ∞F	2700	2900			
Refract. 1 Surf. Temp., ∞F	2580	2781	Convective Air Heater		
Refract. 2 Surf. Temp., ∞F	2358	2542	Gas Temp., ∞F	1800	1800
Refract. 3 Surf. Temp., ∞F	1692	1821	Flue Gas Flow Rate, acfm	3553	4619
Furnace Skin Temp., ∞F	245	258	Gas Velocity, ft/s	50.5	65.6

Assumption: Excess air is 20%.

Primary and Auxiliary Burners

The primary burner will be natural gas- and coal-capable, with coal particle size assumed to be a standard utility grind, 70% - 200 mesh (70% - 75 µm). Burner development and testing are not objectives within the EERC's scope of work. However, some burner turndown is desirable and has been factored into the burner design. Flame stability will be assessed by observing the flame and its relation to the burner wall as a function of secondary air swirl and operating conditions at full load and under turndown conditions. The basic burner design is an International Flame Research Foundation (IFRF)-type adjustable secondary air swirl generator. An IFRF-type adjustable secondary air swirl generator uses primary and secondary air at approximately 15% and 85% of the total air, respectively, to adjust swirl between 0 and a maximum of 1.9.

"Swirl" is defined as the ratio of the radial (tangential) momentum to axial momentum imparted to the secondary air by movable blocks internal to the burner and is used to set up an internal recirculation zone (IRZ) within the flame that allows greater mixing of combustion air and coal. Swirl is imparted by moving blocks to set up alternate paths of radial flow and tangential flow, creating a spin on the secondary air stream that increases the turbulence in the near-burner zone. At the fully open position of the swirl block, the secondary air passes through the swirl burner unaffected, and the momentum of this stream has only an axial component (the air enters the combustion chamber as a jet). As the angle of the blocks changes, the air begins to spin or swirl, and the radial component to the momentum is established, creating the IRZ in the near-burner region. It is the ratio of this radial component of the momentum to the axial component that establishes the quantity defined as swirl.

The adjustable swirl burners currently used by the EERC consist of two annular plates and two series of interlocking wedge-shaped blocks, each attached to one of the plates. The two sets of blocks can form alternate radial and tangential flow channels, such that the air flow splits into an equal number of radial and tangential streams, which combine farther downstream into one swirling flow. By a simple rotation of the movable plate, radial channels are progressively closed and tangential channels opened, so that the resulting flux of angular momentum increases continuously between zero and a maximum value. This maximum swirl depends on the total air flow rate and the geometry of the swirl generator.

Secondary air swirl is used to stabilize the flame. In the absence of swirl, loss of flame may result, increasing the risk of a dust explosion. As swirl is applied to the combustion air, coal particles are entrained in the IRZ, increasing the heating rate of the particles, leading to increased release of volatiles and char combustion. The flame becomes more compact and intense as swirl is increased to an optimum level, which is characterized in existing EERC pilot-scale test facilities as the point at which the flame makes contact with the burner wall. Increasing swirl beyond this level can pull the flame into the burner region, unnecessarily exposing metal burner components to the intense heat of the flame and possible combustion in the coal pipe.

Increasing swirl to provide flame stability and increased carbon conversion can also affect the formation of NOx. The high flame temperatures and increased coal-air mixing associated with increased swirl create an ideal situation under which NOx may form. In full-scale burners with adjustable vanes, swirl is often increased to reach the optimum condition and then decreased slightly to reduce the production of NOx. Although NOx emissions are of interest, their control is not a key objective for the pilot-scale slagging furnace. Therefore, burner operational settings will be based on achieving desired furnace exit temperatures and slag conditions in the furnace. Flame stability under turndown conditions will be characterized by firing the primary burner at reduced load (typically 66% to 85% of the full load rate), maintaining the same primary air flow and adjusting the secondary air flow to meet excess air requirements.

The primary burner design is simply a scaled-up version of the two existing burners based on increased combustion air volumetric flow rates. Materials of construction for the primary burner are entirely stainless steel because of the combustion air (up to 800EF/427EC) temperature ranges to which it will be exposed. Combustion air flow rates through the primary burner will range from about 400 to 600 scfm (11 to 17 m^3/min) depending on furnace firing rate and the fuel type (bituminous, subbituminous, or lignite) fired. Exhibit 2.2-18 is a photograph of the completed burner, excluding the primary air gun/coal pipe.

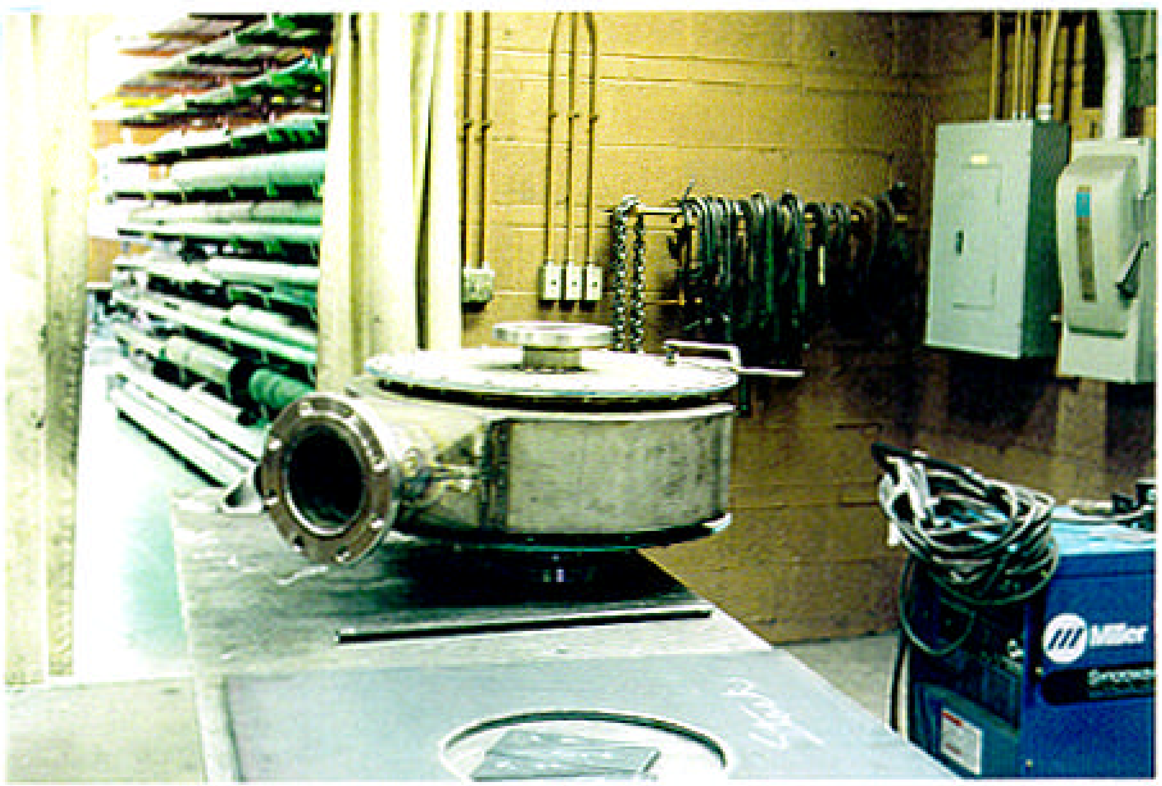

Exhibit 2.2-18
Photograph Of Primary Burner

An auxiliary gas burner (500,000 Btu/hr or 527,000 kJ/hr) will be located in the area of the furnace exit in order to ensure desired slag flow from the furnace and the slag screen. This auxiliary burner will compensate for heat losses through the furnace walls, sight-ports, and RAH test panels. The use of the auxiliary gas burner will be beneficial during start-up to reduce heatup time and to prevent the freezing of slag on the slag screen when initially switching to coal firing. The auxiliary gas burner will be fired near stoichiometric conditions to avoid high excess air levels in the system. The EERC anticipates that the auxiliary gas burner will be fired at relatively low rates (<200,000 Btu/hr or 211,000 kJ/hr) once the furnace reaches thermal equilibrium. Materials of construction for the auxiliary burner are also entirely stainless steel. Exhibit 2.2-19 is a photograph of the completed burner, excluding the primary air gun/coal pipe.

Exhibit 2.2-19
Photograph Of Auxiliary Burner

Inlet combustion air piping to the primary burner will include insulated 6-in. (15-cm) Schedule 5 stainless steel for the secondary air and 1-, 2-, and 4-in. (2.5-, 5-, and 10-cm) Schedule 40 stainless steel for the primary air/coal feed line. The primary burner piping connection to the furnace is 8-in. (20-cm) Schedule 40 material. For the auxiliary burner, inlet combustion air piping sizes will be 1- to 2-in. (2.5- to 5-cm) Schedule 5 and 40 material. The auxiliary burner piping connection to the furnace is 3.5-in. (9-cm) Schedule 40 material.

Thermocouples will be installed to monitor inlet combustion air temperatures for each burner. Thermocouple data will be automatically logged into the data acquisition system. Pressure transmitters and gauges will be used to monitor static and differential pressures in order to monitor burner performance and measure combustion air flow rate. These data will be automatically logged into the data acquisition system, and flow control valves will be used to adjust and maintain desired combustion air flow rates. As a backup, burner data will be recorded manually on data sheets on a periodic basis. During system shakedown, burner performance at full load and reduced load conditions will be evaluated and documented.

Cleaning and maintenance of the burners are expected to be minimal. However, when necessary, burner maintenance will be accomplished by unbolting the flanged connections between the burner and the furnace and secondary and primary air lines. When the top of the slagging furnace is removed to inspect the interior, it will be necessary to first disconnect the combustion air and fuel feed lines and remove the primary burner.

Material procurement for the burners is complete, and fabrication is essentially complete. Burner fabrication was completed in September 1996, except for the primary air guns/coal pipes. These short, flanged sections of straight pipe will be cut to the appropriate length and installed once the refractory-lined furnace has been assembled and final measurements have been made.

Radiant Air Heater Panels

A key furnace design feature will be accessibility for installation and testing of one large RAH panel and one small panel. The furnace design will accept one large RAH panel with a maximum active size of 1 x 6 ft (0.3 x 1.8 m). This size was selected to minimize furnace heat losses and based on panel manufacturing constraints identified by UTRC. Flame impingement on the RAH panels is not necessarily a problem. Cooling air for the large RAH panel will be provided by an existing EERC air compressor system having a maximum delivery rate of 510 scfm (14.4 m^3/min) and a maximum stable delivery pressure of 275 psig (19 bar). Backup cooling air is available from a smaller compressor at a maximum delivery rate of 300 scfm (8.5 m^3/min) and pressure of <100 psig (<7 bar). A tie-in to an existing nitrogen system is also planned as a backup to the existing air compressor system. It will be necessary to heat the cooling air to achieve the 1300F (705C) radiant panel cooling air inlet temperature desired. Outlet cooling air temperatures from the large RAH panel will not be allowed to exceed 1800F (982C) and will generally be controlled at roughly 1700F (927C) by adjusting cooling air flow rate using flow control valves. Cooling air pressure for the large radiant panel will be roughly 150 psig (10.3 bar). Based on recent EERC and UTRC heat-transfer calculations, the cooling air flow rate necessary to cool the large RAH panel will be 200 scfm (5.7 m^3/min). The EERC anticipates using flue gas heat exchange (cooling air preheater) and possibly electrical heating to meet heated cooling air temperature requirements for the large RAH. The advantage of a combination of heat sources for the cooling airstream at this scale is greater flexibility and range of control. Illustrations of the RAH panels were presented in a previous section of this report. Proper insulation and thermocouple location will be required to minimize and document edge effects, respectively, as well as adequately define surface temperature distributions, total heat absorption, and local heat flux.

Furnace design will also permit the installation of one 5- x 1-ft (1.5- x 0.3-m) RAH panel. Cooling air for the small RAH panel will be provided by the EERC air compressor system. Backup cooling air is available from a smaller compressor at a maximum delivery rate of 300 scfm

(8.5 m^3/min) and pressure of <100 psig (<7 bar) and from the existing nitrogen system. Cooling air temperature at the inlet of the small RAH panel will be lower than for the large panel, about 1000F (538C). At this time, the operating pressure of the cooling air system for the small RAH panel is assumed to be 150 psig (10.3 bar), with a maximum flow rate of 100 scfm (2.8 m^3/min). Heated cooling air for the small RAH panel will be supplied from a common 1- and 0.5-in. (2.5- and 1.3-cm) pipe header connected to the outlets of cooling air preheaters No. 2-5 and to the outlet of the CAH supplied by cooling air preheater No. 1. The required amount of unheated pressurized air will be combined with the heated air from the header to allow the exit temperature from the small RAH panel to be controlled to either a specified temperature of up to 1700F (927C) or to an air temperature differential of 600F (333C) across the small RAH panel. Again, actual outlet cooling air temperatures will be controlled as a function of cooling air flow rate using flow control valves. Proper insulation and thermocouple location will be required to minimize and document edge effects, respectively.

Slag Screen

The slag screen design for the pilot-scale slagging furnace system is the result of a cooperative effort between EERC, UTRC, and PSI personnel. The primary objective for the pilot-scale slag screen is to affect the size distribution of ash particles entering the CAH. The design is intended to result in an ash particle-size distribution comparable to that expected in the commercial plant. Other design criteria specific to the pilot-scale slag screen include:

1. a simple design permitting modifications if necessary using readily available, inexpensive materials;
2. matching duct dimensions and flue gas flow rates to maintain turbulent flow conditions;
3. minimizing the potential for plugging as the result of slag deposit growth on tube surfaces or the sloped floor;
4. limiting differential pressure across the slag screen to 2 in. W.C. (4 mm Hg); and
5. limiting heat losses to assure desired slag flow from the slag screen to the furnace slag tap.

Exhibit 2.2-9 illustrates the slag screen and its relationship to the slagging furnace and dilution/quench zone.

The pilot-scale slagging furnace design (based on Illinois No. 6 bituminous coal) anticipates a nominal furnace firing rate of 2.5 million Btu/hr (2.64 x 10^6 kJ/hr) to achieve a furnace flue gas exit temperature/slag screen inlet temperature of 2700F (1483C). The resulting slag screen flue gas approach velocity will be nominally 60 ft/s (18.3 m/s). Increasing the furnace firing rate to 3 million Btu/hr (3.16 x 10^6 kJ/hr) will result in a nominal slag screen flue gas inlet temperature of 2900F (1594C) and an approach velocity of 76 ft/s (23.2 m/s). The flue gas outlet temperature from the slag screen must be >2500F (>1371C) to minimize the potential for slag freezing in the slag screen.

The slag screen will consist of six rows of three 1.5-in. (3.8-cm)-diameter vertical tubes mounted in an upwardly sloped duct (20^o) to facilitate slag flow from the slag screen into the furnace slag tap. The center line-to-center line tube spacing in each row is 3.75 in. (9.5 cm).

Center line-to-center line spacing between individual rows is 4 in. (10.2 cm). Internal duct dimensions for the slag screen will be 10 in. x 13 in. x 3.5 ft (25 cm x 33 cm x 1.1 m). The resulting flue gas velocity through the slag screen will be roughly 91 ft/s (28 m/s). EERC personnel have recommended the use of uncooled high-alumina-content tube material for the slag screen to minimize heat loss and avoid slag freezing in the last few rows of tubes. Apart from the material selected, each tube will be vented in some manner to prevent internal pressure increases upon the heating of trapped air in the tubes and to allow thermal equilibrium between the interior and exterior of the tubes. Also, the tube wall should be a minimum of 0.25 in. (0.64 cm) thick. Promoting thermal equilibrium between the flue gas and interior of the tubes will facilitate the use of Type S thermocouples (one each) in the first and last row of tubes to monitor slag screen temperature without exposing the thermocouples to the slag. Thermocouple data will be automatically logged on the data acquisition system. Pressure taps will be installed in the roof upstream and downstream of the tubes to monitor and record slag screen differential pressure. As a backup to the data acquisition system, slag screen data will be recorded manually on data sheets on a periodic basis.

Routine on-line cleaning of the slag screen is not anticipated to be a requirement. However, two sight ports will be installed in the vertical sidewalls of the slag screen to permit visual observation and the use of an air lance for periodic cleaning if necessary. Placement of sight ports in the walls of the slag screen is a heat loss and materials concern. Therefore, the actual size of the sight ports in the wall of the slag screen will be initially limited to 1 in. (2.5 cm). If heat loss or material problems are identified during shakedown tests, the 1-in. (2.5-cm) holes can be easily plugged with refractory. Sight ports located in the furnace exit and at the inlet of the dilution/quench zone, will permit visual observation of the inlet and outlet of the slag screen. Two additional ports in the furnace exit along with the sight ports in the dilution/quench zone inlet provide access for flue gas sampling around the slag screen. Each of these sight/sample ports is 2.3-in. (5.8-cm) ID. Continuous flue gas sampling is planned between the slag screen and the dilution/quench zone to monitor and control slagging furnace operation.

The refractory component of the slag screen will consist of two refractory layers. The inner high-density layer will be a Plicast Cement Free 96 with an outer insulating layer of Harbison-Walker Castable 26. The high-density refractory will be 2.25 in. (5.7 cm) thick in the sidewalls and 4 in. (10.2 cm) thick in the roof and floor of the slag screen. The insulating refractory will be 4 in. (10.2 cm) thick in the sidewalls, roof, and floor. Properties for the high-density and insulating refractories selected for use in the slag screen are summarized in Exhibit 2.2-15. Exhibit 2.2-20 presents a plan and elevation views of the slag screen showing critical tube and refractory dimensions.

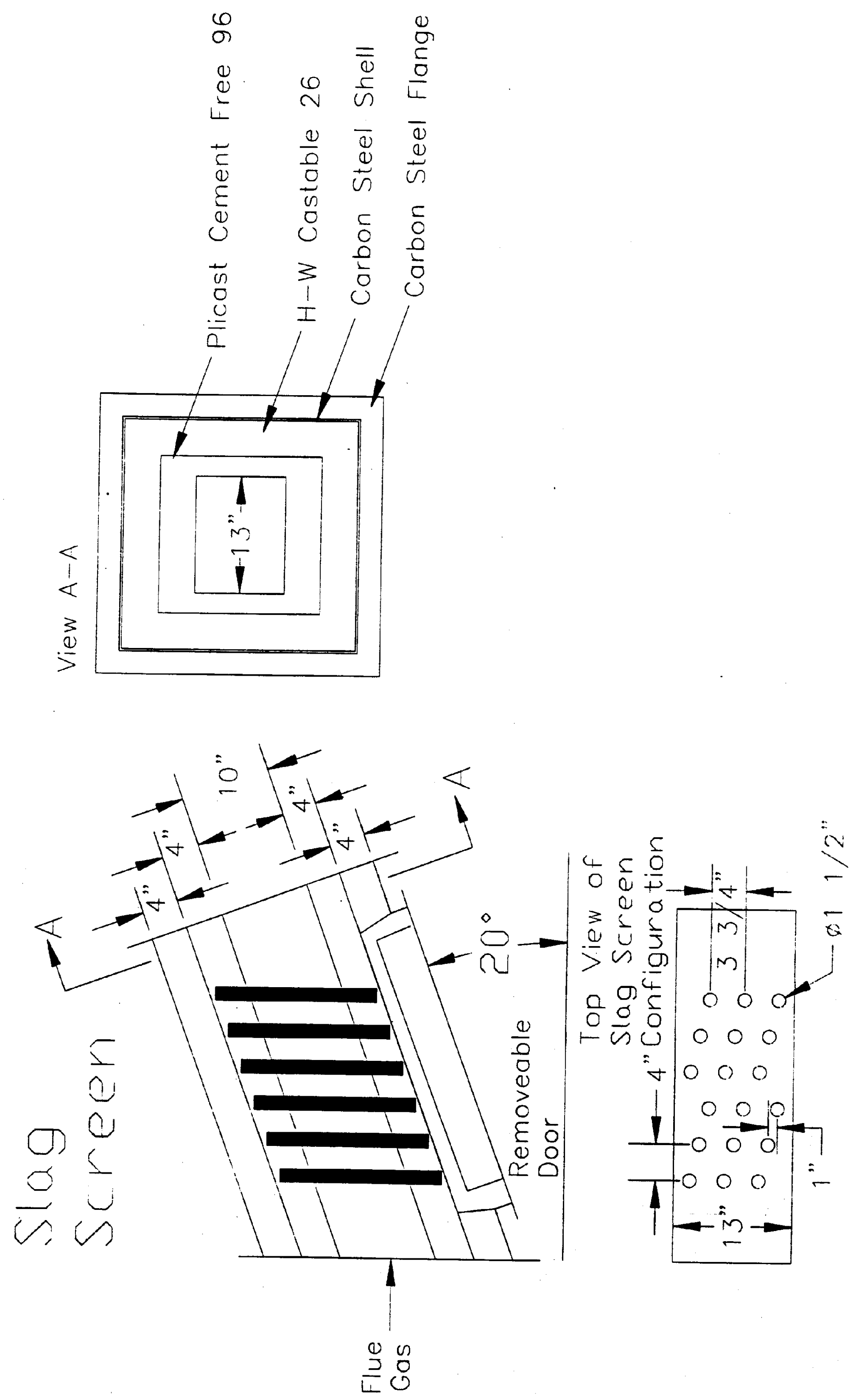

Exhibit 2.2-20
Plan And Elevation Views Of Slag Screen

The construction material for the slag screen shell is carbon steel. The final design package for the slag screen was completed in September and submitted to UTRC and PSI for review and comment. Fabrication was completed in November 1996 and the slag screen was bolted to the furnace exit as shown in Exhibit 2.2-21. The only open question at this time is the material selection for the slag screen tubes. Material selection for slag screen tubes was discussed briefly with UTRC personnel during the November 26, 1996, videoconference. UTRC was planning to discuss these issues with PSI personnel in December in order to finalize material selection and procurement of the slag screen tubes.

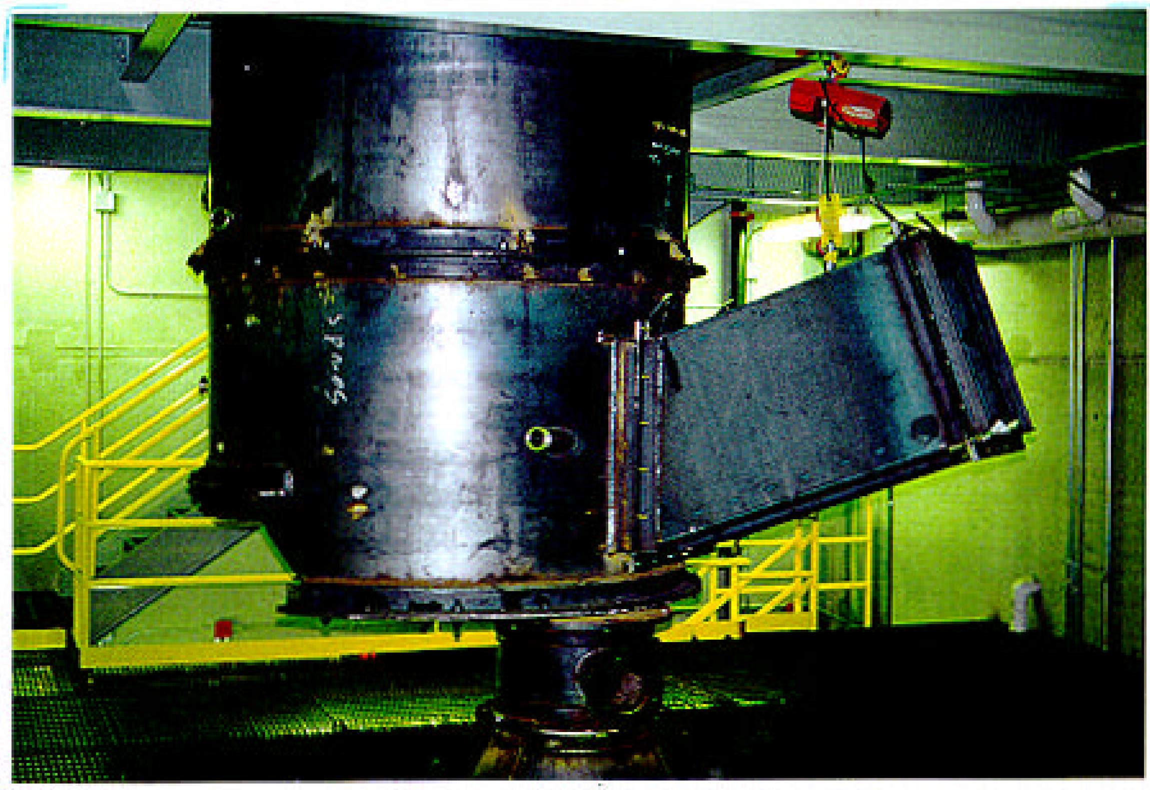

Exhibit 2.2-21
Photograph Of Slag Screen Bolted To Furnace Exit

Dilution/Quench Zone

The circular dilution/quench zone is oriented vertically, maintains a 1.17-ft (0.36-m) diameter in the area of the flue gas recirculation nozzles, and then expands the duct diameter to 2 ft (0.6 m) to provide adequate residence time within duct length constraints. The duct section containing the flue gas recirculation nozzles is a spool piece in order to accommodate potential changes to the size, number, and orientation of the flue gas recirculation nozzles. The vertically oriented dilution/quench zone will be refractory-lined (high-density and insulating refractory) and located immediately downstream of the slag screen. Flue gas recirculation will be used to cool the flue gas in the dilution/quench zone and freeze entrained slag particles. A centrifugal-type flue gas recirculation fan will remove flue gas from the system immediately downstream of the induced-draft fan. The 4-in. (10.2-cm) stainless steel piping transporting the dilution gas will be insulated to avoid condensation problems. Dilution gas will be injected into the dilution/quench zone through eight 1.25-in. (3.18-cm) nozzles at a total flow rate of 286 to 425 scfm (8.1 to 12.0 m3/min), depending on furnace firing rate. The design assumes a dilution gas temperature of 300F (149C) and a flue gas exit temperature of 1850F (1010C) from the dilution/quench zone. A flow control valve will be used to control the flue gas recirculation rate to achieve the desired flue gas exit temperature from the dilution/quench zone.

The evaluation of selective noncatalytic reduction (SNCR) to limit NOx emissions is not a priority at this scale. Therefore, no consideration was given to SNCR evaluation in finalizing the design of the dilution/quench zone. However, ports will be located in the dilution/quench zone to permit the addition of NH_3 or other additives as desired. Flue gas-sampling ports will be located in and downstream of the dilution/quench zone. These options were requested by PSI to permit evaluation of new measurement techniques for NOx, NH_3, and other species in the dilution/quench zone. Fabrication drawings for the dilution/quench zone were completed in October, material procurement was completed in November, and fabrication was initiated in December and will be completed in early January. In the Exhibit 2.2-8 photograph, the top sections of the dilution/quench zone can be seen bolted to the slag screen on the second floor. In the foreground of the photograph, the support section of the dilution/quench zone containing the exit to the CAH can be seen sitting on sawhorses.

Convective Air Heater

The CAH design has been a cooperative effort between the EERC and UTRC. The flue gas flow rate to the CAH tube bank will be 3553 to 4619 acfm at 1800E F (101 to 131 m^3/min at 982C). A rectangular inside duct dimension of 1.17 ft^2 (0.11 m^2) should result in a flue gas approach velocity of 50 to 66 ft/s (15 to 20 m/s) to the CAH. Based on recent discussions, the CAH will consist of three rows of 2-in. (5-cm)-diameter tubes installed in a staggered array. Tube spacing will be a minimum of 4 in. (10.2 cm) on center, with an overall CAH tube bank dimension of 14 in. x 12 in. x 20 in. (36 cm x 30 cm x 51 cm). Primary and backup cooling air for the CAH will be provided by the same EERC air compressor system described for the RAH panels. Cooling air heating and flow rate control will be necessary to achieve the 700F (371C) minimum/1000F (538C) maximum inlet cooling air temperature desired, effectively controlling surface temperatures, and provide for an inside heat-transfer coefficient similar to the commercial design. At this time, the CAH cooling air flow rate and operating pressure is expected to be 100 scfm (2.8 m^3/min) and 150 psig (10.3 bar), respectively. The EERC plans to recover heat from the flue gas to meet heated cooling air temperature requirements for the CAH. The cooling air exit temperature from the CAH is expected to be 1200F (649C) based on UTRC design calculations and will not be permitted to exceed 1300F (705C). Cooling air flow rate will be used to control cooling air exit temperature using a bypass flow control valve.

Observation ports are planned for the CAH section. The number and location of the observation ports will depend on the CAH tube bank design developed by UTRC. In addition, ports for inserting air lances for intermittent manual cleaning of the CAH tube bank will be included. Again, the number and location of these ports will depend on the final CAH tube bank design. Critical measurements relative to the CAH will include accurate surface temperatures, cooling air temperatures, cooling air flow rates, and pressure. CAH testing to evaluate heat-transfer performance is a high priority, requiring extensive instrumentation to monitor performance adequately. An important secondary priority is length of material life in relation to operating conditions and ash deposition. Fabrication drawings for the CAH shell sections were completed and approved in November. Material procurement for and fabrication of the CAH shell were completed in December. Installation of the CAH shell will be completed in early January. The photographs in Exhibit 2.2-22 show the three shell sections comprising the CAH. The top photograph shows the two horizontal sections of the CAH and the bottom photograph shows the transition section between the CAH and the cooling air preheaters.

Cooling Air Preheaters

Design activities for the cooling air preheaters, which will support operation of the RAH panels and CAH tube bank, were essentially completed in September 1996. Because of flue gas temperatures (1700F or 927C) in the vicinity of the first three cooling air preheaters, EERC personnel reviewed material options for fabricating the tube bundles and the inlet cooling air piping to the RAH test panels. These components will be operated at a nominal air pressure of 150 psig (10.3 bar). Stainless steel was ruled out for the first three cooling air preheaters. An alloy capable of handling higher-temperature operation was a better choice to maximize system flexibility and minimize the potential for material failure. Material options considered included a Haynes HR-120, HR-160, HA-230, and HA-556 and an RA253MA. Maximum temperatures for these five alloys at 150 psig (10.3 bar) are 1600, 1750, 1650, 1750, and 1650F (871, 955, 899, 955, and 899C), respectively. Based on material characteristics, availability, and cost, EERC personnel elected to use the RA253MA (1650F at 150 psig or 899C at 10.3 bar) material for all five tube bundles exposed to flue gas and the HR-160 (1750F at 150 psig or 955C at 10.3 bar) material to transfer the heated cooling air to the RAH and CAH test sections. This combination of materials will maximize system flexibility and minimize cost. Use of the HR-160 alloy will permit the installation of electrical heaters in the future to increase the temperature of the cooling air entering these test sections as desired. Because of reduced flue gas temperature, the fourth and fifth cooling air preheaters supporting operation of the RAH panels could be fabricated using stainless steel. However, because of an RA253MA minimum purchase requirement, all five tube bundles will be fabricated using this material.

Fabrication drawings for the cooling air preheaters were completed in October, with material procurement and shell fabrication completed in November 1996. However, the 0.5-in. (1.3-cm) RA253MA pipe for the tube bundles is not expected to be delivered until mid-January 1997. Recent work on the cooling air preheaters focused on evaluating design modifications to accommodate the heated cooling air requirements for the small RAH panel, completing flanged connections for the tube bundles, and preparing coupons for welding certifications. Installation of the cooling air shell sections in the high bay began in December and will be completed in early January to verify fit and complete final connections to the CAH section and tube-and-shell heat exchangers. Once final fitting and connections have been completed, the cooling air preheater shell sections will be removed from the high bay in preparation for pouring refractory. Exhibit 2.2-23 is a photograph of the cooling air preheater shell sections being installed adjacent to the tube-and-shell heat exchangers.

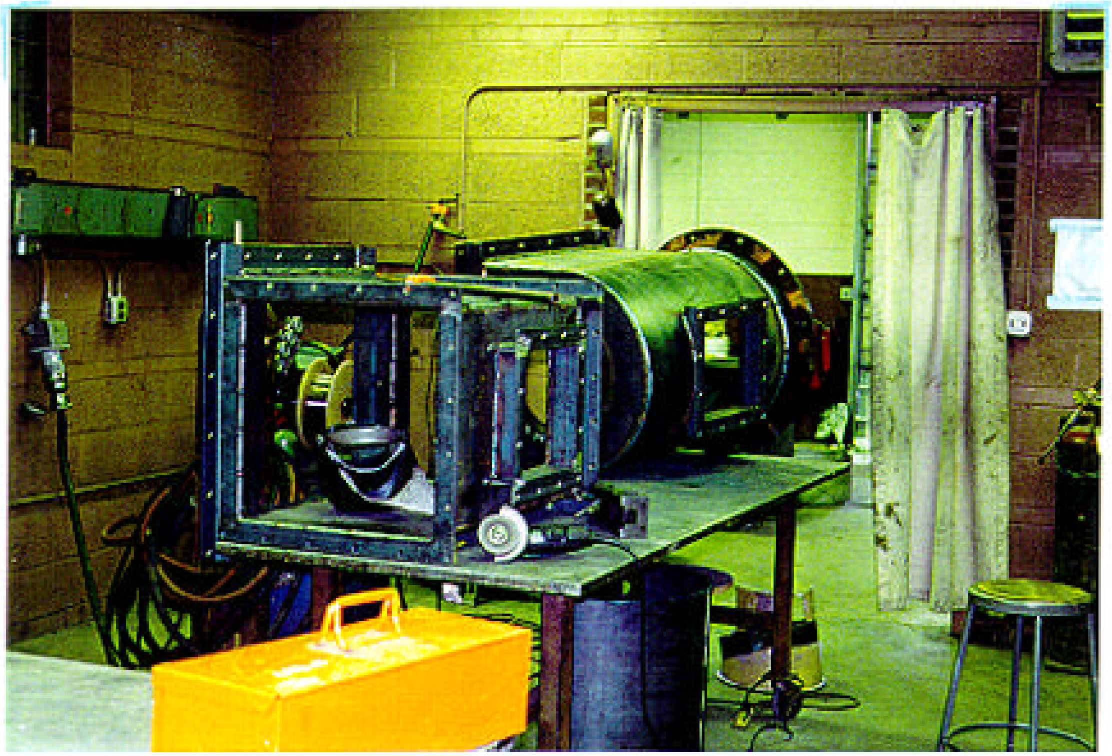

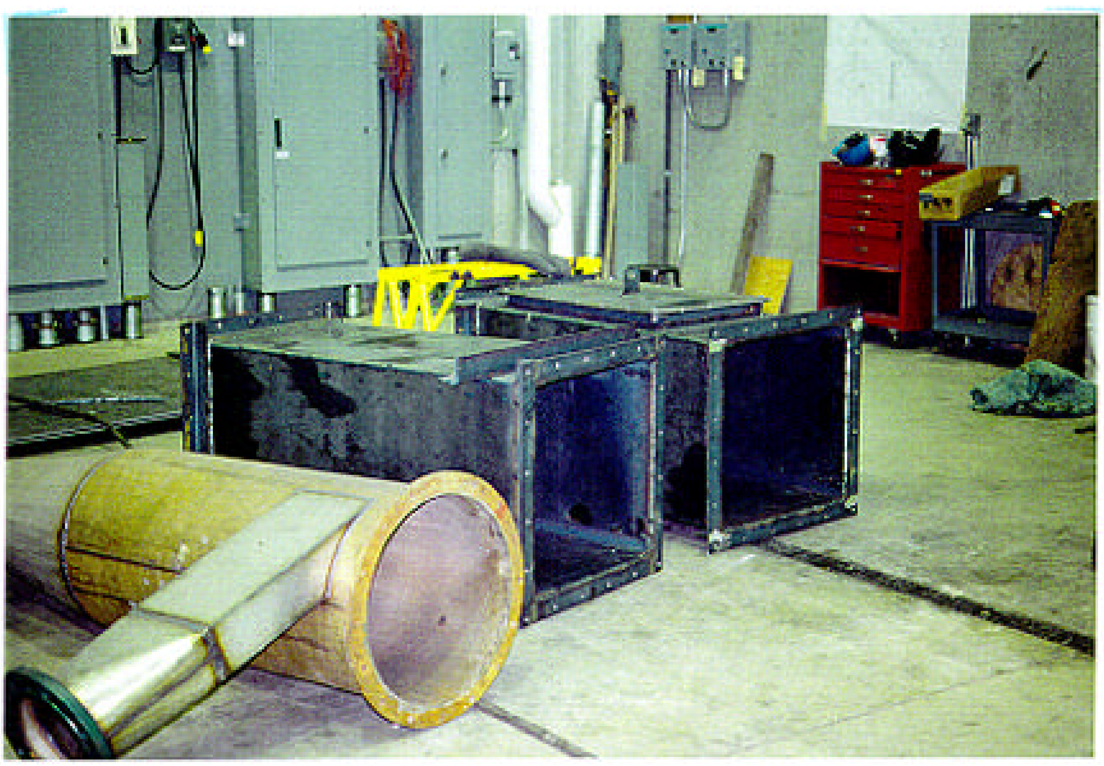

Exhibit 2.2-22
Photographs Showing The Three Rectangular Sections Of The CAH

Exhibit 2.2-23
Photograph Showing Cooling Air Preheat Shell Sections Being Installed Adjacent To Tube-And-Shell Heat Exchangers

Tube-and-Shell Heat Exchangers

The pilot-scale slagging furnace system will include four tube-and-shell heat exchangers for heat recovery and flue gas temperature control. Their location in the overall process layout is illustrated in Exhibit 2.2-16. The first two heat exchangers will reduce flue gas temperature and preheat the secondary air for the primary burner. The third and fourth heat exchangers will be used to control flue gas temperature at the inlet of the baghouse. Materials of construction for the heat exchangers are a combination of 304 stainless steel and carbon steel. Fabrication of the tube-and-shell heat exchangers was completed in August 1996. Installation of the tube-and-shell heat exchangers began in September and was completed in October. Heat exchanger insulation was completed in November, with installation of flue gas piping between the tube-and-shell heat exchangers and the baghouse initiated in December. Flue gas piping installation should be completed in January. Other future activities related to the tube-and-shell heat exchangers include completing cooling air piping connections and installation of thermocouples and static/differential pressure measurement devices. Exhibits 2.2-1, -16, and -17 are photographs showing the installed heat exchangers and some of the completed piping connections.

Exhibit 2.2 -24
Photograph Of Installed/Insulated Tube-And-Shell Heat Exchangers

System Fans

The pilot-scale slagging furnace system will require four fans, a combustion air forced-draft fan, a cooling air forced-draft fan, an induced-draft fan, and a flue gas recirculation fan. All four fans will be centrifugal type fans with variable-speed drives (speed controllers). The combustion air forced-draft blower will supply ambient air to tube-and-shell heat exchangers No. 1 and 2, plus combustion air to the auxiliary swirl burner. A portion of the heated air exiting the heat exchangers will be used as secondary combustion air to the primary swirl burner, with the rest exiting the system through the stack. Valves will be used to control the air flow to the primary and auxiliary swirl burners.

The cooling air blower will supply ambient air to tube-and-shell heat exchangers No. 3 and 4, providing final cooling of the flue gas before it enters the baghouse. The heated air exiting the heat exchangers will go directly to the stack. An electronic speed controller on the fan will adjust the air flow from 0 to 1200 scfm (0 to 34 m^3/min) to maintain a desired flue gas temperature exiting the heat exchangers. This approach will permit the baghouse to be operated at either cold-side (350F/177C) or hot-side (650F/344C) conditions.

Flue gas exiting the baghouse will be drawn through the induced-draft blower and out to the stack. The blower speed will be regulated with an electronic speed controller to maintain a zero-pressure balance point near the exit of the slagging furnace. Hot flue gas (nominally 350F/177C) from the induced-draft fan exit will be drawn through the recirculation blower for use as dilution gas in the dilution/quench zone. An electronic speed controller on the blower motor will regulate the gas flow to maintain the desired flue gas temperature at the exit of the dilution/quench zone.

Exhibit 2.2-25 summarizes the fan specifications. The EERC has solicited vendor recommendations. Subsequent to reviewing final vendor recommendations, the EERC issued a bid package concerning the four system fans, containing flow rate, operating temperature, and discharge pressure requirements. Based on the bids received from four prospective vendors, a purchase order was issued to Winger Associates, representing American Fan Company, for all four system fans in late August 1996. Two of the fans arrived in November and two arrived in late December. As of this report, installation of two fans has been completed, and installation of the other two will be completed in early January 1997, followed by piping and electrical connections. Exhibit 2.2-26 presents photographs showing the two forced-draft fans and the system induced-draft fan sitting on the sixth floor of the high bay and the flue gas recirculation fan sitting on its shipping pallet.

Preparation of bid packages for process control and other valves was completed in September 1996, and the bid packages were issued to potential vendors in early October. Vendor selection and the issuing of purchase orders was completed in November. As of the this report, all but a few miscellaneous valves have been delivered.

Exhibit 2.2-25
Pressure, Temperature, and Flow Specifications for Combustion 2000 Blowers

	Inlet Pressure, psig	Exit Pressure, psig	Avg. Inlet Temp., °F	Min. Inlet Temp., ∞F	Max. Inlet Temp., ∞F	Max. Inlet Flow, scfm	Max. Inlet Flow, acfm	Avg. Inlet Flow, acfm	Motor Horsepower Range
Forced-Draft Blower	0	3	60	-20	100	1200	1292	1200	25-40
Cooling Air Blower	0	1.5	60	-20	100	1200	1292	1200	15-20
Induced-Draft Blower	-1	0.5	350	250	450	1200	2255	1755	25-30
Flue Gas Recirculation Blower	0	1.5	350	250	450	450	788	701	10-15

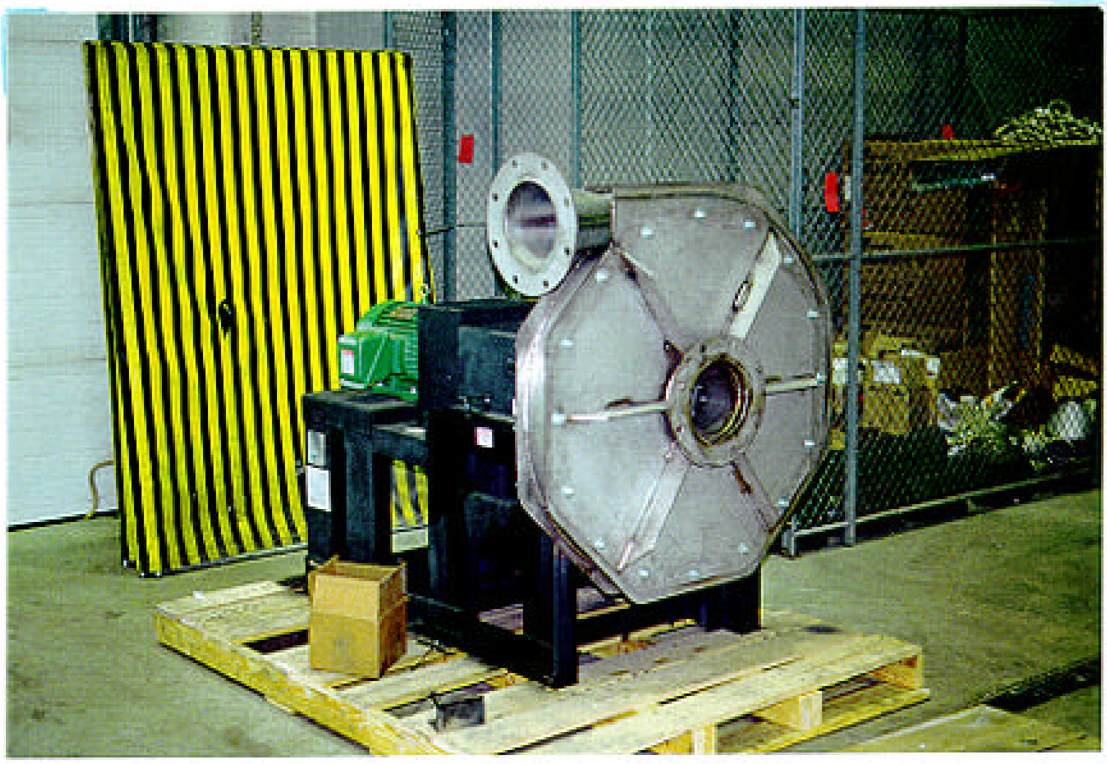

Exhibit 2.2-26
Photographs of system fans

Emissions Control

A pulse-jet baghouse will be used for final particulate control on the pilot-scale slagging furnace system. The intent is that the baghouse design will permit operation at both cold-side(250 to 400F/121 to 205C) and hot-side (600 to 700F/316 to 371C) temperatures. The primary baghouse chamber and ash hopper walls are electrically heated and insulated to provide adequate temperature control to minimize heat loss and avoid condensation problems on start-up and shutdown. Inlet and outlet piping and the clean air plenum will be insulated. Because of the planned operating conditions, materials of construction are primarily 304L stainless steel. The main baghouse chamber was designed with internal angle iron supports to handle a negative static pressure of 15 in. W.C. (28 mm Hg).

Flue gas flow rates to the baghouse are expected to range from a low of 630 scfm (17.8 m^3/min) (980 acfm [27.8 m^3/min]) at 350F [177C], based on a furnace firing rate of 2 million Btu/hr [2.1 x 106 kJ/hr]) to a maximum of 1063 scfm (30.1 m^3/min) (2371 acfm [67.1 m^3/min] at 700F [371C]), based on a furnace firing rate of 3 million Btu/hr [3.16 x 106 kJ/hr]). Therefore, the baghouse design is based on an average flue gas flow rate of 850 scfm (24.1 m^3/min) (1325 acfm [37.5 m^3/min] at 350F [177C] or 1900 acfm [53.8 m^3/min] at 700F [371C], based on a nominal furnace firing rate of 2.5 million Btu/hr [2.64 x 106 kJ/hr]). The baghouse is sized to accommodate a maximum of 36 bags mounted on wire cages with 2-in. (5.1-cm) bag spacing. Bag dimensions will be nominally 6 in. (15.2 cm) in diameter by 10 ft (3.0 m) in length, providing a total filtration area of 565 ft^2 (52.5 m^2). Arranging the bags in six rows of six bags each allows the number of bags on-line to be changed by installing different tube sheets. For example, when the baghouse is operated at 350F [177C] and 850 scfm (24.1 m^3/min) (1325 acfm [37.5 m^3/min]), only 24 bags will be required to achieve a filter face velocity of 3.5 ft/min (1.1 m/min). If all 36 bags were installed, the filter face velocity would be roughly 2.3 ft/min (0.7 m/min). In the event that the baghouse is operated at a hot-side condition (1900 acfm [53.8 m^3/min] at 700F [371C]), 30 bags would result in a filter face velocity of 4 ft/min (1.2 m/min), and 36 bags would decrease the face velocity to 3.4 ft/min (1.0 m/min). At a maximum potential flow rate of 2371 acfm (67.1 m^3/min) (1063 scfm [30.1 m^3/min]) at 700F [371C]), 36 bags would result in a filter face velocity of 4.2 ft/min (1.3 m/min).

Initially only one tube sheet will be constructed, permitting the installation of 36 bags (565 ft^2 [52.5 m^2] of filtration area) arranged in a six-by-six array. Installing the maximum number of bags will permit the overall system to be evaluated over the broadest potential range of operating conditions during shakedown while minimizing the potential impact of the baghouse on overall system performance. Each filter bag will be secured to the tube sheet using a snap band sewn into the top cuff. Stainless steel wire cages with 20 vertical wires and 6-in. (15.2-cm) ring spacing will provide bag support. The pulse-jet baghouse will be a single compartment capable of either on- or off-line cleaning. Flue gas will enter the baghouse in an area just below the bottom of the cage-supported bags and above the ash hopper. Access to the filter bags and stainless steel wire cages will be gained by removing the clean air plenum at the top of the baghouse. The baghouse ash hopper will be supported at the fourth level (roughly 40-foot [12.2-m] elevation), providing access to the clean air plenum on the fifth level to facilitate installation, inspection, and removal of filter bags and cages.

Low-watt-density heat cable made for conductive surfaces was installed to preheat the surface of the baghouse chamber to prevent moisture condensation during start-up and to minimize baghouse heat losses over the operating range of interest (350F to 700F [177C to 371C]); heat cable was run vertically on each of the four baghouse walls spaced on 6-in. (15.2-cm) centers. The individual elements will be wired in parallel to minimize the impact of single-element failures. The baghouse ash hopper is heated in a similar manner. Five temperature controllers will be used to control electrical resistance heating on the pulse-jet baghouse.

Pulse-jet cleaning will be triggered as a function of baghouse differential pressure or as a function of time. The baghouse pulse-jet cleaning system will be operated/controlled by a program written for the Genesis data acquisition software that permits adjustment of cleaning frequency and pulse duration. Timers written into the program will be used to set pulse duration and off time, while total baghouse operating time and test time in hours and total and test cleaning cycles will be documented by the data acquisition system. Filter bag cleaning will occur when the program opens the solenoid-operated valves between the pulse-air reservoir and the six pulse-air manifold lines. Each manifold line will provide pulse air to six filter bags. Six filter bags will be cleaned simultaneously, with a short delay between each set of filter bags to allow air pressure to recover in the pulse-air reservoir.

Air for bag cleaning will be provided by the same existing EERC air compressor system that will be supporting the RAH and CAH test sections. High-pressure/low-volume and low-pressure/high-volume cleaning options are included in the design of the pulse-air system. In order to operate at a low-pressure/high-volume condition, a pulse volume of 0.03 ft^3/ft^2 (0.009 m^3/m^2) of fabric surface, or roughly 0.5 ft^3 (0.01 m^3)/bag, will be necessary at a pulse-air reservoir pressure of <40 psig (<3 bar). The pulse volume for each set of six bags would be 3 ft^3 (0.08 m^3). For a high-pressure/low-volume case, 0.01 to 0.02 ft^3/ft^2 (0.003 to 0.006 m^3/m^2) of fabric surface is common, and the pulse-air reservoir pressure will be 40 to 100 psig (3 to 7 bar). Therefore, a maximum pulse volume of 1.9 ft^3 (0.05 m^3) will be required to clean one set of six bags. The required pulse duration to achieve a desired pulse-air volume as a function of pulse pressure will be determined during system shakedown. Assembly of the pulse-air manifold and installation of compressed air piping to the pulse-air reservoir were completed in November.

Flue gas sample ports will be installed in the inlet and outlet piping of the baghouse to permit flue gas flow rate measurements and sampling for gaseous/vapor-phase constituents as well as fly ash. Specific routine measurements to be made will include flue gas oxygen, sulfur dioxide, and nitrogen oxide concentrations using on-line instruments. Fly ash particle-size distribution and mass loading will be determined periodically using standard U.S. Environmental Protection Agency (EPA) methods. Hazardous air pollutants (HAPs) will be measured on a limited basis using EPA Method 29. Sight ports (4 in. [10.2 cm] OD) are located at two elevations in the baghouse to permit inspection of bag surfaces on the dirty side and two locations in the clean air plenum to permit visual inspection of the tube sheet surface and the exit of several bags.

Thermocouples will be installed in the inlet and outlet piping, as well as at four locations along the length of the baghouse chamber. Differential pressure across the chamber and static pressure at the outlet of the chamber will be monitored continuously with pressure transducers.

Gauges will also be used to visually monitor baghouse differential and static pressure at the main combustor control panel. Baghouse thermocouple and pressure transducer data will be automatically logged on the data acquisition system. As a backup, baghouse data will be recorded manually on data sheets on a periodic basis.

Baghouse ash removal will be accomplished by opening a 6-in. (15.2-cm) knife valve at the bottom of the hopper, allowing ash material to drain through a 6-in. (15.2-cm) stainless steel pipe into a 55-gallon (208-liter) drum on the main floor level. The photographs in Exhibits 2.2-1, --8, and -17 show the baghouse ash removal line and valves. Ash containers of this size facilitate handling and are adequate for ash accumulation during 100-hr and longer test periods, with only periodic replacement required.

Procurement activities are essentially complete for the baghouse. The baghouse was installed, insulated, and covered with galvanized sheet metal in September 1996. Bags and cages were ordered in October. The bags were delivered in late October, but were found to have an oversized snap band and were returned to the vendor for modification. The fit of a modified sample bag was verified in late December and the modified bags and cages are expected in January. Installation of the baghouse inlet and outlet valves was completed in December, with the bypass valve installation expected in early January as flue gas piping installation progresses. Remaining activities related to the baghouse include completing flue gas piping installation and insulation, installation of flue gas sample ports, and installation of thermocouples and static/differential pressure measurement devices.

The EERC is not planning to install a sulfur dioxide control system. Initial dispersion modeling data developed by the North Dakota State Department of Health indicate that sulfur dioxide emissions would have to be limited to 16 lb/hr (7.2 kg/hr) to avoid exceeding the ambient standard. Based on a 2.5-million Btu/hr (2.64 x 10^6 kJ/hr) coal-firing rate, the EERC is not concerned about the potential 16-lb/hr (7.2-kg/hr) sulfur dioxide limit or the need for a sulfur dioxide control system. Recent conversations with the North Dakota State Department of Health have confirmed that the dilution effect of the system cooling air that will be exhausted through the stack will permit a 23-lb/hr (10.4-kg/hr) sulfur dioxide emission rate.

Instrumentation and Data Acquisition

The instrumentation and data acquisition components for the pilot-scale slagging furnace system will address combustion air, flue gas, cooling air, cooling water, and other appropriate measurements (temperatures, static and differential pressures, and flow rates). Flue gas will be monitored for oxygen, sulfur dioxide, carbon monoxide, carbon dioxide, and total nitrogen species (nitric oxide and nitrogen dioxide) on a continuous basis at the furnace exit. A set of existing gas analyzers for oxygen, sulfur dioxide, and nitrogen species will be available to monitor a second system location simultaneously. Surface temperature measurements are anticipated for the RAH panels and CAH tube bank. In addition, heat flux measurements for the furnace, RAH panels, and CAH section have been recommended. Orifice plates and venturis (monitored with pressure transducers and gauges on the main combustor control panel) will be installed at various points in the system to measure combustion air flow rate, flue gas flow rate, flue gas recirculation rate, and cooling air flow rates.

The data acquisition system will be based on a Genesis software package and two personal computers. This type of data acquisition system is currently used at the EERC on a number of pilot-scale combustion and gasification process systems. All process data points will be logged on the data acquisition system. However, the EERC is uncertain at this time of how much integrated system control will be required or desired. Final decisions concerning the level of integrated control implemented will be made based on system performance during shakedown and relative cost. Detailed P&IDs and an instrumentation list were submitted to UTRC for review and approval in July 1996. Following UTRC approval, EERC initiated procurement of system instrumentation and components for the data acquisition system in August.

Specific items ordered and received to date include one of two computers to handle process control and data acquisition, the data acquisition software and hardware packages, an uninterruptable power supply, a pulse-air programmable logic controller for the baghouse, K-type and S-type thermocouples, the pressure transmitters, pressure gauges, flowmeters for cold high-pressure cooling air, some of the control valves and flow measurement devices, miscellaneous tubing and fittings, and rotometers for air, water, and natural gas. Items ordered but not yet received include a second computer, some of the control valves and flow measurement devices, and a few pressure relief valves. The balance of items to be ordered related to instrumentation/process control include a few cooling air control valves and flow measurement devices and some miscellaneous items. During a November 26, 1996, videoconference, UTRC and the EERC agreed that a high-temperature optical pyrometer and a high-temperature videocamera system were desirable components for the pilot-scale slagging furnace system. UTRC agreed to discuss the selection and procurement of these items with PSI personnel. Procurement of flue gas instrumentation and components for process control and data acquisition is expected to continue through February 1997.

HITAF Air Heater Materials

Ceramic Materials

The fused cast materials available from Glass Refractory Products (GRP) for the RAH hot wall liner have been down-selected to 3 types of compositions, which will be further modified to meet all of the requirements, including high resistance to slag corrosion, high thermal conductivity, stable thermomechanical properties to temperatures at least up to 1427°C (2600°F), and resistance to mechanical and thermal shock. These compositions include high alumina (Al_20_3); alumina-magnesia, including spinel ($MgAl_20_4$); and chromia-alumina or chromia-magnesia-alumina. Each of the compositions meet different combinations of the above requirements; but none meet all of the requirements. Therefore, an optimized combination of these compositions is being developed currently with the manufacturers of these refractories.

The current Monofrax L (spinel) is the material selected for initial testing in the UNDEERC RAH demonstrator planned for May, since it has excellent refractoriness and thermal conductivity, and should be a good material to test the heat transfer characteristics of the RAH design. However, its resistance to coal slag corrosion is limited; and in order to greatly increase its resistance to slag attack, chromia additions to the composition will be necessary. The

Monofrax M (high alumina) also has high thermal conductivity, but has poor resistance to slag attack.

GRP is now using their own IR&D funds to develop an optimized composition, which is based on various combinations of three compositions: Monofrax L, Monofrax M, and Monofrax K-3 or E (high chromia-alumina), plus some small additions of other oxides. Equally important, however, is the melting and casting of these compositions into small molds [457 mm x 229 mm x 102 mm (18" x 9" x 4")], compared to the production molds which often are as large as [1829 mm x 1219 mm x 610 m (6' x 4' x 2')], where the solidification kinetics are vastly different.

During this reporting period, GRP has cast Monofrax L, K-3, and E into the small molds, and has sent these materials to UTRC for characterizing their properties, including macro- and microstructure, flexural strength of Monofrax L [to 1538°C (2800°F)], emissivity, and slag resistance. The data will be used to fill in the baseline properties not yet available, and also will be used to compare these properties with those of the new, modified compositions that are to be cast in the experimental facility at GRP in January.

Machined blocks of Monofrax L [330 mm x 152-178 mm x 73 mm (13" x 6-7" x 2 7/8") from the thermal conductivity tests at the Orton Foundation] have been further sliced into sections and then cut into flexure test specimens. Exhibit 2.2-27 shows the cutting diagram of slices taken from one of the Monofrax L blocks. Both thick [15.9 mm (5/8")] and thin [6.4 mm (1/4")] slices are being used to prepare flexural specimens that will have different orientations of the grain structure. The purpose of this characterization study is to evaluate the effects of the internal structure of the cast material (examine grain growth and morphology during solidification, document the location of porosity and voids, and other features) on the flexural properties of the material.

An additional sample of the Monofrax L material, which was recently cast into a 457 mm x 229 mm x 102 mm mold, is also being machined into flexure bars in order to determine the statistical variation of the strength of the cast material and the Weibull modulus.

Another chromia-magnesia composition from Corhart is also being considered for the RAH lining.. The material is designated C104, and has attractive thermal conductivity of approximately 6 W/mºK at 1093ºC. The material may need some additional process development to overcome some wormhole casting defects, however its high chromia content should provide good corrosion resistance and high emissivity.

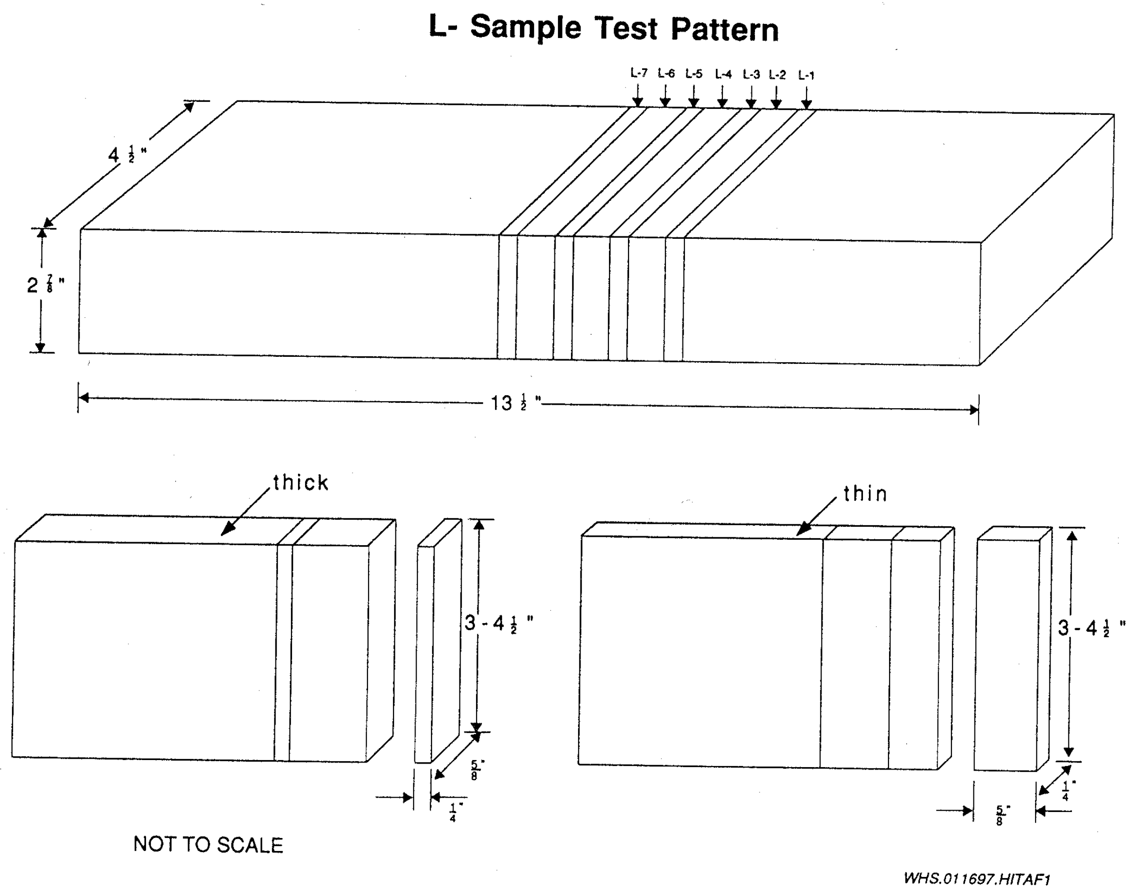

Exhibit 2.2-27
Cutting Pattern for Flexural Test Specimens Taken from Thick [15.8 Mm (5/8")] and Thin[6.4 mm (1/4")] Slices of Monofrax L

Ash Dipping Exposure Testing

Also during the reporting period, a preliminary series of ash dipping exposure tests was completed. This test, which involves dipping a group of refractory samples in molten slag, then pulling them above the surface and allowing the slag to run off (refractory sample kept hot at all times). The dipping/run-off sequence is repeated every 460 seconds (7.67 minutes). This interval was determined by observing the amount of time needed for the slag to finish dripping from the sample surface. In this manner, the erosive, as well as corrosive, effects can be determined in a relatively low amount of technician monitoring.

Breakage of the support rod systems and some thermal shock induced cracking of the fusion cast chromia-alumina crucibles were encountered, thus no results were reported in the previous quarterly report. By switching to sapphire support rods, and slowing down the heating and cooling cycles, some successful tests were run. One each of Monofrax K-3, Monofrax E, and Jargal M were run simultaneously for approximately 50 hours at 1440ºC (2630ºF), whereupon the sapphire rod broke in the vicinity of the Monofrax E sample, due to interfacial corrosion of some type. The Jargal M refractory had clearly become thinner due to corrosion.

During the reporting period, new crucibles were purchased, and an upgrade to the ash dipping furnace power supply were performed. During the coming quarter, more detailed analysis of the samples tested for 50 hours, as well as longer duration tests of the baseline, and "improved composition" materials.

Coatings for RAH Refractories

Coatings will be required on the backside, and potentially the fire side, of the Monofrax L being employed in the first trials of the 2 MM Btu/hr rig at UNDEERC. The coatings are being used to enhance emissivity and radiant heat transfer on the backside (tube side) of the bricks, and potentially to provide some limited corrosion resistance on the fire side of the refractory. In the full scale RAH, coatings may still be required to enhance emissivity and improve heat transfer. During the reporting period, coatings produced by jet vapor deposition, painting, flame spraying and plasma spraying. The last two techniques, plasma and flame spraying, were chosen for initial laboratory trials, for application to the first combustor trial at UNDEERC.

The marriage of ceramics by either plasma or flame spray is state gas turbine technology. High temperature ceramics such as chromia and alumina are married to the zirconia ceramics employed as thermal barrier coatings in advanced gas turbine engines. During the next reporting period, flame sprayed chrome oxide (Norton Rockide C) and plasma sprayed chromia-alumina coatings will be applied to samples of Monofrax M and Monofrax L. The samples will undergo thermal cycling tests to check for coating spallation, and emissivities will be evaluated at elevated temperatures.

Lastly, efforts in ceramics included final selection of materials for the support rails, and the "small RAH" test panel for the UNDEERC test. Aurex 30 was selected for the support rails on the basis of its expected high emissivity, good resistance to thermal shock, and relatively high mechanical strength. The small RAH is designed for comparison of different fireside lining materials, and initial tests will focus on coated Monofrax L and Monofrax M (both from GRP), and the C104 (chromia-magnesia) as hot lining materials. In addition, mechanical testing of Monofrax L will be performed to provide data for design validation of the Large RAH test panel, during the next quarter.

Alloy Matertials

The efforts during this reporting period were focused on (a) the high temperature surface stability of MA 754 and MA 758 and (b) joining strategy . As shown in Exhibit 2.2-28, the principle differences between MA 754 and 758 is in the quantity of chromium in the alloy. The increased concentration of chromium in MA 758, barely increases the strength of the alloy but significantly increases the reservoir of chromium thereby increasing the high temperature life expectancy of the alloy.

Exhibit 2.2-28
Chemical Composition of Candidate Alloys

			Concentration weight percent				
Alloy	Ni	Cr	C	Al	Ti	Yttria	Fe
MA 754	Bal	20	0.05	0.3	0.5	0.6	1
MA 758	Bal	30	0.05	0.3	0.5	0.6	1

Specimens of Ma 754 and MA 758 were exposed for 1000 hours at 1000 and 1100C. The oxidation behavior obeyed a parabolic relationship as shown in Exhibit 2.2-29, a plot of the weight gain squared versus time. The data is in excellent agreement with the accepted behavior of a chromia former.

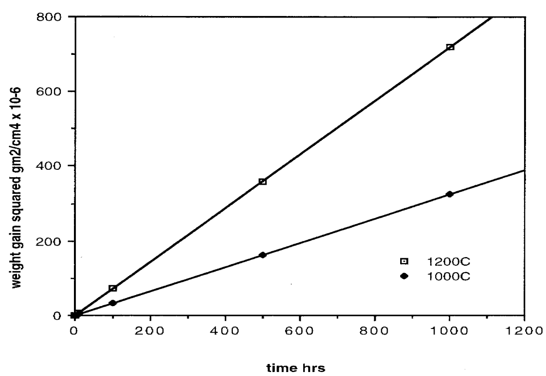

Exhibit 2.2-29
Parabolic Oxidation of MA-754/758

The normally acceptable loss in thickness associated with oxidation is 0.5mm per year. The calculated time to consume 0.5mm per year in the temperature range from 1000C to 1300C is shown in Exhibit 2.2-30. In the temperature range of interest, both alloys meet program requirements.

Exhibit 2.2-30
Calculated Metal Loss Rates

Alloy	time, hours for 0.5mm loss at			
	1000C	1100C	1200C	1300C
MA 754	24,900	22,700	8,000	300
MA 758	53,800	31,400	10,800	1,500

The mechanically alloyed materials , unlike conventional alloys, are not weldable. The difficulties are associated with the inability to maintain the fine dispersion strengthening oxide phase in the weldment . However the MA alloys are successfully joined by both conventional brazing techniques and by transient liquid metal processing, TLP. In this process , the joining alloy contains one or more elements that suppress the melting point of the alloy, and at temperature rapidly diffuse into the matrix, thereby changing the composition of the union, which results in a significant increase in the melting point of the joined material. Increases in melting points greater than 200C is not uncommon.

Initial joining of pipes and elbows necessary for the construction of the RAH will incorporate a basis thread design. Tests are currently in progress to verify the ease in which both male and female threads are machined . Studies are also underway to determine the most cost effective method of insuring leak tightness of the joints. Methods of sealing include the conventional use of high temperature gaskets, high temperature brazes, TLP, as well as reaction bonding in which the active metal or alloy unites with the threads to form a intermetallic which “welds” the materials.

Laboratory- and Bench-Scale Activities

The high-temperature physiomechanical properties of engineering materials such as structural ceramics make them suitable for use as furnace liners, heat exchangers, hot-gas filters, and other components for operation at temperatures above 1300C (2372F). For such applications, it is necessary to know and understand the effects of corrosion on mechanical properties such as strength, creep, fatigue behavior, and stability.

Corrosion is the degradation of material surfaces or grain boundaries by chemical reactions causing loss of material and consequently a decrease in strength of the material. The major challenges from a corrosion standpoint are to identify where at the surface or in the microstructure the attack occurs; why that feature is attacked; and what are the rates of the attack. To understand those localized attacks, EERC personnel are conducting detailed slag corrosion studies of engineering materials suitable for use in the HITAF using the simulated conditions of the dynamic slag application furnace (DSAF). Some of the questions to be addressed include:

- What reactions will occur?
- What are the conditions for the reaction?
- How are corrosion rates affected by silicate melt type, gas velocity, stress, temperature, and gas composition?
- How do the corrosion rates translate to flaw severity in the refractories or the ceramic?
- Can we identify specific reaction rates with specific increases in flaw severity?

Laboratory Activities

The Plibrico Company provided 100 lb (45 kg) of refractory castable material (Plicast 96 and 99) at no charge for duplication of the slag flow corrosion tests. Another 50 lb (22.5 kg) of an experimental refractory castable, Plicast 98, has also being received at no charge and is currently being tested. The bulk chemistry for these refractories varies by the amount of silica present:

0%, 2%, and 4% for the Plicast 99, 98, 96 material respectively. Test samples for both dynamic and static tests of the three castables were prepared and sintered to 1500C (2732F). Two of the refractory samples (Plicast 96 and Plicast 99) were also modified with rare earth oxides (REOs). The purpose of the REO addition was to develop refractories of high strength, high fracture toughness, and poor slag wettability characteristics for the HITAF.

Preliminary morphology evaluations have been completed on the corroded samples of Plicast 96, Plicast 99, Hydrecon Tabcast, and Narcocast 60. The refractories were tested at 1500°C (2732°F): 63 hr for Plicast 99, 140 hr for Plicast 96, and 50 hr for Narcocast under flowing slag conditions. The corroded blocks were cross-sectioned through the slag channel and analyzed in a scanning electron microscope (SEM). The latest observations indicate that earlier conclusions on the sources of some of the test sample fracture patterns were premature. Most of the cracks were found to originate from defects created in the castable refractory during processing or the fabrication process. X-ray mapping on these refractories shows the presence of a calcium silicate phase at the grain boundaries, a corrosion-promoting material. The quantity of this phase is controlled by the silica content of the refractory. For example, more of the calcium silicate phase is found at the grain boundary for Plicast 96 than for Plicast 99. For Narcocast (60% alumina to 40% silica), these phases are dominant, whereas for Hydrecon Tabcast (90% alumina to 10% chrome), they were insignificant. The SEM was also used to measure slag diffusion or penetration into the refractories. The average slag diffusion depths were 0.63 (1.6), 0.56 (1.42), 0.68 (1.72), and 0.48 in. (1.22 cm) for Plicast 96, Plicast 99, Narcocast 60, and Hydrecon Tabcast, respectively.

Energy-dispersive x-ray fluorescence (EDXRF) analysis was completed on three spent slags from tests of Plicast 96, Plicast 99, and Hydrecon Tabcast at 1500°C. For all of the slag reactant products, there was generally a decrease in the silica and in the alkalies, with an increase in the alumina content from the original Illinois No.6 slag chemistry, Exhibit 2.2-31.

Exhibit 2.2-31
EDXRF Data for Refractory Samples

Time, hr	Oxide	As Received	Plicast 96	Plicast 99	Narcocast 60
50	SiO_2	54.4	48.6		
	Al_2O_3	19.0	25.5		
	Fe_2O_3	15.6	14.3		
	NaO	0.0	1.5		
	MgO	1.3	1.2		
12	SiO_2	54.4		50.9	51.0
	Al_2O_3	19.0		22.8	23.7
	Fe_2O_3	15.6		16.4	15.9
	NaO	0.0		0.1	0.0
	MgO	1.3		1.0	0.8

Bench-Scale Activities

Both static and dynamic corrosion tests were performed simultaneously in the DSAF for Plicast 96, 98, and 99 refractory castables. For the static test, about 0.024 lb (11 g) of Illinois No. 6 slag was placed in a 1-in.(25-mm)-square hole in a 2-in. (50-mm) cube. The Plicast 96 and 99 tests were duplicates of previous tests. To date, 140 hr have been completed for the static test and 65 hr for the continuous slag flow experiments. The slag diffusion depth for the samples tested in the dynamic mode, as measured by SEM, was 0.93 in. (24 mm) and 0.92 in. (23 mm) for Plicast 96 and 99, respectively. For the static test samples, the measured diffused layer was 0.42 in. (11 mm) and 0.47 in. (12 mm) for Plicast 96 and 99. The average measured eroded/corroded surface for the Plicast 96 and 99 was 0.35 in. (8.9 mm) and 0.26 in. (6.5 mm) for the dynamic test samples. It was very minimal for the static test samples, 0.012 in. (0.31 mm) and 0.022 in. (0.56 mm) for Plicast 96 and 99, respectively. For Plicast 98, 130 hr have been completed for the static test and 25 hr of flowing slag at 130-hr retention time at 1500C (2732F) for the dynamic test. The slag diffusion layer and the eroded and/or corroded layer have not been measured in either the static or dynamic tests of the Plicast 98.

The data from the duplicate dynamic tests seem to correlate well with those from the previous run. For example, for Plicast 99 at 63 hr of slag flow time, the average corroded/eroded surface was 0.22 in (5.7 mm). For the static test, very little corrosion activity was measured because of the formation of a saturated reaction product between the slag and the refractory material, which is a function of experimental set temperature and time. This saturated reaction product promoted minimal corrosion activity.

Based on the dynamic test evaluation, the Plicast 99 refractory material performed better than Plicast 96. However, it should be stated that mechanical strength for Plicast 99, as expressed by the modulus of rupture at room temperature, is much lower than for Plicast 96. For example, for Plicast 99, the measured strength is 300 psi (0.003N) at 1370C (2500F), whereas for Plicast 96, it is 6000 psi (0.6 N). To increase the strength of the Plicast 99, it should be sintered at elevated temperatures (greater than 1500C [2732F]).

The EERC has also evaluated experimentally developed silicon-based (silicon carbide [SiC]) ceramics for use in the RAH region of the HITAF. Silicon-based ceramics possess attractive physical, mechanical, and chemical properties, with an oxidation passivity that makes them good candidates for high-performance structural applications such as those that would be required for the RAH areas of the HITAF, with high thermal conductivity.

The experimental SiC castable was made of 90% silicon carbide granules, (37-CrystolanTM, Norton Company) and 10% Alphabond 200 Hydratable AluminaTM binder (Alcoa Industrial Chemicals). The binder is a reactive alumina, which contains no calcium compounds that can form low-melting-point compounds, especially at the grain boundaries in the refractory matrix, that might reduce resistance to corrosion. To date, a 50-hr slag flow time over the 90:10 silicon carbide-to-alumina refractory test sample has been completed in the DSAF, with a total retention time of 95 hr at 1400C (2552F).

This experimental SiC refractory presented challenging but interesting problems. The slag flow into the quench vessel was sluggish, first, because of the lower test temperature and second, because of the formation of gaseous reaction products, i.e., CO and/or CO_2 at the near surface of the refractory, which caused the slag to flow not only through the channel, but also along the entire vertical face wall. There were very fine, pinlike holes at the surface (surface pits), where the slag had interacted with the refractory. These surface pits might indicate the path for the outward diffusion of the gaseous phases in this SiC refractory. Another possible explanation for this localized surface pitting could be the formation of iron silicides, one of the reaction phase products formed from the direct contact of the SiC with the slag. It also must be noted that the population distribution of both these flaws will control the strength and the performance characteristics for this refractory. Large, bubblelike structures were also observed running parallel to the drain channel and measuring about 0.79 in. (2.0 cm) wide and 0.084 in. (0.21 cm) high.

At 1400C, (2552F), the quenched slag droplets were hollow and relatively large compared with the slag droplets for the other refractories, which were dense and beadlike. It is interesting that the color of the quenched slag beads was very different from that of the reactant bubbles at the near surface. The quenched slag beads were very dark in color, nearly black, compared with the light brown color for the reactant bubbles. This may be explained by the oxidation state of the iron in the slag. The residual slag layer in the channel made it difficult to measure recession for both of the directions of the refractory channel; however, a 0.38-in. (0.98-cm) recession across the diameter was the best estimate.

Although the postcorrosion test evaluations have not yet begun, preliminary theoretical suggestions indicate that the corrosion attack path of this SiC refractory material could have started with the dissolution of the silicon dioxide layer by the slag melt, followed by oxidation of the free silicon phase, and then the silicon carbide phase, and finally the grain boundary attack. However, it should be noted that the level of corrosion would also be dependent on the composition and structure of the SiC base material and on the slag type. There seems to be some evidence in the literature suggesting that the depth of the flowing slag layer can modify the local oxygen partial pressure at the slag-refractory interface, thereby also influencing the corrosion mechanism, *Ferber* <u>A Characterization of Corrosion Mechanism Occurring in a Sintered SiC Exposed to Basic Coal Slag</u>.

Discussions are still continuing with UTRC on the design and selection of the refractory samples to be tested in the DSAF at the EERC for the RAHs.

Status Assessment and Forecast

- Continue morphology studies on refractory samples
- Continue corrosion tests on SiCBalumina and REO-modified test samples
- Continue discussions with UTRC on refractory samples for RAH
- Evaluate Plicast 98 refractory castable
- Evaluate with other types of coal slags

Structural Analysis

Alloy Material Analysis

No new stress analysis of the radiative air heater tubes was performed. Stress analysis of the North Dakota pilot scale convective air heater (CAH) was performed. The purpose of this analysis is to verify that a sufficient margin of safety exists in the design.

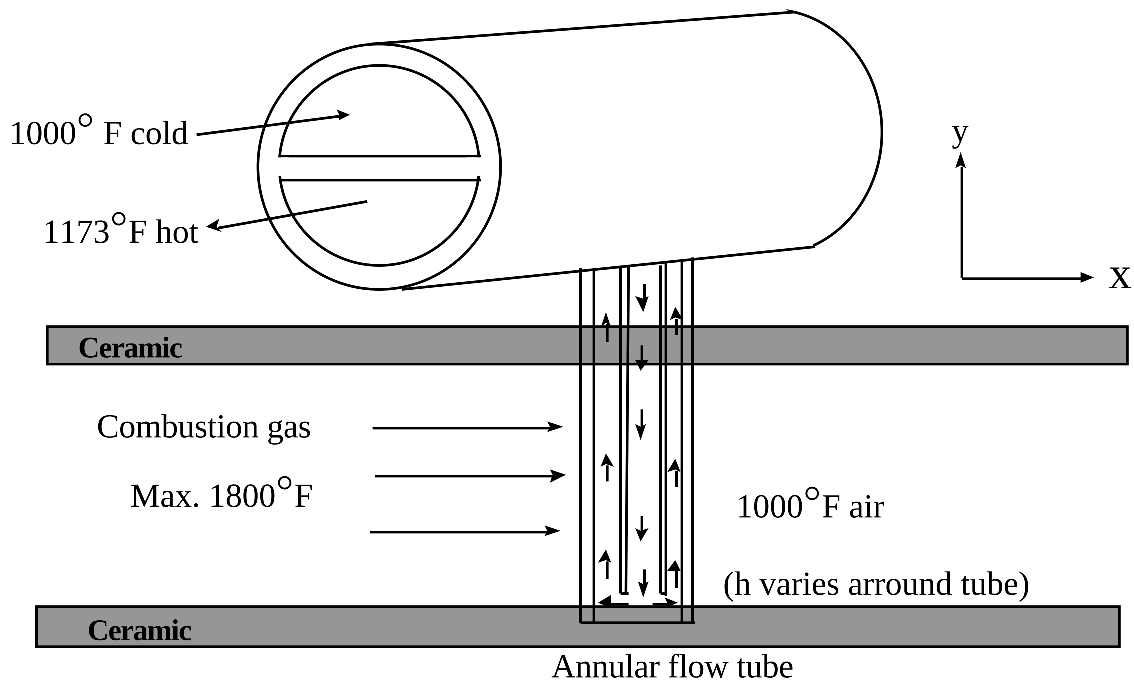

Exhibit 2.2-32
Convective Air Heater

Exhibit 2.2-32 is a sketch of the convective air heater design. The sketch shows the header and one of several annular flow tubes supplied by the header. The header is a partitioned cylinder. The top compartment distributes the cool inlet air flow and the lower compartment collect the heated outlet flow. The tubes are a tube in a tube design where the cool air travels down the center and is returned to the top through the outer annular flow area. A spiral vain in the annulus will force the air to circle the tube as it travels upward. This was done to encourage even heating of the air flow. The header is supported by a saddle that is not shown in the figure. The tubes are inserted directly in to the combustion gas stream.

Header Analysis

A 2D model of the cross section of the header was constructed. This model was used to find the bending stress in the cylindrical header caused by thermal gradients.

Geometry

Partitioned cylinder	OD (y direction)	15 in. (38.1 cm)
	OD (x direction)	14 in. (35.6)
	Length 22 in.	(55.9 cm)

Material

Haynes 214

Thermal Boundary Conditions

Hot side

Air flow temp	1173°F	(634°C)

Cold side

Air flow temp	1000°F	(538°C)

OD of header is perfectly insulated

Analysis

Due to symmetry, only _ of the header was modeled. The cross section of the header lies in the x-y plane. The axial length of the header lies in the z direction. The header was constrained in the x direction by a symmetry plane. One node was fixed in the y direction. A minimum number of constrains was used to avoid inducing additional stress. Both thermal and stress analyses were performed. Generalized plane strain elements were used. The cylinder was allowed to expand in the z direction. The cross section must remain planer but it is allowed to rotate about the x and y axis. The model assumes the material has infinite strength and that the deformation is elastic.

Results

See Exhibit 2.2-33

Exhibit 2.2-33
Header Model Results

Haynes 214	
Deflection	**inch (cm)**
y deflection each edge (height)	.060 (.152)
x deflection each edge (width)	.061 (.155)
z max. (total increase in length)	.188 (.478)
Stress	**psi (kPa)**
Max Tensile Sigma X	3,614 (24,915)
Max Compressive Sigma X	-1,430(-9,858)
Max Tensile Sigma Y	3,189 (21,985)
Max Compressive Sigma Y	-461 (-3,178)
Max Tensile Sigma Z	3,953 (27,252)
Max Compressive Sigma Z	-3,219(-22,192)
Max Von Mises	4,833(33,319)
Max Tresca	5,839(40,254)
Temperature	**°F (°C)**
Maximum Minimum	1,165(629) 1,008 (598)
Safety Factor	12.75

Tube Analysis

A 2D model of the cross section of a tube was constructed. This model was used to find the bending stress in the tube due the thermal gradients caused the circumferential variation in convective heat transfer coefficient (h). Away from the ceramic duct walls there is no axial variation in h.

Geometry

Cylindrical tube	Outside Diameter	2.0 in. (5.08 cm)
	Wall thickness	1875 in. (.476 cm)
	Length 19 in.	(.48.26 cm)

Material

Haynes 214

Thermal Boundary Conditions

Hot (outside) side		
Air flow temp	1800°F	(982°C)
Cold (inside) side		
Air flow temp	1000°F	(538°C)

Analysis

Due to symmetry, only _ of the tube was modeled. The cross section of the tube lies in the x-y plane. The axis of the tube lies in the z direction. The tube is constrained by the symmetry plane in the y direction. One node was fixed in the x direction. A minimum number of constrains was used to avoid inducing additional stress. Both thermal and stress analyses were performed. Generalized plane strain elements were used. The cylinder was allowed to expand in the z direction. The cross section must remain planer and it is not allowed to rotate about the x and y axis. This boundary condition was imposed because the tube end fits into a pocket in the ceramic. The tube may expand deeper into the pocket but bending will be prevented. The model assumes the material has infinite strength and that the deformation is elastic.

Results

See Exhibit 2.2-34.

Exhibit 2.2-34
Tube Model Results

Haynes 214	
Deflection	**inch (cm)**
y deflection each edge (height)	.0070 (.018)
x deflection each edge (width)	.0068 (.017)
z max. (total increase in length)	.132 (.335)
Stress	**psi (kPa)**
Max Tensile Sigma X	3,499 (24,122)
Max Compressive Sigma X	-1,881(-12,968)
Max Tensile Sigma Y	3,237 (22,316)
Max Compressive Sigma Y	-1,503 (-10,362)
Max Tensile Sigma Z	4,901 (33,787)
Max Compressive Sigma Z	-6,801(-46,886)
Max Von Mises	6,419(44,253)
Max Tresca	6,469(44,597)
Temperature	**°F (°C)**
Maximum Minimum	1,554 (846) 1,513 (823)
Safety Factor	8.3

Ceramic Material Analysis

A three dimensional model of a wedge shaped brick made from a modified Monofrax M material was constructed. A thermal analysis was performed to determine the temperature profile through the brick. These results were read into a second model that calculated the resulting stress and deflections. A summary of the geometry and thermal boundary conditions follows.

Geometry

Ceramic shape	Wedge Rectangular 18 in by 30 in by 1.0 to 2.0 in thick (45.7 cm by 76.2 cm by 3.8 cm)

No vertical slip joints, horizontal slip joints

Thermal Boundary Conditions

Hot side

Sink temp	2800°F (1520°C)
Convective heat transfer coefficient	21.2E-5 Btu/sec/in2/°F
	110 Btu/hr/ft2/°F
	(625 W/m2/C)

Cold side (directly exposed to tubes)

Sink temp	1700°F (900°C)
Convective heat transfer coefficient	9.6E-5 Btu/sec/in2/°F
	50 Btu/hr/ft2/°F
	(284 W/m2/C)

Cold side (covered by support brick)

Sink temp	1700°F (900°C)
Convective heat transfer coefficient	4.8E-5 Btu/sec/in2/°F
	25 Btu/hr/ft2/°F
	(142 W/m2/C)

Analysis

Due to symmetry, only _ of the brick was modeled. The face of the brick lies in the y-z plane. The thickness of the brick lies in the x direction. The brick was constrained by the symmetry plane in the y direction. One node was fixed in the z direction and 2 nodes were fixed in the y direction. A minimum number of constrains was used to avoid inducing additional stress. The model assumes the material has infinite strength and that the deformation is elastic.

Results

See Exhibit 2.2.-35.

Exhibit 2.2-35
Model Results

Modified Monofrax M	
Deflection	**inch (cm)**
y deflection each edge (width)	.17 (.43)
z deflection (height)	.16 (.41)
x max. deflection at center	.13 (.33) .000 at four corners
Stress	**psi (kPa)**
Max Tensile Sigma X	2,800 (16,500)
Max Compressive Sigma X	-1,000(-6,900)
Max Tensile Sigma Y	8,600 (59,300)
Max Compressive Sigma Y	-1,900 (-13,100)
Max Tensile Sigma Z	2,800 (19,300)
Max Compressive Sigma Z	-800(-5,500)
Max Von Mises	8,519 (58,800)
Temperature	**°F (°C)**
Hot Face	2,650 (1454) 2,773 (1523)over lap
Cold Face	2,000 (1204) 1,830(999)under lap
Delta Temp Center	650 (360)

The model indicates that Modified Monofrax M results in low levels of stress. The under lap area of the brick does have high tensile loads. These loads result from thermal stress. The under lap area is cooler than the rest of the brick and the thermal expansion is less than the hotter sections of the brick. Cracking at flaws maybe a problem in this area. The modified Monofrax M is expected to have tensile strengths of greater than 3,500 psi at 2,750°F and 5,000 psi at 2,400°F. The high stress under lap area is less than 1900°F. Testing is needed to determine if cracking is a problem in the under lap area.

Ceramic Attachment Analysis

A two dimensional model of a wedge shaped brick attached to the support refractory by two ceramic pins was constructed. A two D thermal model was constructed. The film coefficients and sink temperatures used were the same as the three-D analysis. The temperature profile through the two D model was compared with that predicted by the three D model and found to be in good agreement. These results were read into a two D stress analysis model. A summary of the geometry and thermal boundary conditions follows.

<u>Geometry</u>

Ceramic shape	Wedge Shape 18 in tall by 1.0 in to 2.0 in thick (45.7 cm by 2.54 cm to 5.08 cm)
Simple horizontal slip joints	
.25 in ceramic pins	

<u>Thermal Boundary Conditions</u>

Hot side	
Sink temp	2800°F (1520°C)
Convective heat transfer coefficient	21.2E-5 Btu/sec/in2/°F 110 Btu/hr/ft2/°F (625 W/m2/C)
Cut out and over lap surfaces	
Sink temp	2000°F (900°C)
Convective heat transfer coefficient	2.12E-5 Btu/sec/in2/°F 5.0 Btu/hr/ft2/°F (28.4 W/m2/C)
Cold side (covered by support brick)	
Sink temp	1700°F (900°C)
Convective heat transfer coefficient	4.8E-5 Btu/sec/in2/°F 25 Btu/hr/ft2/°F (142 W/m2/C)

<u>Analysis</u>

The cross section of the brick lies in the x-y plane. The thickness of the brick lies in the z direction. Contact between ceramic tiles and the support structure was simulated. The model assumes the material has infinite strength and that the deformation is elastic. The weight of the ceramic tile and 3in H2O air pressure on the cold side of the tile was included.

<u>Results</u>

See Exhibit 2.2-36.

Exhibit 2.2-36
Model Results

Modified Monofrax M	
Deflection	**inch (cm)**
y deflection (height)	.20 (.51)
x max. deflection at center	.030 (.076)
Stress	**psi (kPa)**
Max Tensile Sigma X	1,300 (9,000)
Max Compressive Sigma X	-400(-2,800)
Max Tensile Sigma Y	1,100 (7,600)
Max Compressive Sigma Y	-,400 (-2,800)
Max Shear Stress	600 (4,200)
Temperature	**°F (°C)**
Hot Face	2,673 (1467) 2,750 (1510)over lap
Cold Face	2,216(1214) 1,800(982)under lap
Delta Temp Center	457(236)

The model, run with just the mechanical loads (weight and pressure) resulted in a maximum stress of 500 psi (3,500 kPa) in areas around the pins. The slanted pins carry loads only when the brick above is removed. With careful design of the vertical pin height and the clearance of the slanted cut out, a single brick would be replaceable.

The outward displacement (bowing) of the brick at the edge is much less than at the center. The less this edge deforms the better the barrier to slag infiltration.

Ceramic Thermal Test

Small scale testing of the candidate ceramic materials is about to begin. The test will verify the modeling done and determine the materials resistance to thermal gradients and thermal shock. Thermal cycling will be performed. Tests to measure mechanical properties after thermal cycling will be performed. A test plan was written and the first pair of ceramic test specimens has been prepared. The rig is being calibrated and testing is about to begin.

Design Layout of the CAH

A preliminary design layout of the CAH has been completed, see Exhibit 2.2-37, -38, and -39. The design is 90% complete for an all stainless steel assembly, minus the radiation tubes. Because of the combination of temperatures and pressures that are expected, stainless steel has its limitations and therefore other more materials are being investigated.

Quotes the cost, delivery and availability of alternative materials such as the Inconel Alloy's 617, 800, 802, 601, 601GC, 333 and Haynes 214 are being obtained. These materials are preferred over the stainless steels, because they have better resistance to the harsh environments and have better mechanical properties at the high temperatures. Once a material selection has been made, an analysis of the structural integrity of the CAH at its operating conditions will be performed.

The current operating conditions show a design of 7 active radiation tubes and 5 dummy tubes. The outside tube dimension is 2.0" [.051m] OD x 0.188" [.005m] wall. The inner tube dimension is 1.0" [.025m] x .065" [.002m] wall. The temperature of the air flowing into the inner radiation tube from the inlet plenum is 1000 F [538 C] and the temperature of the air in terms of the exit plenum from the radiation tubes is 1173 F [634 C].

A threaded joint interface which would incorporated a high temperature metal o-ring has been designed. This will permit two dissimilar materials to be connected. This condition would exist if the CAH were to be made from stainless steel and the radiation tubes were made from an Inconel Alloy or Haynes type material.

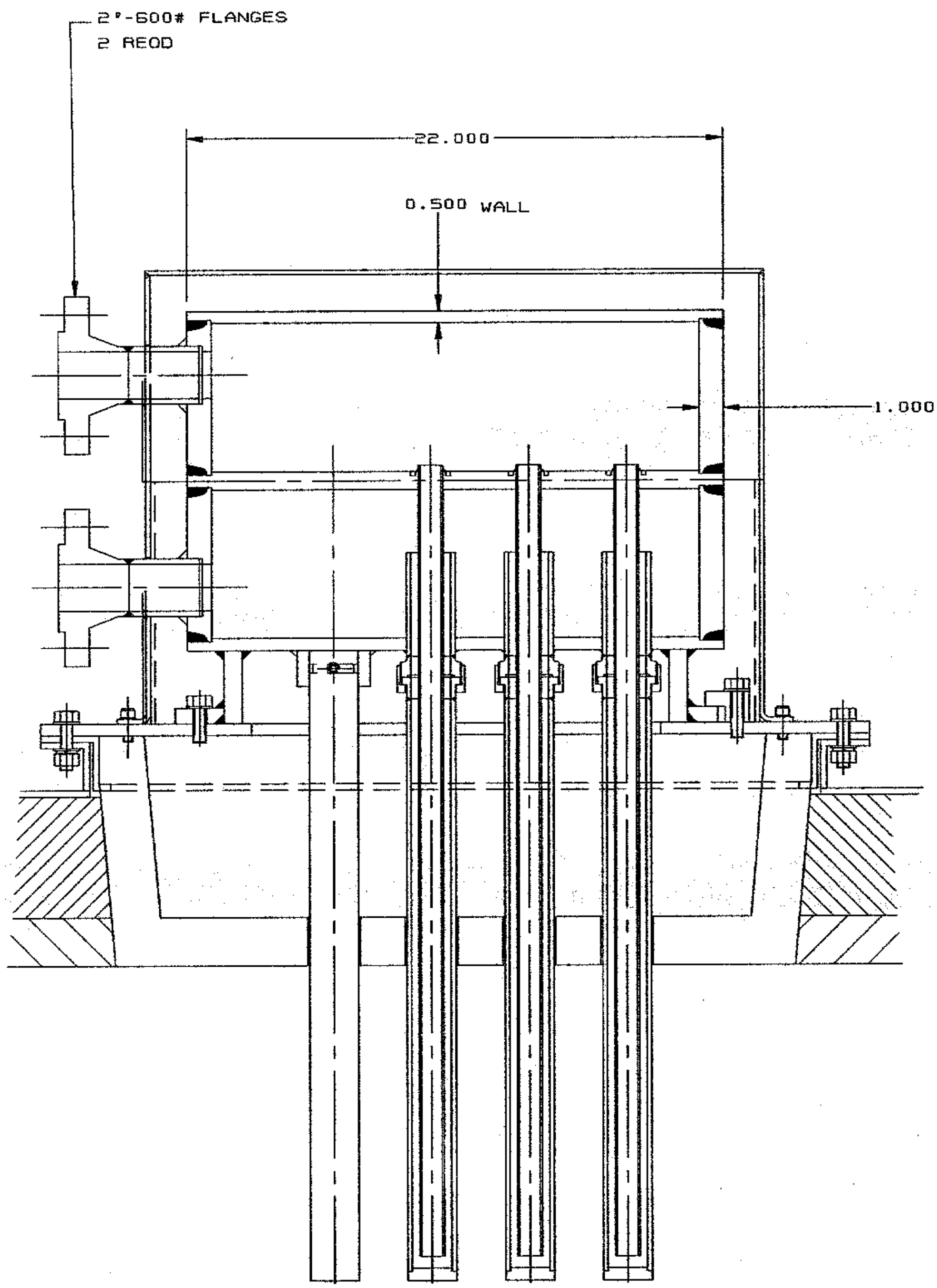

Exhibit 2.2-37
Preliminary Design of CAH Test Unit - Side View

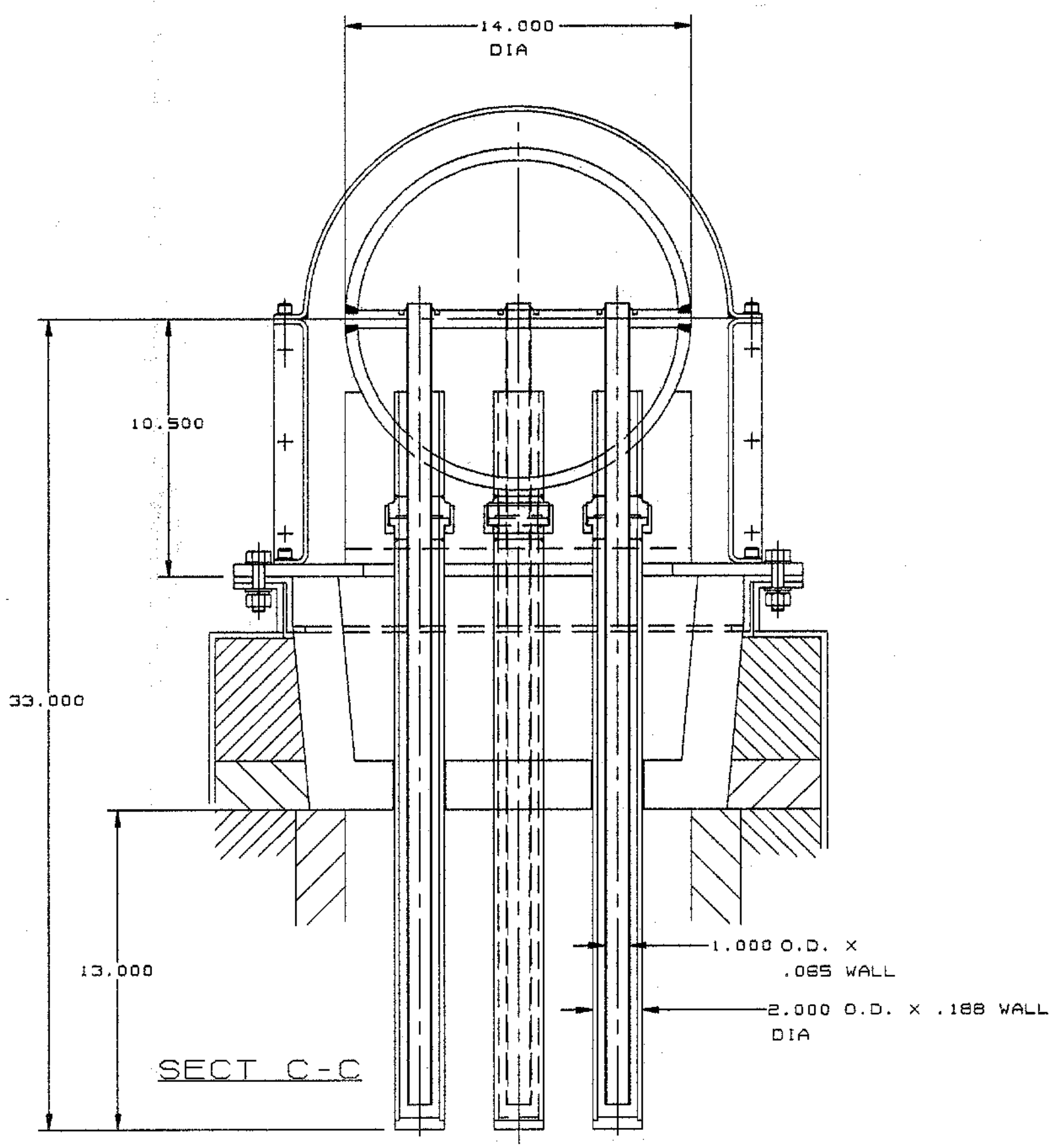

Exhibit 2.2-38
Preliminary Design of CAH Test Unit - Front View

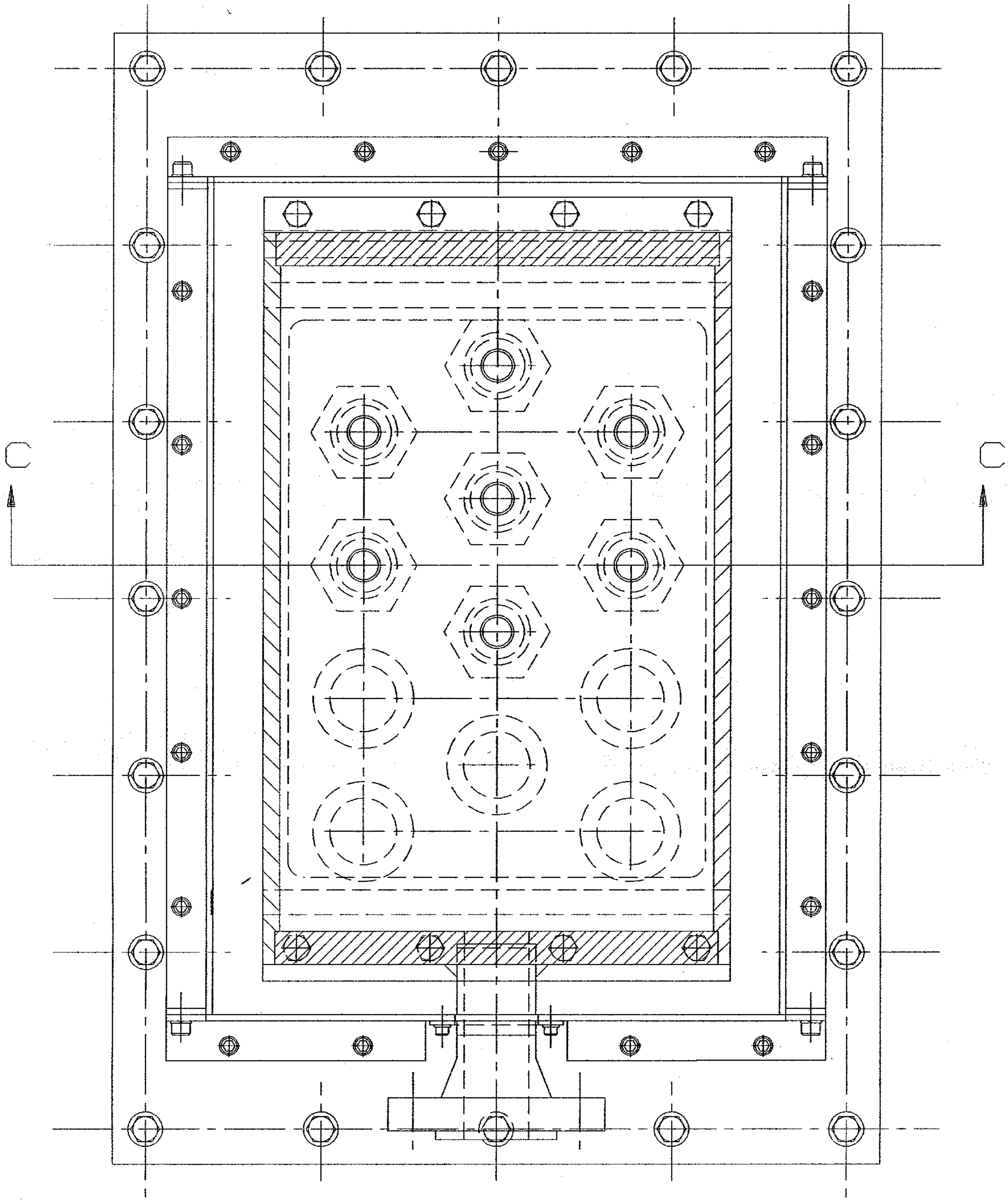

Exhibit 2.2-39
Preliminary Design of CAH Test Unit - Top View

Design Layout of the RAH

A preliminary design as been laid out for the RAH, see Exhibit 2.2-40 and -41, showing all the major components and orientations as required for the initial EERC tests. The material for the flanges, elbows and the 3 vertical radiation tubes has been selected and ordered. The material specified is an Inconel alloy type MA 754. This material was selected because of its high strength and good oxidation resistance at elevated temperatures.

A sample test specimen assembly has been designed to investigate the machinability and feasibility of making threaded joints as one method of joining the tubes to the flanges and elbows using this MA 754 Inconel alloy. This test will provide information on the ability to machine internal and external threads and their ability to seal air at 150 psig for ambient and elevated operating temperatures.

The air manifold that feeds the inlet and exit lines of the radiant tubes outside the RAH door assembly will probably be made of an Inconel alloy material yet to be determined. A design study will be done to determine whether the radiant tubes should be hung from above or supported from below.

The design of the RAH door frame support structure is continuing. A structural and thermal analysis will be done once an optimal structural design has been selected that has considered the material properties of available metals and insulating materials. The amount of heat transfer that can radiate to the metal structure through insulation barriers must be limited or some type of cooling must be provided wherever there is a potential for over heating of the main structural members.

There is a preliminary design for the ceramic bricks (panels) and the brick supports. There are at least two attachment schemes for attaching the bricks to the brick supports. Using machinable wax a half scale assembly will be made that will test the feasibility of the brick attachment scheme and the ability of the bricks to be removed and replaced if one should crack or fail. These wax panels will provide an appreciation of the assembly process and the overlapping between the top, bottom & side bricks. This exercise will also provide a clear and visual demonstration of the attachment scheme.

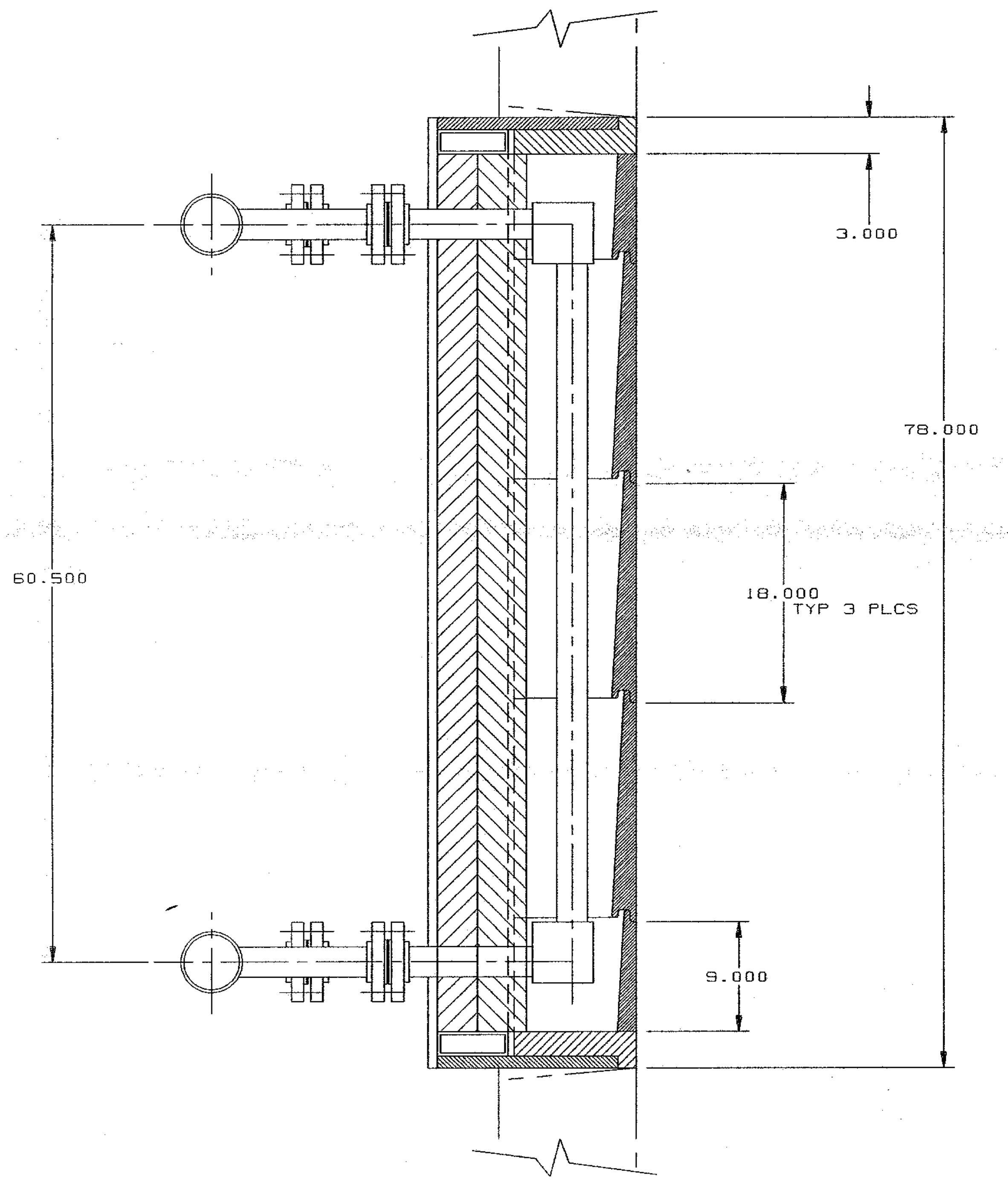

Exhibit 2.2-40
Preliminary Design of CAH Test Unit - Side View

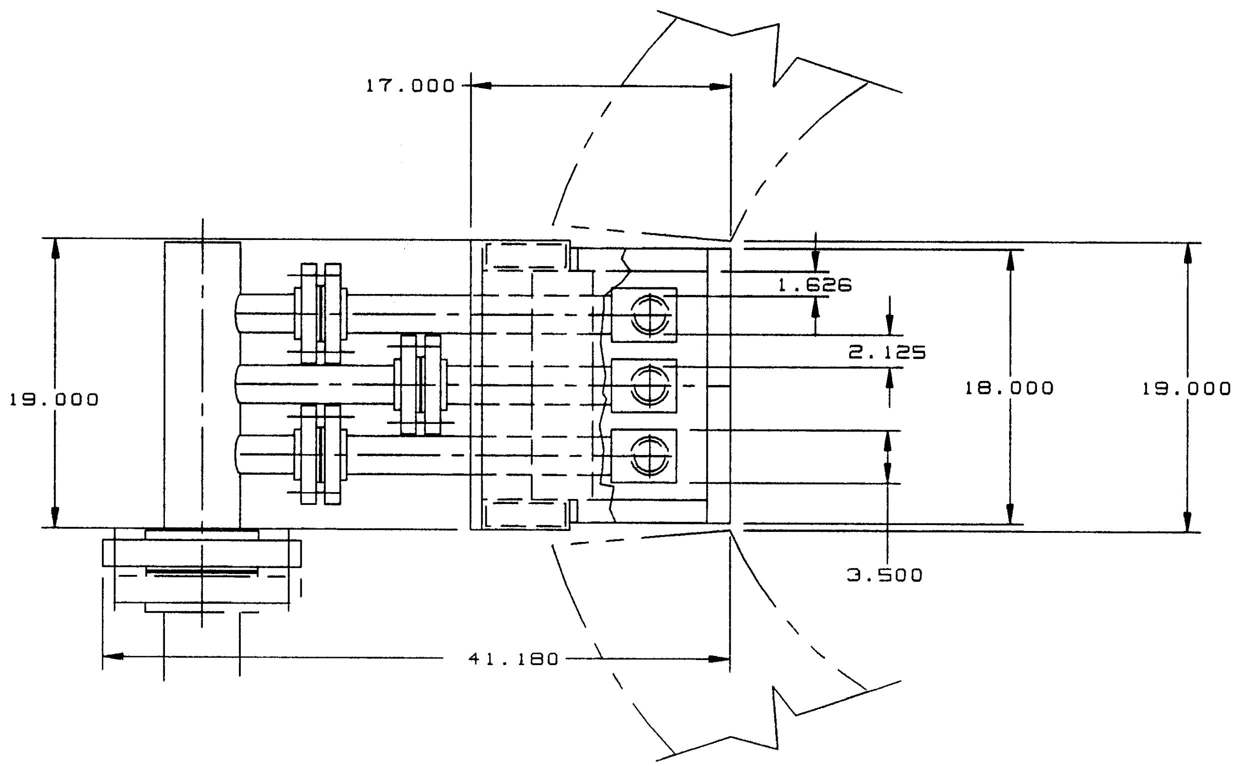

Exhibit 2.2-41
Preliminary Design of CAH Test Unit - Top View

Task 2.4 Duct Heater

Duct Heater Test Facility Preparation

During this reporting period, design and layout of the high pressure combustion facility to be installed in the UTRC JBTS has continued. Several variations to the combustor design have been considered based upon the data that will be necessary to obtain to properly evaluate the performance of the low NOx emission in-duct boost heater. Initially, a combustor with four planes of optical access was designed, but the combustor cost was prohibitive. This combustor design was scaled down to that shown in Exhibit 2.4-1 below. This combustor is designed for operation at 600 psia with a discharge temperature of 2550°F (1673K) with an inlet temperature of 1700° F (1200K). The scaled-down combustor has 4 rectangular quartz windows located at the discharge plane of the mixer, followed by four round quartz windows for a second viewing plane downstream of the injector. Each of these quartz windows can be replaced with a steel insert into which a traversing thermocouple or gas sampling probe can be inserted. An instrumentation spool assembly with radial gas sampling ports and thermocouples will be located at the exit of the combustor, prior to the converging section, to obtain an exit species and temperature profile. The combustor is lined with a high temperature alloy, backed by a ceramic insulation, so that carbon steel can be used in its construction. Vendor quotations are being obtained for the forging of the pressure vessel, combustor weldment, and window flange fabrication.

Vendor quotations for the high temperature, high pressure inlet piping to the test cell are being obtained, and ancillary valving and ductwork are being designed. The Facilities Instrumentation Group in the JBTS is now obtaining the necessary flow and temperature monitoring hardware for the combustor installation and operation. Of critical importance is the ability to monitor and interlock the operation of the JBTS facility with the Phoenix Solutions designed electric air heater to ensure that all operating parameters of the heater are within specification. In addition, the combustor instrumentation necessary to ensure safe operation at the high exit temperatures (1673K [2550° F]) and pressures (27 atmospheres) are being outlined and obtained. Data acquisition hardware is being reviewed and ordered so that the combustor exit temperature profiles, and combustor emissions can be measured. As outlined in the previous report, the optical system for planar imaging of mixing profiles within the combustor is being designed and preliminary testing in laboratory flames is being scheduled. Because of the very high centripetal acceleration to be experienced in the mixer/injector, Rayleigh scattering will be used as the primary flow visualization technique in the combustor in lieu of Mie-scattering since the seed particles would not reliably follow the gas flow path.

The combustor (Exhibit 2.4-1) is capable of operation with natural gas or methane fuel with a combustor exit temperature of 1673K (2550° F) and pressure up to 40 atmospheres. The optical ports located at the discharge plane of the mixer/injector are of uv-grade quartz and are 3 x 10 inches (7.6 x 25.4 cm) in dimension. There are 4 ports at each axial station. There are also 4 round optical ports downstream of the rectangular windows. As stated above, each window location will have an optional metal insert into which a traversing gas sample or thermocouple probe can be mounted. Because of the arrangement of the optical and sampling ports, a three-dimensional distribution of temperature and species can be produced which will aid in the evaluation of the mixer performance. The combustor outer shell is composed of carbon steel, with an Inconel liner and ceramic insulation layer on the ID to reduce heat loss to the walls and reduce the combustor wall thickness. The windows will be purged with nitrogen to maintain an acceptable quartz or metal temperature. The centrifugal mixer will be housed in a modular insert located at the inlet to the combustor, just downstream of the inlet diffuser. Air flow, fuel flow, and purge flow will be metered with venturis.

Exhibits 2.4-2 through -4 show the layout of the combustor, air heater, and inlet piping in the JBTS test facility. The inlet piping is unlined stainless steel, whereas the outlet piping from the electric air heater will be lined stainless steel pipe. Stainless piping is required for the inlet to the electric heater to prevent any corrosion particles from the inlet pipe being transferred to the resistance screens. A double valve safety system is required by facility safety standards to allow two levels of shutoff from the air supply system to the combustor. The layout of the cell shows the relative positions of the electric power supply, air heater, and combustor.

The electric resistance air heater which was manufactured by Phoenix Solutions of Minneapolis was inspected at Phoenix Solutions on December 6, prior to final assembly of the heating elements into the pressure vessel. Shakedown tests were then conducted at Phoenix Solutions to verify heater performance at low power. The heater and power supply with associated switchgear were delivered to UTRC on December 23, 1996. The power supply and switchgear were positioned by crane into the UTRC JBTS Cell 4 facility prior to the facility shutdown due to the Christmas holiday. However, in removing the high temperature heater from the enclosed-box trailer in which it was shipped, the heater was damaged. The heater was externally inspected, and a decision made to return it to Phoenix Solutions for a thorough examination to assess any internal damage. The results of this inspection have not yet been obtained. However, repair will be expedited on the heater at no cost to DOE since this item was purchased as UTRC capital. Based upon preliminary estimates of time to repair, the heater will be returned to UTRC prior to completion of the construction of the combustor. In the interim, work will proceed on connection of the switchgear and power supply to the UTRC 4160 Vac electrical substation to be used to supply the needed power; design and fabrication work will proceed as well on the combustor.

Cold Flow Mixing Studies

The facility is being prepared for conducting mixer evaluations in cold flow prior to design and construction of the hot test mixer hardware. In order to obtain meaningful data on the performance of the centrifugal mixer for the duct heater, the cold flow facility will use propane as the high density marker gas, due to its large Rayleigh cross-section, and a helium/air mixture in the outer flow to simulate the density ratio to be expected in the actual duct heater. Once again, Rayleigh scattering from the propane molecules will be used to generate a planar image of the distribution of the center (fuel) flow in the overall fuel and air mixture. Based upon prior data, reported previously, nearly complete mixing is expected within 2 swirler diameters downstream of the injector.

At the present time, detailed design of the components for the high pressure combustor is proceeding. It is estimated that the combustor will be completed in May, 1997; this is in agreement with the estimated delivery of the heater from Phoenix Solutions so that there will be no further delay in the program schedule. Cold flow mixing studies will be conducted in the interim to refine the mixer/injector design prior to construction of the hot test facility mixer. A test matrix will be devised to determine the flow velocities, swirl geometries, inlet temperatures, and inlet pressures which will be needed to provide an understanding of the centrifugal mixing concept.

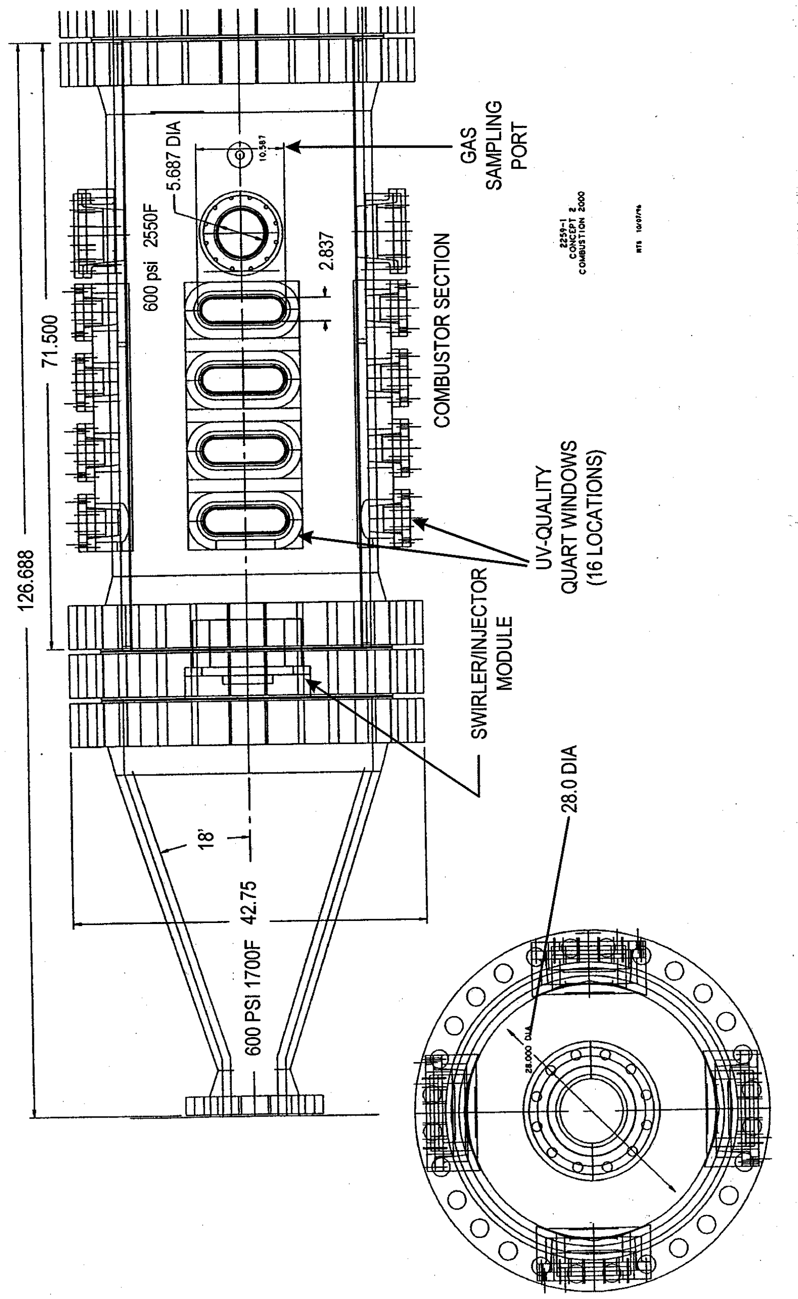

Exhibit 2.4-1
Original In-duct Boost Heater Sub-scale Test Combustor

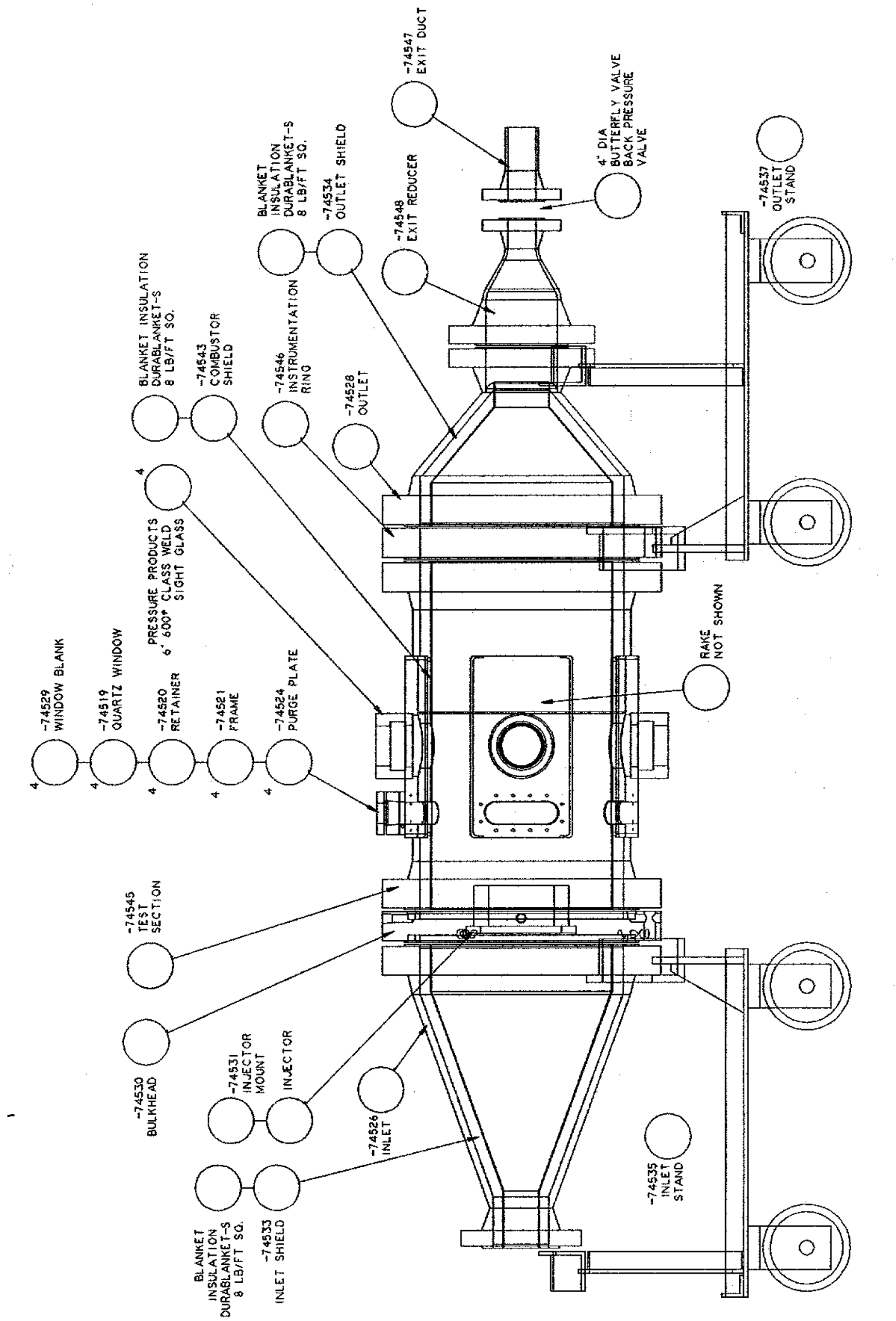

Exhibit 2.4-2
Reduced Optical Access Duct Heater Test Combustor and Support Stand

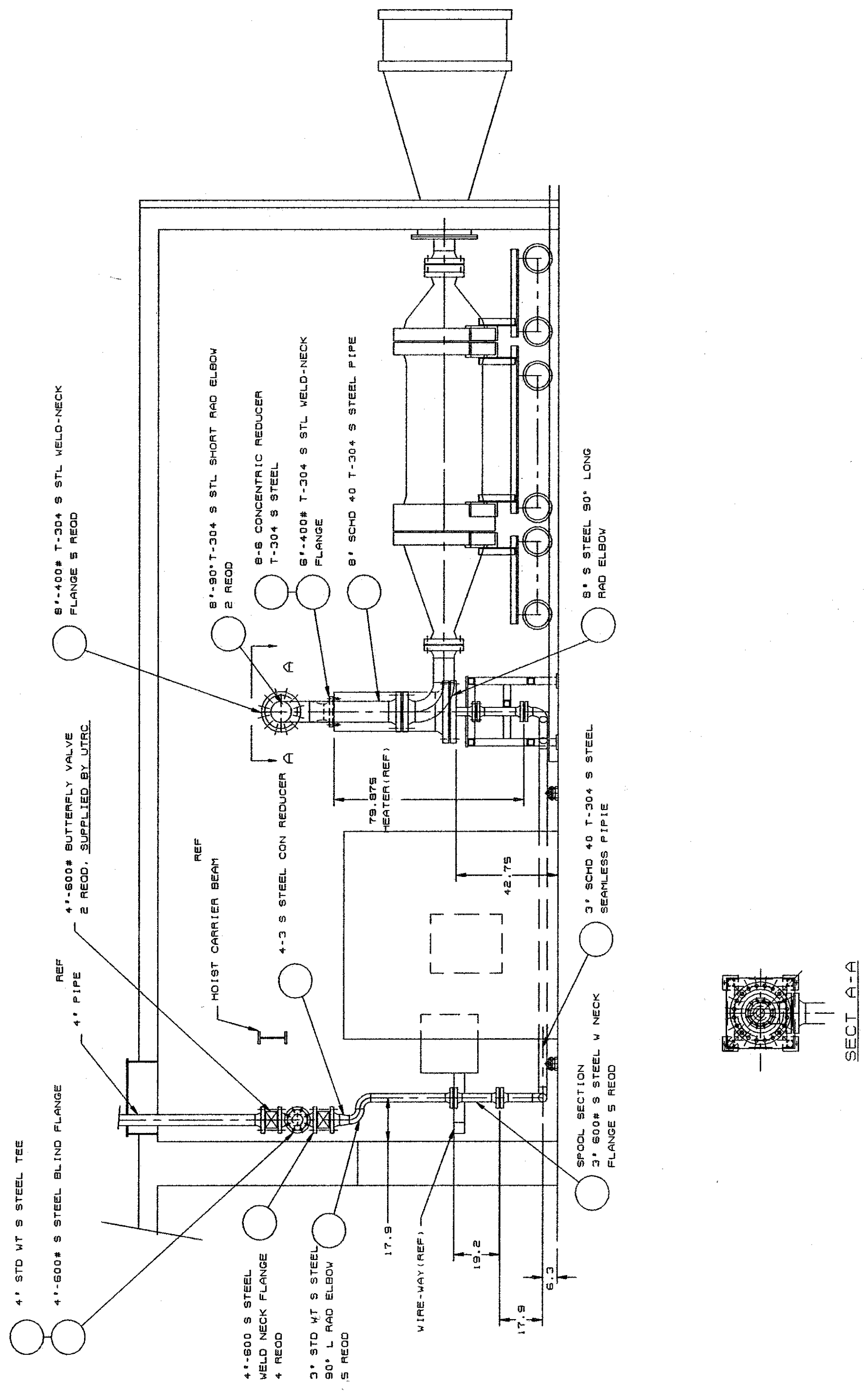

Exhibit 2.4-3
Duct Heater Test Facility Air Heater and Combustor Layout

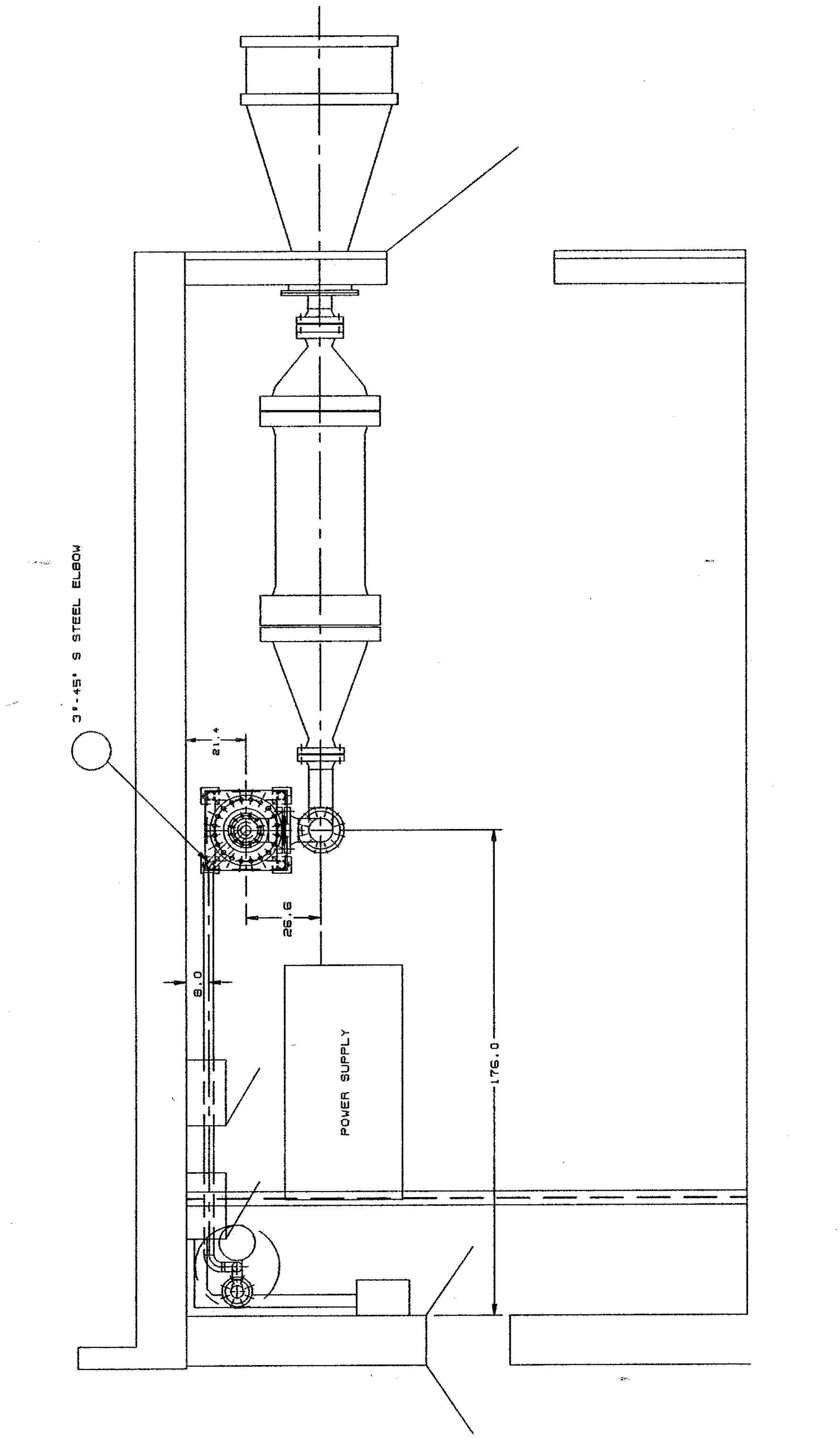

Exhibit 2.4-4
Plan View of Duct Heater Test Facility at UTRC JBTS